Teemu Ovaska

Exhaust Particle Numbers of High- and Medium-Speed Diesel Engines with Renewable and Recycled Fuels

ACTA WASAENSIA 451

Vaasan yliopisto
UNIVERSITY OF VAASA

ACADEMIC DISSERTATION

To be presented, with the permission of the Board of the School of Technology and Innovations of the University of Vaasa, for public examination on the 13th of November, 2020, at noon.

Reviewers

Adjunct Professor, Dr Mika Huuhtanen
University of Oulu, Faculty of Technology,
Environmental and Chemical Engineering
P.O. Box 8000
FI-90014 University of Oulu
Finland

Dr Jyrki Ristimäki
Royal Caribbean International,
RCL (UK) Ltd.
Telakkakatu 1 P 33,
FI-20101 Turku
Finland

Julkaisija	**Julkaisupäivämäärä**	
Vaasan yliopisto	Lokakuu 2020	
Tekijä(t) Teemu Ovaska	**Julkaisun tyyppi** Artikkeliväitöskirja	
ORCID tunniste orcid.org/0000-0001-6181-8437	**Julkaisusarjan nimi, osan numero** Acta Wasaensia, 451	
Yhteystiedot Vaasan yliopisto Tekniikan ja innovaatiojohtamisen yksikkö Energiatekniikka PL 700 FI-65101 VAASA	**ISBN** 978-952-476-928-0 (painettu) 978-952-476-929-7 (verkkoaineisto)	
	http://urn.fi/URN:ISBN:978-952-476-929-7	
	ISSN 0355-2667 (Acta Wasaensia 451, painettu) 2323-9123 (Acta Wasaensia 451, verkkoaineisto)	
	Sivumäärä 118	**Kieli** Englanti

Julkaisun nimike

Nopea- ja keskinopeakäyntisten dieselmoottorien pakokaasun pienhiukkaslukumäärä uusiutuvia ja kierrätyspolttoaineita käytettäessä

Tiivistelmä

Dieselmoottorien pakokaasun pienhiukkaslukumäärää säädellään maailmanlaajuisesti. Tämän väitöskirjan tavoitteena oli tutkia, miten uusiutuvat ja kierrätyspolttoaineet vaikuttavat nopea- ja keskinopeakäyntisten dieselmoottorien pakokaasun pienhiukkasten lukumäärään. Kierrätyspolttoaineen lisäksi selvitettiin uusiutuvien polttoaineiden sekä polttoaineiden seosten vaikutus. Tulokset perustuvat viiteen tutkimukseen, joissa pienhiukkaslukumäärä mitattiin laboratorio-olosuhteissa kokoalueella 5,6–560 nm.

Sekä kierrätyspolttoaine että uusiutuvan naftan ja fossiilisen polttoaineen seos vähensivät keskinopeassa voimala- ja laivamoottorissa hiukkasten kokonaislukumäärää. Nopeakäyntisessä työkonedieselmoottorissa nämä polttoaineet eivät pienentäneet hiukkasmäärää.

Yhdessä tutkimuksista nopeakäyntisen moottorin hiukkaslukumäärä oli pienin, kun ajettiin vähärikkisellä fossiilisella dieselpolttoaineella. Rypsi- ja soijapohjaiset metyyliesterit tuottivat kuitenkin yleensä vähiten hiukkasia välillä 70–200 nm.

Toisessa tutkimuksessa saman moottorin kokonaishiukkaslukumäärä pieneni, kun seospolttoaineessa puuperäisen uusiutuvan dieselin määrä lisääntyi. Joutokäynnillä seostamaton uusiutuva diesel vähensi pienimpiä hiukkasia merkittävästi.

Työkonemoottorin 500 tunnin pitkäaikaiskokeessa soijametyyliesterin (20 %) ja fossiilisen dieselöljyn seos ei juurikaan lisännyt yli 50 nm hiukkasia, mutta pienempien hiukkasten määrä nousi. Todennäköinen syy oli voiteluöljyssä havaittu kuparin lisääntyminen eikä seospolttoaineen palamiseen liittyvä tekijä.

Kokonaisuudessaan tulokset osoittivat, että uusiutuvien ja kierrätyspolttoaineiden käyttö auttaa vähentämään nopea- ja keskinopeakäyntisten dieselmoottorien pienhiukkasten lukumääräpäästöä niin työkone- kuin voimala- ja laivamoottoreissakin.

Asiasanat

dieselmoottori, pakokaasu, hiukkaslukumäärä, vaihtoehtoiset polttoaineet

Publisher	**Date of publication**	
Vaasan yliopisto	October 2020	
Author(s) Teemu Ovaska	**Type of publication** Doctoral thesis by publication	
ORCID identifier orcid.org/0000-0001-6181-8437	**Name and number of series** Acta Wasaensia, 451	
Contact information University of Vaasa School of Technology and Innovations Energy Technology P.O. Box 700 FI-65101 Vaasa Finland	**ISBN** 978-952-476-928-0 (print) 978-952-476-929-7 (online)	
	http://urn.fi/URN:ISBN:978-952-476-929-7	
	ISSN 0355-2667 (Acta Wasaensia 451, print) 2323-9123 (Acta Wasaensia 451, online)	
	Number of pages 118	**Language** English

Title of publication

Exhaust Particle Numbers of High- and Medium-Speed Diesel Engines with Renewable and Recycled Fuels

Abstract

The number of exhaust particles emitted from non-road diesel engines is regulated worldwide. This dissertation aimed to evaluate how different alternative fuels affect the exhaust particle number in high- and medium-speed engines. The fuels, all originating either from renewable or circular-economy feedstock, were used either neat or as blending components. Five experimental studies were performed in the laboratory, recording particle numbers within the size range of 5.6 to 560 nm.

Circular-economy-based marine gas oil and a blend of renewable naphtha and light fuel oil reduced the exhaust total particle number in a medium-speed engine compared with neat light fuel oil. However, similarly produced marine gas oil and another blend of naphtha and light fuel oil did not lead to particle reductions in a high-speed engine.

In another study with a high-speed engine, low-sulphur fossil diesel produced the lowest total particle number at most loads, while methyl esters of rapeseed and soy bean oil mostly reduced particles within a size range of 70 to 200 nm. In one high-speed engine study, increasing the share of renewable diesel in the fuel blend consistently reduced the exhaust particles. At low idle, neat renewable diesel reduced ultrafine particles significantly.

A blend containing 20 vol.-% soy bean oil methyl ester in fossil diesel fuelled another high-speed engine in a 500-hour endurance test. The number of particles above 50 nm remained almost constant but finer particles increased. The probable reason seemed to be wear-out copper in the lubricant, not combustion degradation.

As a whole, the results showed that alternative fuels originating either from renewable or circular-economy feedstock will not bring penalties in terms of number-based particle emissions in high- or medium-speed non-road engines.

Keywords

diesel engine, exhaust, particle number, alternative fuels

ACKNOWLEDGEMENT

The research work for this doctoral thesis started in 2012. In the autumn of that year, I was hired as a research assistant by Professor Seppo Niemi. My main task was Master´s Thesis work as a part of TREAM project (Trends in real world emissions of diesel and gasoline vehicles) in the former Faculty of Technology in the University of Vaasa. Before completing the thesis work I expressed my interest in the doctoral studies and I was granted the opportunity to study as a doctoral student of technology on 1st of January 2014.

Since then, I have worked as a project researcher and a grant-funded researcher. The research data and the results for the present thesis have been acquired during two company-based projects, in addition to the publicly financed TREAM and Hercules-2 research programs.

I owe my deepest gratitude to Professor Niemi: I could not have had a better supervisor than he. I have been privileged to have had rewarding work under such supportive and appreciative guidance.

I wish also to thank my other supervisor, Dr Jukka Kiijärvi, for his support during this dissertation work. Dr Kiijärvi has given valuable insights, especially relating to consideration of uncertainty during the data analysis. Moreover, numerous other discussions about the world of road cycling with Dr Kiijärvi have had restorative effects on my ability to think.

In addition to my supervisors, I also wish to thank Dr Katriina Sirviö with whom I have had an opportunity to collaborate during all the research projects since 2012. Many fuel-related studies which have been essential for this thesis could not have been possible without Dr Sirviö´s expertise as a chemist and her willingness to share her knowledge so freely.

I have also been privileged to work in a research group full of great colleagues. My thanks go to Mr Olav Nilsson, Dr Petri Välisuo, Mr Thileepan Paulraj, Mrs Michaela Hissa, Mrs Sonja Heikkilä, Mrs Kirsi Spoof-Tuomi, Ms Saana Hautala and Mrs Anne Mäkiranta among others.

I wish to thank the School of Technology and Innovations at the University of Vaasa as well as AGCO Power, Wärtsilä and the Novia University of Applied Sciences. They have provided the equipment, facilities and working time necessary for the experiments and publishing the research. Moreover, I am thankful to all the co-authors of the five scientific papers that underpin this thesis.

The experimental research and dissertation work have been funded by the European Union, Business Finland (former Tekes), Vaasa University Foundation and Henry Ford Foundation. I was awarded a personal grant by Vaasa University Foundation in the 2018–19 semester for dissertation work. In 2014, I was awarded a personal scholarship by Henry Ford Foundation for postgraduate studies, and another in 2019, for finishing this doctoral thesis. I am much obliged for its financial support.

Alongside my university studies, since 2010 Mr Janne Suomela, Mr Tomi Vaappo, Mr Juho Aitonurmi and Mr Nicolas Remy have influenced me as a person in many ways by being my great friends. What is more, without the research work at the university, I could not have had the chance to get to know such outstanding people as Mr Teemu Närvä and Mr Harri Lehtinen and his family. Thanks to you all.

My family has been the catalyst that allows me to demonstrate my capabilities, so I am very grateful to my caring parents Erkki and Merja, who have always encouraged me to study. They did not have the opportunity for advanced study, whereas I and my elder siblings have always had that option. My sister Minna and my brother Kimmo have been excellent role models for me.

Finally, something had been missing among the finest flavours of life until the 1st of May 2014. Since then, for almost as long as I have been working towards this thesis, I have also learnt the lessons of first real love. Thus, I wish to express my special gratitude to Elisa for her continuous love and support.

Contents

Figures

Tables

Symbols and abbreviations

D_p	particle diameter
$dN/dlogD_p$	normalised particle number concentration (1/cm^3)
N	particle number concentration (1/cm^3)

CI	compression ignition
CTO	crude tall oil
DFO	diesel fuel oil
EEPS	engine exhaust particle sizer
EU	European Union
FAME	fatty acid methyl ester
ICE	internal combustion engine
ISO	International Standard Organization

LFO	light fuel oil
MGO	marine gas oil
NRMM	non-road mobile machinery
NRSC	Non-Road Steady Cycle
PM	particulate matter
$PM_{2.5}$	ambient air borne particles which have a diameter up to 2.5 microns
PM_{10}	ambient air borne particles which have a diameter up to 10 microns
PN	particle number
PSD	particle size distribution
RDOA	renewable diesel fuel oil derived from waste fat, residues or vegetable oils
RDOB	renewable diesel fuel oil derived from crude tall oil
RDOB10	10 vol.-% crude tall oil derived renewable diesel-90 vol.-% fossil diesel fuel blend
RDOB20	20 vol.-% crude tall oil derived renewable diesel-80 vol.-% fossil diesel fuel blend
RDOB50	50 vol.-% crude tall oil derived renewable diesel-50 vol.-% Fossil diesel fuel blend
RDOB100	100 vol.-% crude tall oil derived renewable diesel (same as RDOB)
RME	rapeseed methyl ester
SME	soy bean oil methyl ester
TPN	total particle number
VEBIC	Vaasa Energy Business Innovation Centre
WHO	World Health Organization

Publications

This doctoral dissertation consists of the following five publications, referred to in the text by their Roman numerals:

I. Ovaska, Teemu; Niemi, Seppo; Sirviö, Katriina; Nilsson, Olav. 2019. Exhaust Particle Number of a Non-Road Diesel Engine Fuelled by Methyl Esters with Different Fatty Acid Compositions. *Agronomy Research*, volume 17, issue Special Issue 1, pages 1165–1180. ISSN: 1406-894X.

II. Ovaska, Teemu; Niemi, Seppo; Katila, Tapani; Nilsson, Olav. 2018. Exhaust Particle Size Distributions of a Non-Road Diesel Engine in an Endurance Test. *Agronomy Research*, volume 16, issue Special Issue 1, pages 1159–1168. ISSN: 1406-894X.

III. Niemi, Seppo; Vauhkonen, Ville; Mannonen, Sari; Ovaska, Teemu; Nilsson, Olav; Sirviö, Katriina; Heikkilä, Sonja; Kiijärvi, Jukka. 2016. Effects of Wood-Based Renewable Diesel Fuel Blends on the Performance and Emissions of a Non-Road Diesel Engine. *Fuel*, volume 186, pages 1–10. ISSN: 0016-2361.

IV. Ovaska, Teemu; Niemi, Seppo; Sirviö, Katriina; Nilsson, Olav; Portin, Kaj; Asplund, Tomas. 2019. Effects of Alternative Marine Diesel Fuels on the Exhaust Particle Size Distributions of an Off-Road Diesel Engine. *Applied Thermal Engineering*, volume 150, pages 1168–1176. ISSN: 1359-4311.

V. Ovaska, Teemu; Niemi, Seppo; Sirviö, Katriina; Heikkilä, Sonja; Portin, Kaj; Asplund, Tomas. 2019. Effect of Alternative Liquid Fuels on the Exhaust Particle Size Distributions of a Medium-Speed Diesel Engine. *Energies*, volume 12, page 2050. ISSN: 1996-1073.

Author´s contribution

Paper I: Ovaska is the main author. Ovaska, Nilsson and Sirviö implemented the engine experiments. Sirviö performed the laboratory analyses. Ovaska analysed the emission data and visualised the results. Ovaska and Niemi wrote the paper.

Paper II: Ovaska is the main author. The research was within a wider context of engine experiments designed by Katila and Niemi. Nilsson and Ovaska carried out the engine experiments. Ovaska analysed the emission data and visualised the results. Ovaska and Niemi wrote the paper.

Paper III: Ovaska is the co-author. The research was part of a wider range of engine experiments designed by Vauhkonen, Mannonen and Niemi. Nilsson, Sirviö, Ovaska and Heikkilä conducted the engine experiments. Ovaska analysed the emission data and visualised the results. Niemi wrote the paper. Kiijärvi was responsible for the layout of the paper.

Paper IV: Ovaska is the main author. The research formed part of a series of engine experiments designed by Portin, Asplund and Niemi. Nilsson, Ovaska and Sirviö conducted the engine experiments. Ovaska and Niemi wrote the paper.

Paper V: Ovaska is the main author. The research was part of a wider range of engine experiments designed by Portin, Asplund and Niemi. Ovaska, Sirviö and Heikkilä carried out the engine experiments. Ovaska and Niemi wrote the paper.

1 INTRODUCTION

Human beings need oxygen to keep their vital organs working. The oxygen comes from breathing-in ambient air. Unpolluted air is favourable for human health (Apte et al. 2018; Heft-Neal et al. 2018; Im et al. 2018). According to the global ambient air quality database published by the World Health Organization (WHO), the air is polluted for nine out of 10 people around the world (WHO 2019). WHO estimated that each year seven million lives are exposed to potentially fatal diseases as a consequence of breathing polluted air that contains fine particles (WHO 2018). The fatal effects of polluted air can be avoided by improving ambient air quality i.e. reducing the annual mean concentrations of fine particulate matter (PM_{10} and $PM_{2.5}$) in the air. $PM_{2.5}$ refers to ambient airborne particles that have a diameter of up to 2.5 microns, PM_{10} particles have a diameter of up to 10 microns. Fatal effects of particles on human health are usually associated with the concentrations of $PM_{2.5}$ or PM_{10} in the ambient air (Oberdörster, Oberdörster & Oberdörster 2005; Janssen et al. 2011). There is special concern for the smallest particles, as they readily deposit into the respiratory system and may penetrate into the cardiovascular and even cerebrovascular system via respiratory organs. (Anderson, Thundiyil & Stolbach 2012; Oravisjärvi et al. 2014).

Road traffic is the main source of $PM_{2.5}$ in urban ambient air globally. Out of the total contribution to the concentration of $PM_{2.5}$, road traffic accounts for 25%; combustion and agriculture 22%; domestic fuel burning 20%; natural soil dust and sea salt 18%; and industrial activities 15%. (Karagulian et al. 2015). Road traffic-related PM originates mainly from the combustion of liquid fuels that are burned incompletely inside vehicles´ internal combustion engines (ICE). Additionally, compression ignition (CI) engines are widely used for other purposes unrelated to conventional traffic, such as generating power for non-road vehicles or providing electricity in stationary applications. (Mollenhauer & Tschöke 2010).

As is widely known, PM arising from the use of non-road vehicles or power generation can be effectively reduced by using natural gas as the main fuel (Burel, Taccani & Zuliani 2012; Andresson, Salo & Fridell 2015; Srinivasan et al. 2019). However, the need for new liquid fuels and fuel blends will remain over the next few decades (Kalghatgi, 2018). Before the introduction of new fuels or fuel blends, they need to be assessed for compatibility with combustion engines and engine systems (Florentinus et al. 2012; Sirviö et al. 2016; Sirviö et al. 2019).

Non-road PM emissions are regulated worldwide. Engine manufacturers have to satisfy the relevant local emission limits in order to sell their products. Moreover,

fuel and lubricating oil refiners, plus the end-users of the engines and oil products, must also comply with the local emission legislation. The particle number (PN) emission from non-road mobile machinery (NRMM) has been regulated in the EU since 2019 (EU Regulation 2016/1628).

The main goal of this thesis was to investigate and evaluate how different alternative fuels, originating either from renewable or circular-economy feedstock, affect the exhaust PN in non-road diesel engines. In particular, PN describes the fatality and adverse effects of exhaust fine particles more precisely than particulate mass. PN was therefore selected as the main measure for the detrimental effects of exhaust particulates. A total of seven alternative fuels were studied. They were two renewable diesels from different feedstocks (RDOA, RDOB); circular-economy-based marine gas oil (MGO); a blend of renewable naphtha and marine light fuel oil (LFO); rapeseed methyl ester (RME); soy bean oil methyl ester (SME); and a blend of SME and low-sulphur fossil diesel fuel oil (DFO). Two fossil diesels, DFO and LFO, were used as baseline fuels. The selection of fuels was based on the needs of corporate partners and on the availability of fuels.

Five experimental studies were carried out to achieve the thesis´ main goal. All research was performed in the School of Technology and Innovations at the University of Vaasa.

This dissertation produces new scientific conclusions about the effects of alternative fuels on the exhaust particle numbers in non-road diesel engines. Engine manufacturers, fuel producers and refiners in particular, as well as authorities, can utilise the conclusions. The dissertation´s principle novelty is its evaluation of completely new alternative fuels, such as circular-economy-based MGO and renewable naphtha. This includes their comparison with other renewable fuels and commercial low-sulphur fossil fuels.

This thesis consists of five research papers in which the results were originally presented.

The effects of current alternative fuels on the exhaust PN are not yet sufficiently clear. In Paper I, "*Exhaust Particle Number of a Non-Road Diesel Engine Fuelled by Methyl Esters with Different Fatty Acid Compositions*," the main aim was to find out how different methyl esters affect exhaust PN. The non-road diesel engine was also fuelled with RDOA, produced from waste fats, residues or vegetable oils.

Of particular relevance to end-users is long-term adherence to PN limits when a non-road engine is fuelled by a blend. In Paper II, "*Exhaust Particle Size Distributions of a Non-Road Diesel Engine in an Endurance Test*," the main

objective was to investigate exhaust PN from a high-speed non-road diesel engine subjected to a 500-hour running period when the engine is fuelled by a blend of SME and DFO.

Paper III was entitled "*Effects of Wood-Based Renewable Diesel Fuel Blends on the Performance and Emissions of a Non-Road Diesel Engine*." One of this study´s goals was to clarify how blending RDOB derived from crude tall oil (CTO) with DFO affects the exhaust PN of a non-road diesel engine. This paper set out to provide valuable information about the use of innovative renewable diesel and its blends in a modern non-road diesel engine.

More extensive use of renewable energy sources includes the introduction of novel liquid fuel types. In Paper IV, "*Effects of Alternative Marine Diesel Fuels on the Exhaust Particle Size Distributions of an Off-Road Diesel Engine,*" the main aim was to investigate how seldom-used alternative fuels affect the exhaust PN. Circular- economy-based MGO and a blend of renewable naphtha and marine LFO have hitherto received little attention. The fuels were intended for marine applications and the study was the first stage of a large marine fuel research project (see Paper V).

In Paper V, "*Effect of Alternative Liquid Fuels on the Exhaust Particle Size Distributions of a Medium-Speed Diesel Engine,*" the main objective was to establish how circular-economy-based MGO and naphtha-LFO blend affect exhaust PN in a medium-speed engine. The novelty of this paper was the use of these fuels in a marine diesel engine. The study was the second stage of the large marine fuel research project.

Kerosene also was one of the fuels studied in Papers IV and V. However, kerosene was not included in this dissertation because it is a conventional fossil fuel, not based on feedstocks that are renewable or part of a circular economy.

2 BACKGROUND

High-speed CI engines are widely used in mobile land-use applications whereas medium-speed CI engines are largely used for electrical power generation on land and at sea. In addition to base load and peak-shaving in power generation, combustion engines are used to stabilise the electricity grid in the event of sudden peak power demands if the energy production is largely based on renewable sources. CI engines have been the main choice for a long time in ships. Regardless of an engine application, harmful pollutant emissions may be generated by combustion of either liquid or gaseous fuel in the engine cylinders. However, gaseous and particulate emissions are tightly regulated worldwide to inhibit the effects of pollutants on ambient air quality, human health and climate change. Pollutants can be reduced by several means including selection of fuels, a large number of in-cylinder methods, and exhaust after-treatment. The present study decided on finding out how renewable and circular-economy-based fuels affect the reduction of harmful particulates.

2.1 Exhaust particles

Diesel engine exhaust particles often conform to a size distribution which has two distinctive particle modes; nucleation mode and accumulation mode. The mean diameters of particles in nucleation mode are less than 50 nm, whereas the mean diameter range in accumulation mode is 50–500 nm (Kittelson 1998; Rönkkö et al. 2006; Rönkkö et al. 2007; Filippo & Maricq 2008; Lähde et al. 2010; Heywood 2018).

Initiation of particle nucleation is a very complex process, still not fully understood (Heywood 2018). Some researchers assume that sulphur promotes the initiation (Vaaraslahti et al. 2004; Arnold et al. 2006; Giechaskiel et al. 2007; Rönkkö et al. 2007; Biswas et al. 2008). Initiation is followed by particle formation. Nucleation mode particles are believed to form during dilution as exhaust gas mixes with ambient air.

Accumulation mode is thought to consist mainly of the agglomerated carbon soot particles which result from the incomplete burning of either the fuel or the lubricating oil remnants inside the cylinder (Kittelson, Arnold & Watts 1999; Rönkkö et al. 2007; Nousiainen et al. 2013). Moreover, black carbon is the fraction of the agglomerated carbon soot particles that actively absorbs the visible light (Petzold et al. 2013; Maricq 2014; Timonen et al. 2019). Combustion air and material breakdown from engine components are also sources of particles in diesel exhaust gas (Mason et al. 2016).

The maximum PN limits are specified in the EU Stage V standard of the NRMM regulations. This standard applies to land-based mobile machines; items of transportable industrial equipment (or vehicles); stationary engines of generating sets of above 560 kW; and inland waterway vessels. The EU Stage V standard is phased into effect in 2019–2020.

2.2 Effects of fuel properties on exhaust particle numbers

The physical properties of liquid fuel tend to control its spray characteristics, while the fuel´s composition determines the pathways of chemical reactions during combustion (Eastwood 2008). Particle formation with low-sulphur fuels is influenced by fuel characteristics such as its density (Szybist et al. 2007; Bach, Tschöke & Simon 2009), viscosity (Mathis et al. 2005; Tsolakis 2006), cetane number (Li et al. 2014; Alrefaai et al. 2018) and the fuel´s water content (Samec et al. 2002). The fuel´s aromatic content acts as a precursor of particulates during the combustion (Ntziachristos et al. 2000, Tree & Svensson 2007, Zetterdahl et al. 2017). Nevertheless, researchers have obtained divergent results about the effect of fuel aromatic content on PM emission (Bach, Tschöke & Simon, 2009).

Earlier studies have reported how fatty acid methyl esters (FAMEs), either as neat or as blending components, reduced the number of accumulation mode particles (Jung et al. 2006; Heikkilä et al. 2009; Rounce et al. 2012; Sun et al. 2019). However, Sun et al. (2019) reported that the exhaust PN of a turbocharged CI engine increased under the size category of 22 nm with increasing RME content in the fuel blend. PN above 22 nm decreased compared to petroleum diesel. Nyström et al. (2016) detected a lower PN around the peak size values of 75–116 nm when a high-speed, non-road diesel engine was fuelled with RME instead of low-sulphur diesel. In the study of Hellier et al. (2019), waste date pit methyl ester led to a reduction in PN within the size range of 100 to 200 nm compared to petroleum diesel. However, they did not detect a corresponding PN reduction with RME or SME. Even though many researchers report on the reducing effect of FAMEs on accumulation-mode particles, the mechanism and results are not unambiguous but seem to depend on several factors.

Zhu et al. (2016) investigated three different FAME fuels, based on rapeseed oil, soy bean oil and palm oil. They concluded that palm oil methyl ester increased the nucleation mode PN but decreased the accumulation mode PN. The researchers (Zhu et al. 2016) discussed whether the presented PN result could have been influenced by a lower fraction of unsaturated molecules and shorter carbon chain

length in palm oil methyl ester than those in RME and SME. According to a study by Pinzi et al. (2013), the oxygen content in the FAME molecule structure controls PM formation, which depends quantitatively on the carbon chain length of the molecule. Barrientos et al. (2015) expressed the view that reactivity of soot particles, e.g. their ability to oxidise, was affected by the chain length and the type and location of carbon-carbon bond. Wang et al. (2016b) also found that the smaller the fraction of unsaturated fatty acids, the lower the soot particle precursors from FAME fuel combustion.

Ushakov & Lefebvre (2019) assessed RDOA´s use as an alternative marine fuel. Within the measured size range of 14–750 nm, the total particle number (TPN) was 30% higher for RDOA compared to low-sulphur MGO. There are only a few published studies concerning CTO-derived RDOB´s effect on PN emissions of a CI engine. Therefore, Papers III and IV of the present study provide valuable additional knowledge about the effects of this renewable diesel.

Nabi et al. (2012) investigated total concentrations of fine particles of up to 10 000 nm with a high-speed marine engine. The engine was fuelled by MGO and also by diesel fuel with sulphur contents of 50 and 10 mg/kg respectively. The results showed that TPN was lower with diesel fuel than with MGO. This study also measured particle mass emissions. The authors stated that the lower PM for diesel probably resulted from fuel properties such as sulphur content, density, viscosity and carbon-to-hydrogen ratio, all of which were lower for diesel than for MGO.

Consequently, fuels clearly affect the PN emissions of CI engines. Therefore, additional knowledge of those effects is essential when adopting new fuel options. Compliance with the prevailing particle emission legislation has to be ensured before the introduction of novel liquid fuels. The increasingly stringent limits of future emissions legislation mean this information is always in demand by engine manufacturers, fuel producers and refiners, as well as end users. This dissertation aims to increasing information about the effects of alternative fuels on exhaust particle numbers from non-road diesel engines. Moreover, the research primarily focused on the type of renewable and recycled fuels that will become necessary.

3 MATERIALS AND METHODS

The experimental measurements were performed by the University of Vaasa at the ICE laboratories of the Technobothnia Research Centre and Vaasa Energy Business Innovation Centre (VEBIC) in Vaasa, Finland.

3.1 Engines

The research was conducted by using three different engines at laboratory conditions. Table 1 lists the engines´ main specifications. All the experimental engines were in service at the laboratory. Maximum torques quoted are measured values obtained with commercial low-sulphur DFO in Papers I, III and IV. In Paper II, the maximum torques are those obtained when the fuel consisted of 20 vol.-% SME and 80 vol.-% DFO.

Table 1. The specifications of the experimental engines.

Paper	I, III, IV	II	V
Cylinder number	4	4	4
Bore (mm)	108	108	200
Stroke (mm)	120	134	280
Swept volume (dm^3)	4.4	4.9	35.2
Rated speed (rpm)	2200	2100	1000
Rated power (kW)	101	103	
Maximum torque at rated speed (Nm)	455	462	
Maximum torque at 1500 rpm (Nm)	583	583	
Selected maximum alternator power output at 1000 rpm (kW)			600

The engines used in Papers I–IV were high-speed, non-road diesel engines. Paper V´s was a medium-speed diesel engine. All engines had a common-rail fuel injection system. The engines were not equipped with exhaust aftertreatment systems, except in Paper II, in which a diesel oxidation catalyst and a urea-based

selective catalyst reactor were incorporated into the exhaust pipe. No engine parameter optimisation was applied during the experiments.

An eddy-current dynamometer (Horiba WT300) was used to load the high-speed engines for Papers I–IV. The medium-speed engine in Paper V was loaded by an ABB alternator.

3.2 Fuels

The selection of fuels was based on the needs of corporate partners and on the availability of fuels. Table 2 lists the properties of the investigated fuels. The properties were analysed by the fuel laboratory of the University of Vaasa if not otherwise mentioned in Table 2. The reference fuel used for Papers I and III was DFO which conformed to the EN 590 fuel standard (SFS-EN 590:2013). The same DFO was a constituent part of the fuel blend in Paper II.

In Paper I, the aim was to evaluate how different methyl esters affect the exhaust PNs. A high-speed, non-road diesel engine was fuelled in turn by four different fuels: RME, SME, RDOA and the reference DFO. RME and SME fulfilled the requirements of EN 14214 fuel standard (EN 14214:2012+A1:2014). The RDOA´s feedstock consisted of waste fats, residues or vegetable oils. The RDOA was originally referred to as HVO in Paper I.

In Paper II, the objective was to investigate exhaust PN from a high-speed non-road diesel engine subjected to a 500-hour running period when the engine is fuelled by a blend of 20 vol.-% SME and 80 vol.-% DFO. The length of the running period corresponds to the oil change interval of the studied non-road engine.

In Paper III, one of the goals was to clarify how blending CTO-derived RDOB with DFO affects the exhaust PN of the non-road engine. Blends containing 10, 20, and 50 vol.-% of RDOB were studied, described in this dissertation as RDOB10, RDOB20 and RDOB50, respectively. Additionally, the engine was also operated with neat RDOB (RDOB100). In Paper III, the blends were originally referred to as HB10, HB20 and HB50, and neat RDOB as HB100. The baseline fuel was DFO. Small shares of 10 and 20% are realistic in practical commercial applications while the stronger blend and neat option extended the range to show trends about the effects of renewable diesel.

In Paper IV, the aim was evaluate how various alternative fuels affect the exhaust PN when used in a high-speed diesel engine. The investigated alternative fuels were circular-economy-based MGO, RME, CTO-derived RDOB and a

Table 2. Properties of studied fuels in Papers I and III–V.

		Kinematic viscosity, mm^2/s (40 °C)	Density, kg/m^3 (15 °C)	Cetane number	Sulphur content, mg/kg	Water, mg/kg	Carbon, wt. %	Hydrogen, wt. %
Fuel	Paper	EN ISO 3104/ ASTM D7042 [a] Fuel supplier´s info	EN ISO 12185/ ASTM D7042	EN 15195/ [b] ASTM D6890	EN ISO 20884/ EN ISO 2084 [c] ASTM D7039	EN ISO 2937	ASTM D5291	ASTM D5291
DFO	I.	-	834	-	3.6	-	-	-
RME		4.5[a]	883	54[b]	<2[c]	132	77.4	12.2
SME		4.1[a]	885	47[b]	3[c]	353	77	11.9
RDOA		2.9[a]	779	75[b]	<1	19	84.2	15.1
DFO	III.	3.0[a]	841[a]	59[a]	8[a]	30[a]		
RDOB10		3.0[a]	839[a]	60[a]	7[a]	<30[a]		
RDOB20		3.1[a]	835[a]	61[a]	6[a]	<30[a]		
RDOB50		3.2[a]	828[a]	65[a]	4.6[a]	<30[a]		
RDOB100		3.5[a]	814[a]	65[a]	<1[a]	<30[a]		
LFO	IV.	1.84	827	52	8.3			
MGO		7.69	843	68	<100			
RME		4.49	883	53	<5			
RDOB		3.5	813	65	<5			
Naphtha-LFO		1.37	805	51	6.8			
LFO	V.	3.1	836	58	6		84.5	13.4
MGO		3.7	838	54	30		84.8	13.7
Naphtha-LFO		1.8	810	52	4.5		85	13.8

20/80 vol.-% blend of renewable naphtha and LFO. The baseline fuel was low-sulphur marine LFO.

In Paper V, the objective was to establish how alternative fuels affect the exhaust PN when used in a medium-speed diesel engine. The engine was fuelled by circular-economy-based MGO, but now with different properties from those of the MGO used in Paper IV. The second alternative fuel tested was a 26/74 vol.-% blend of renewable naphtha and LFO. The baseline fuel was LFO.

3.3 Measurement of particle numbers

PN of raw exhaust gas was measured by using an engine exhaust particle sizer (EEPS 3090, TSI Inc.). It measures the particles in a size range of 5.6 to 560 nm. The term TPN in this dissertation refers to all particles that were detectable by using the EEPS device. Mobility particle size spectrometers, such as EEPS, have been found to be most accurate when measuring particle numbers within the size range of 20–200 nm (Wiedensohler et al. 2012). Greater uncertainties may exist outside this size range, as described by Wiedensohler et al. (2018).

The EEPS classifies particles based on their differential electrical mobility. The particles in the incoming sample are charged negatively by a first charger. Thus, the number of highly positive charged particles is reduced and overcharging of the second charger is prevented. The particles are then charged positively by the second charger. Each particle carries a charge that relates to its size. Positively charged particles are led into the central column which contains a central rod with a high voltage. The rod´s electrical field repels the particles radially outward to 22 electrically isolated electrometers on the outer wall of the column. Large particles are detected near the bottom of the column while smaller particles are higher up. When a particle hits an electrometer, the resultant electrical current is measured. The currents from the 22 electrometers are interpreted as the concentration of PN and converted into 32 size channels of output by using a data inversion algorithm. The noise level of the EEPS electrometers may increase as they become dirty. Thus, determination of zero current values for the electrometers is recommended in order to compensate as the noise level increase. (TSI 2009). These zero current values were determined in all measurements performed for the papers.

The determination of the exhaust PN requires dilution of the sample. The EEPS measures PN from the partial exhaust flow. During the research work, the sample was processed to meet the requirements set for EEPS inlet aerosol, including inlet sample flow rate, temperature and dilution.

In Paper I, the exhaust gas sample was diluted at two stages. First, the sample was diluted with ambient air by means of a porous tube diluter. Then, the sample was led through secondary dilution, performed with a Dekati ejector diluter. The overall dilution ratio was determined by simultaneously measuring carbon dioxide concentration before and after the dilution stages. The total dilution ratio varied from 118:1 to 286:1.

In all the other papers, the exhaust sample was first diluted with ambient air by means of a rotating disc diluter (model MD19-E3, Matter Engineering AG, currently Testo AG). This used a constant 60:1 dilution ratio during the measurements. The dilution air was kept at 150 °C in order to control the presumed drop in the temperature from raw sample state to the diluted sample state. Control of the dilution air temperature targeted to prevent condensation of any vapours in the exhaust sample during the first dilution (Testo 2016). The diluted sample (5 dm^3/min) was further diluted by purified air with a dilution ratio of 2:1, giving an overall dilution ratio of 120:1.

During every study (Papers I–V), the PN was recorded once, for a period of three minutes. The stability of the PN level during recording was checked to ensure reliable results.

3.4 Engine running procedures

Standardised ICE running procedures ensure that similar conditions of engine operation are used during the measurements. They also enable comparison of the results with other experiments and legislative limits. The standardised procedures define the engine speeds and loads to be used in the parameter recordings. In Papers I, III and IV, the load points selected for the high-speed engine were based on the eight-mode C1 driving cycle of the ISO 8178 standard. The C1 steady state cycle is known as the non-road steady cycle (NRSC), shown in Table 3. The intermediate speed was chosen to be 1500 rpm.

With each fuel, the same engine torques were used in each study. At each speed, the maximum torque selected for Paper I was 90% of the full load torque. This allowed the test engine to always run at the same loads, irrespective of the studied fuel. The same torque values were used in Paper III. In Paper IV, each maximum torque was 80% of the full load torque, and the engine was also run at 25% load at intermediate speed. The maximum torque values were lower than full load values to ensure the whole cycle could run with all fuels.

Table 3. Experimental matrix with high-speed engine in Papers I, III and IV.

Point	1	2	3	4	5	6	7	8
Speed	Rated				Intermediate			Idle
Load (%)	100	75	50	10	100	75	50	0
Torques in Papers I, III (Nm)	410	308	205	41	525	394	263	0
Torque in Paper IV (Nm)	351	263	176	35	450	338	225	0
Weighting factor	0.15	0.15	0.15	0.10	0.10	0.10	0.10	0.15

In Paper II, the total engine running time was 500 hours. Before starting the running period, PN measurements were performed with the new engine installation. Thereafter, the engine was operated each day according to a defined running procedure, consisting of sequential load points chosen to represent typical actual engine use as accurately as possible. Table 4 sets out the daily running cycle. The PN measurements performed with the new engine were repeated after 250 hours of engine operation, and again after 500 hours.

In Paper V, the maximum electrical power from the alternator used to load the engine was set at 600 kW, at a fixed engine-speed of 1000 rpm. The output was measured as net electrical power downstream of the frequency converter used to control the engine-driven generator set. Measurements were also taken at partial electric loads of 450, 300, 150 and 60 kW. These load points were selected according to the D2 test cycle of the ISO 8178-4 standard.

At the beginning of each measurement day, the zero current values for the EEPS electrodes were determined in order to avoid the increase in the EEPS noise level. This procedure entailed running the EEPS for 60 seconds with a high-efficiency particulate air filter on the inlet. Additionally, for the high-speed engines (Papers I–IV), the intake air temperature was adjusted to 50 °C downstream of the charge-air cooler at the selected maximum torque at rated speed. The temperature was controlled manually by regulating cooling water flow to the heat exchanger. After this initial adjustment, the temperature was allowed to freely change with engine load and speed.

Table 4. Daily cycle between measurements in Paper II.

Point	Speed (rpm)	Load (%)	Torque (Nm)	Duration (min)
1	1000	0	0	15
2	1300	14	75	15
3	1600	21	123	15
4	1800	29	175	30
5	2000	40	214	15
6	2100	51	236	15
7	1900	60	346	15
8	1700	49	293	15
9	1500	30	175	30
10	1200	25	127	15

To ensure reliable results, the engines were always allowed to stabilise at each load point before PN recordings were taken. The criteria for this were stable temperatures of coolant water, intake air and exhaust.

3.5 Processing of particle number data

The EEPS data inversion algorithm involves an instrument matrix that is used for the representation of the relationship between particle diameters and electrometer currents. Studies have shown that the original instrument matrix of EEPS (IM-2004) is not capable of estimating the geometric mean diameters of diesel exhaust particles in a way that agrees with other commercial devices for measuring PN within the comparable size range (e.g. Zimmerman et al. 2014; Quiros et al. 2015). Thus, TSI Inc. developed a new instrument matrix for engine exhaust particles (IM-Soot) in order to improve EEPS accuracy (Wang et al. 2016a). Apart from the results presented in Paper III, the IM-Soot data inversion algorithm was used to process the PN data. In the original Paper III, the IM-2004 data inversion algorithm was applied, but for this dissertation, Paper III´s results were reanalysed using the new instrument matrix IM-Soot.

Processing of PN data for this dissertation differed from that of the original papers. In all this dissertation´s papers, the PN results presented were based on three-minute stable time periods. The averaging interval of two seconds was used. For Papers I, IV and V, the three-minute PN recordings were split up into three one-minute recordings. The uncertainty of the PN measurement was approximated by calculating the standard deviation of the PN averages, taken from each one-minute recording. For Papers II and III, in contrast, the full three-minute recordings were used without any division. The uncertainty of the PN measurement was not presented.

For this dissertation, the TPN in the size range of 5.6 to 560 nm was calculated from the original PN recordings, each of which was three minutes long. The PN concentrations of the 32 size resolution channels in the EEPS spectrometer output were added up at the time intervals of 0.1 s in order to calculate TPN. The time interval of 0.1 s corresponds to the time resolution capability of EEPS.

The TPN results represent the calculated three-minute averages of PN sums. Moreover, the averages of the normalised PN concentrations were calculated from each size resolution channel ($dN/dlogD_p$, where N is particle concentration and D_p the mobility diameter of a particle). The averages of the calculated TPN and of the normalised PN concentrations were multiplied by the overall dilution ratio of the exhaust sample, thus translating the values into corresponding concentrations in the raw exhaust.

With regard to the EEPS output´s size channels, the first 10 channels represent particle geometric mean sizes from 6.0 to 22.1 nm. The data analysis includes a calculation of PN sum of these first 10 size channels as a proportion of TPN from all 32 size channels. This calculation was used to approximate the PN split between nucleation and accumulation modes of TPN.

4 RESULTS

This chapter revises the exhaust TPN results from each study (Papers I–V) in which renewable or recycled fuels fuelled either high- or medium-speed diesel engines.

Differences in TPN were detected within the studied fuel sets of Papers I, III, IV and V, as well as during the 500-hour endurance test (Paper II). With the exception of Paper V´s tests, nucleation mode particles accounted for the greater proportion of the detected TPN. Within this mode, the distinct PN differences between fuels were mostly detected around the size category of 10 nm.

4.1 High-speed engine with methyl esters and renewable diesel

Paper I´s aim was to assess how different methyl esters affect the exhaust PN. Along with DFO and RDOA, the studied fuels were methyl esters RME and SME. Figure 1 shows the TPN at rated speed. Each bar represents the mean value of TPN, with standard deviation depicted as error bars. As at rated speed, the studied fuels also produced distinctly different TPN emissions at all other load points of the NRSC.

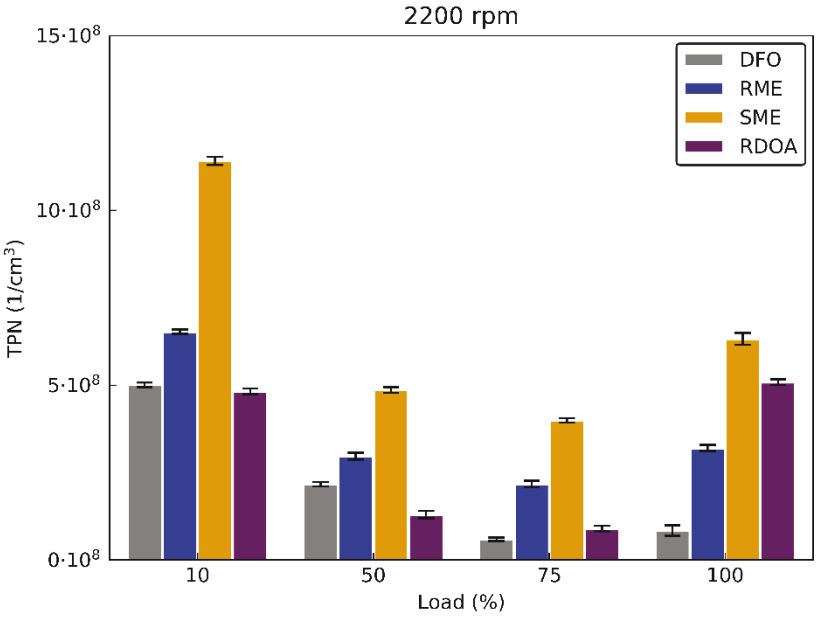

Figure 1. The effect of methyl esters and RDOA on exhaust TPN at rated speed.

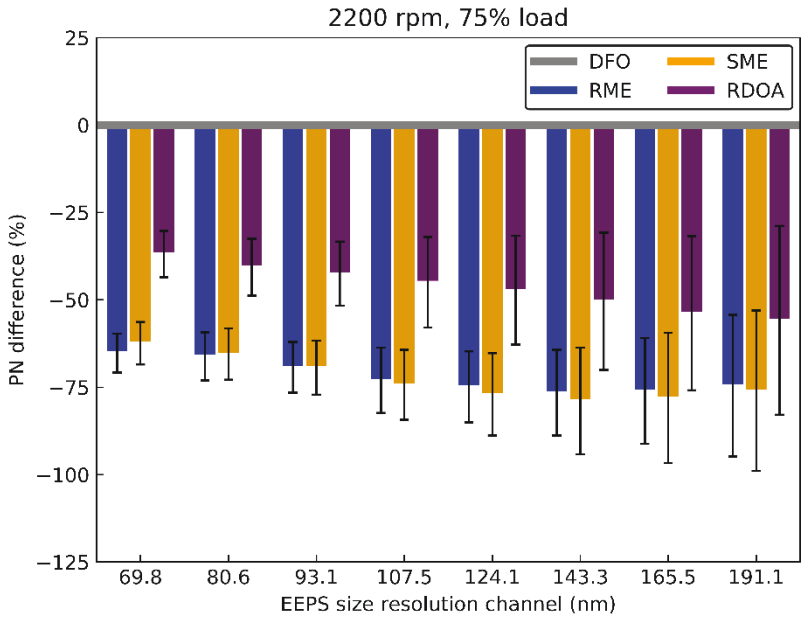

Figure 2. The effect of methyl esters and RDOA on exhaust PN within the size range of 70 to 200 nm at 75% of rated speed. PN with DFO forms the zero line.

The lowest TPN was mostly detected with baseline DFO and the highest with SME. Figure 2, however, illustrates how methyl esters significantly reduced PN (by 62 to 78%) within the size range of 70 to 200 nm at 75% load at rated speed. A similar trend was detected at several load points. RDOA also was beneficial in this size range, relative to DFO. However, methyl esters were not observed to reduce PN emission outside the size range of 70 to 200 nm.

4.2 Endurance test of high-speed engine with a methyl ester blend

In Paper II, the objective was to investigate how a 500-hour running period affects the exhaust PN of a high-speed, non-road diesel engine when fuelled by a 20/80 vol.-% blend of SME and DFO. Figure 3 illustrates the TPN results at two loads at intermediate speed. The TPN increased clearly with running hours. It also increased distinctly between initial and final measurements at every other load point. The TPN was affected by the considerable increase of PN within an approximate size range of 7 to 30 nm. In contrast, no notable differences were, observed in PN of above 50 nm during the 500-hour period. Analysis showed that copper concentration in the lubricating oil increased considerably (from 49 to

420 ppm) between the running hours of 357 and 553. The increase in TPN with running hours was assumed to be caused by the copper particles, not by the effects of SME in the fuel blend.

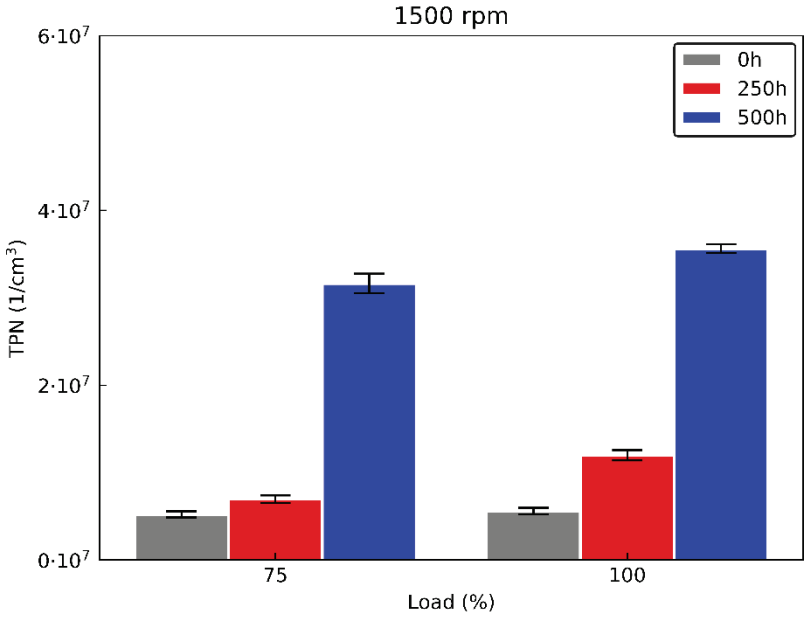

Figure 3. The effect of a 500-hour running period on exhaust TPN at intermediate speed.

4.3 High-speed engine with blends of wood-based renewable diesel fuel

One of the goals of Paper III was to evaluate how blending CTO-derived RDOB with DFO affects the exhaust PN of a non-road diesel engine. The studied blends contained 10, 20, and 50 vol.-% of RDOB, termed RDOB10, RDOB20 and RDOB50, respectively. The two neat constituents, DFO and neat RDOB (RDOB100), were also tested. Figure 4 shows the effects of the various fuels on the exhaust particle size distribution (PSD) at low idle. The averages of the normalised PN concentrations are represented as data points which are connected by lines. The shaded area illustrates the size of standard deviation. As shown, neat RDOB gave a clear PN reduction at a particle size category of 10 nm. However, no equally coherent trend was observed in the PSDs at other engine loads. Nevertheless, RDOB improved the TPN performance. Figure 5 depicts the weighted TPN emissions over the C1 driving cycle of the ISO 8178 standard. Throughout the entire test cycle, the TPN emissions decreased with increasing share of renewable

diesel. Fuelling with RDOB100 produced a TPN reduction of 33% compared with fossil DFO. With RDOB10, the TPN decreased by approximately 8%.

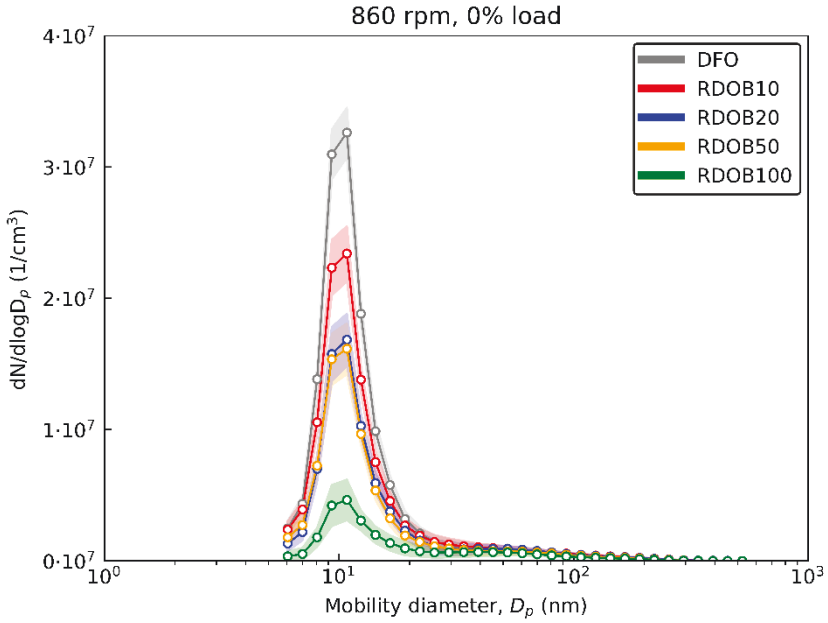

Figure 4. The effect of CTO-derived RDOB fuel blends on the exhaust PSD emission at low idle.

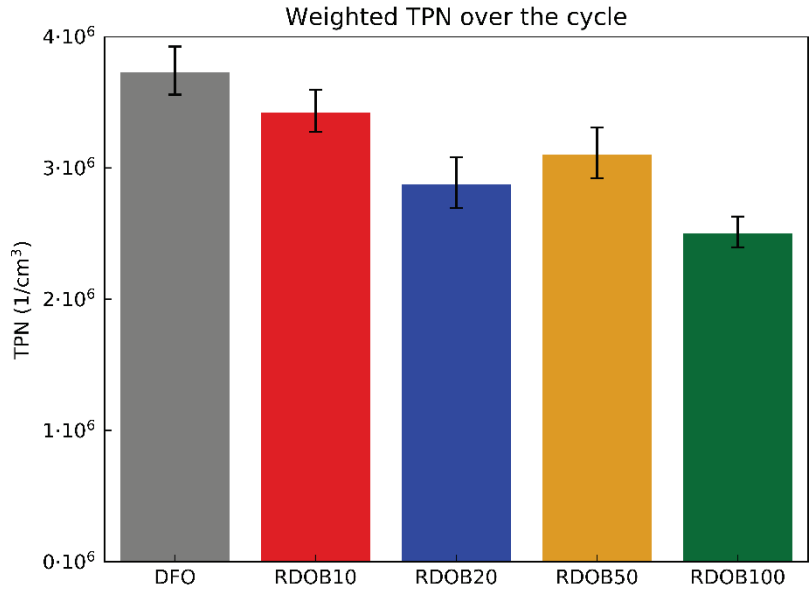

Figure 5. TPN emission for blends of CTO-derived RDOB and DFO within a size range of 5.6–560 nm, weighted over ISO 8178 C1 cycle.

4.4 High-speed engine with alternative marine diesel fuels

Paper IV´s aim was to find out how potential alternative marine diesel fuels affect the exhaust PN of a high-speed diesel engine. Five fuels were studied: LFO, MGO, CTO-based RDOB, RME and a naphtha-LFO blend. Figure 6 illustrates the TPN results at intermediate speed. Results at both intermediate and rated speeds, and at all loads, show none of the alternative fuels led to a distinctive TPN reduction relative to the baseline LFO. Nevertheless, RDOB and the naphtha-LFO blend were quite similar to LFO with regard to TPN. Depending on the load, RDOB and the blend slightly decreased or increased TPN compared to LFO. At some loads, MGO emitted TPNs similar to baseline LFO, but at other loads, slightly higher.

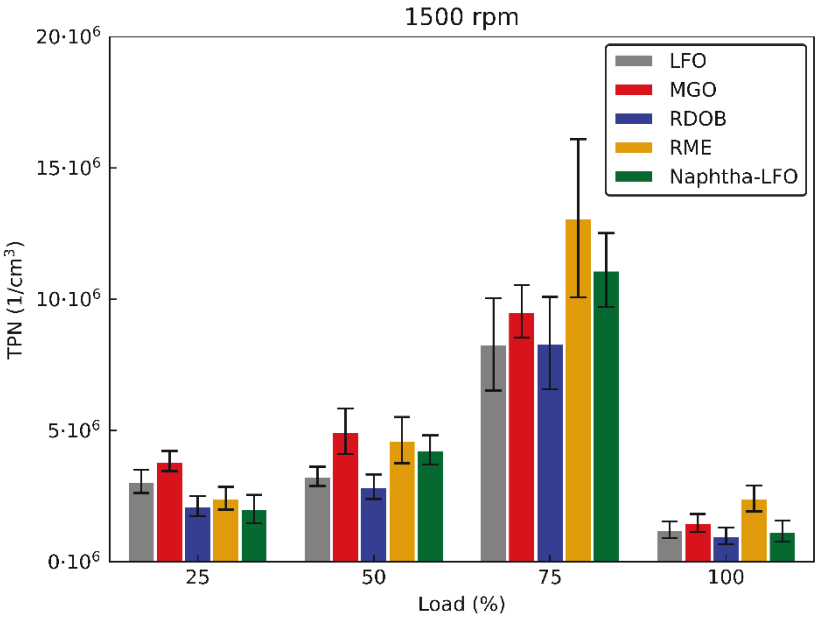

Figure 6. The effect of selected alternative fuels on the exhaust TPN of a high-speed engine at intermediate speed.

4.5 Medium-speed engine with alternative liquid fuels

In Paper V, the objective was to establish how alternative marine diesel fuels (LFO, MGO and the naphtha-LFO blend) affect the exhaust PN when the fuels are used in a medium-speed diesel engine. Figure 7 depicts the TPN differences between the two alternative fuels in relation to LFO. Compared to the LFO baseline, MGO and the renewable naphtha-LFO blend both proved to be beneficial in terms of TPN. The blend and MGO generated fairly similar TPNs at the higher electric loads

from 300 to 600 kW, with both fuels showing clear reductions in comparison to LFO. Depending on the load, the blend reduced TPN by between 5 and 51% whereas MGO reduced TPN by between 24 and 44%. At low loads (60 and 150 kW) the TPN was lowest with MGO and the decrease in TPN with the blend was not so great. Overall, blending renewable naphtha with LFO resulted in a clear reduction of TPN emissions within the particle size range of 5.6 to 560 nm. Circular-economy-based MGO was even better at low loads.

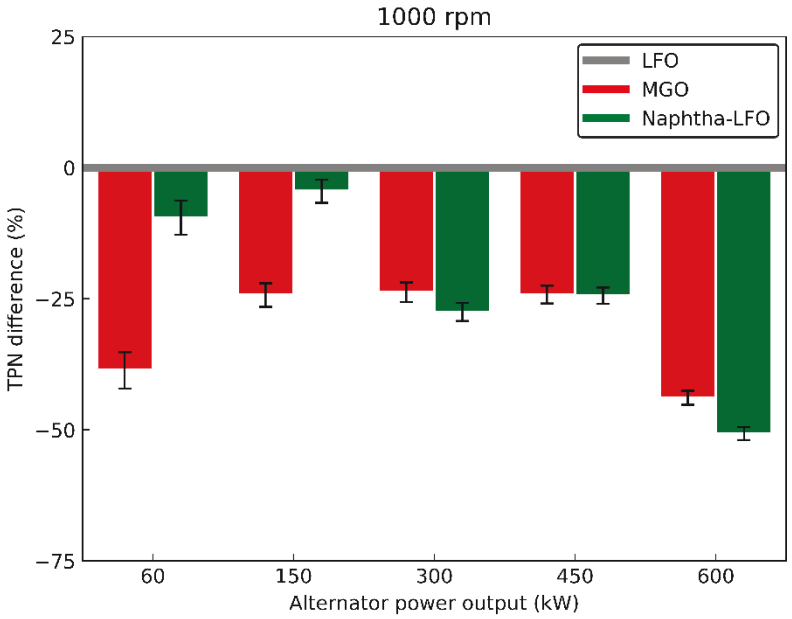

Figure 7. The effect of selected alternative fuels on the exhaust TPN of a medium-speed engine at different loads. TPN with LFO forms the zero line.

Irrespective of the load or fuel, the TPN now consisted almost solely of particles above the size category of 23 nm. For all fuels, the share of particles larger than 23 nm was the highest at full load, being always above 95%. At each load and with all three fuels, the PSD had a distinct peak between 20 and 100 nm.

5 DISCUSSION

The exhaust gas TPN of a CI engine is measured under critical physical conditions due to the instability of the emitted particles. TPN undergoes continuous changes since the initiation of single particles inside the engine cylinder. (Heywood 1988). Thus, numerous uncertainties are intrinsic to the presented TPN results. The uncertainties that may have affected the TPN results during the research work are next discussed.

Liquid fuel has to be mixed with intake air prior to proper combustion inside the engine cylinder in which PM initiation occurs. Several factors affect air-fuel mixture preparation that then affect PM initiation. Mason et al. (2016) mention that PM initiation depends on the time available for mixture preparation, air-fuel ratio and fuel composition. Initiation and evolution of PM continues during the exhaust gas transport. Thus, in addition to differences in the actual TPN, subsequent losses may affect the results. Giechaskiel et al. (2012) divide the particle loss mechanisms into two categories: sampling and transport. The transport category includes issues related to particle dynamics and particle losses. Transport-related loss may occur not only inside the sampling line but also inside the exhaust pipe (Mason et al. 2016). This study performed all the measurements under very stable engine conditions. PN number was also followed up at each load. It was not recorded until the level remained stable. Therefore, the results are completely comparable for all fuels independent of possible sampling or transport losses.

This dissertation´s TPN results comprise all particles that were detectable by the EEPS device within its size range capability of 5.6 to 560 nm. Thus, the presented TPN results include particles from both the nucleation mode and the accumulation mode (Kittelson 1998; Rönkkö et al. 2006; Rönkkö et al. 2007; Filippo & Maricq 2008; Lähde et al. 2010; Heywood 2018).

The nucleation mode formation has been reported to be sensitive to the engine parameters (Lähde et al. 2011), fuel and lubricating oil characteristics (Vaaraslahti et al. 2005) and exhaust aftertreatment (Maricq et al. 2002). Dilution conditions such as dilution ratio, temperature and relative humidity of the dilution air are also seen to affect nucleation mode formation (Mathis et al. 2004). On the other hand, Rönkkö et al. (2007) reported that the PSD dominated by nucleation mode was unaffected by the changes in dilution air temperature and relative humidity between 20 °C and 82 °C and 0% and 60%, respectively. The TPN remained unchanged although the fuel sulphur increased from 10 to 48 ppm (Rönkkö et al. 2007). These results indicate that nucleation mode formation might be insensitive

to fuel sulphur content, dilution air temperature and relative humidity of ambient air. So, it seems that there are contradictory results and perceptions regarding how dilution conditions affect formation of nucleation mode particles. However, unlike the nucleation mode, the accumulation mode is not sensitive to dilution conditions (Maricq et al. 2002; Kittelson, Watts & Johnson 2002).

With the exception of Paper I, the first dilution stage was made with heated air (at 150 °C) in order to prevent condensation of ambient moisture in the sampling lines. According to Vaaraslahti et al. (2004), the nucleation mode evaporates completely when an exhaust sample is heated sufficiently after the dilution stage. However, nucleation mode formation was not disabled during the present research work, so the TPN included both nucleation mode and accumulation mode particles. The TPN results would have been different without the nucleation mode particles. Nevertheless, each study used completely similar sampling methods for all fuels, so this consistent methodology does favour comparability of the results. Stable TPN levels over the three-minute measurement period also facilitated thorough comparison of the fuels. Figure 8 illustrates an example of this, drawn from Paper V´s study. It shows the actual TPN of LFO, MGO and naphtha-LFO blend as a function of measurement time at 100% load at 1000 rpm. Similar follow-up recordings were used in all the studies to ensure reliable and comparable results.

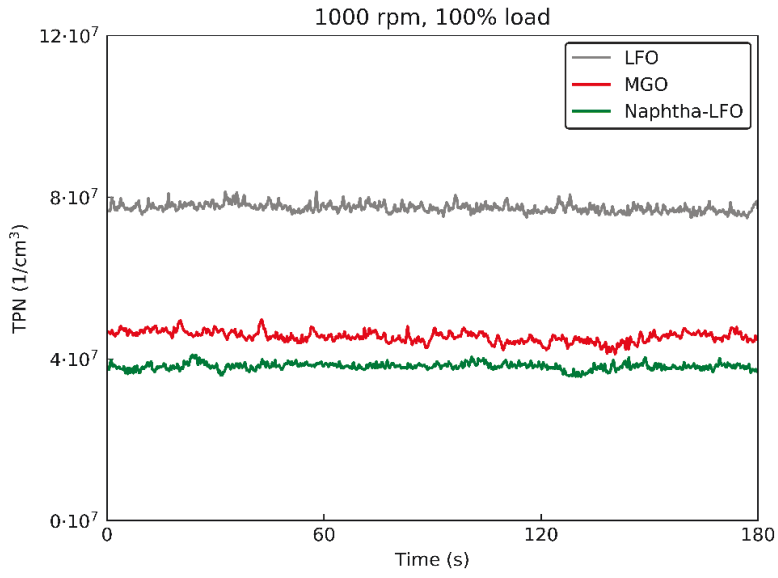

Figure 8. The actual TPN of LFO, MGO and the blend of naphtha and LFO during three-minute measurement period at 100% load at 1000 rpm.

Paper I´s conclusion that methyl esters reduce accumulation mode PN in the 70 to 200 nm size range is consistent with the earlier findings (e.g. Jung et al. 2006, Heikkilä et al. 2009, Rounce et al. 2012, Sun et al. 2019). They reported how FAMEs, either neat or as blending components, had a reducing effect on the number of accumulation mode particles. Similar results were also obtained in Paper I. In any case, the PN reductions in accumulation mode can be most likely explained by oxygen bounded in mono-alkyl-ester molecules (Yang et al., 2007; Lapuerta et al., 2008). Promotion of soot oxidation was more effective with methyl esters than with DFO and RDOA. The DFO and RDOA evaluated in Paper I were similar to the studied fuels of Happonen et al. (2010), who reported that the soot oxidation properties for both fuels were similar. However, in the present study, RDOA also reduced accumulation mode particles when compared with baseline DFO, although to a lesser extent than the methyl esters (Figure 2). Vaporisation of water releases oxygen that also promotes soot oxidation (Samec et al. 2002). In Paper I, however, the water content of both methyl esters was low, and for DFO and RDOA it was negligible. The water contents of alternative fuels were assumed to be too low to explain the obtained PN reductions in accumulation mode.

Paper II´s objective was to find out how a 500-hour running period affects the exhaust PN emission of a high-speed, non-road diesel engine fuelled by a blend of SME and DFO. Addressing the detected increase of copper concentration in the lubricating oil, one assumption was that these copper particles might have caused the considerable PN increase within an approximate size range of 7 to 30 nm. Copper is one of the metallic elements originating from engine wear (Chu-Van et al. 2020). However, there were no increases in the oil´s level of other wear metals, such as lead, as would have been probable in the case of damage to bearings or other engine parts (Sirviö et al. 2016). Schumacher, Peterson & Van Gerpen (2005) suggested that the high levels of copper in their lubrication oil samples originated from a copper oil-cooler. Thus, one possible reason for the substantial increase in the nucleation mode PN was assumed to be copper originating from the break-in of a new oil-cooler (Paper II). Therefore, the increase in the TPN with running hours, depicted in Figure 3, could be explained by the copper particles, not by the effects of SME in the fuel blend. It should be noted that the number of particles larger than 50 nm did not increase during the 500-hour running period. The use of the blend of SME and DFO proved, thus, not deteriorate the combustion-derived PN performance of the engine during this period.

Turning to Paper III´s studies, there are only a few publications available on the effect of CTO-derived RDOB on PN emissions from a CI engine. Laurikko et al. (2014) performed a field test of four cars fuelled by a blend of 20 vol.-% CTO-derived RDOB and 80 vol.-% DFO. No clear differences in PM mass emissions was

detected compared with the DFO reference fuel during the 20 000 km of on-road driving covered by each car. One of Paper III´s goals was to clarify how blending CTO-derived RDOB with DFO affects the exhaust PN emission of a non-road diesel engine. The polyaromatic hydrocarbon content of the blend fell as the share of RDOB increased. Thus, the reduction in aromatics was most likely one of the main reasons for the lower TPN emissions throughout the entire test cycle. Furthermore, the clear PN reduction at a particle size category of 10 nm at idle with neat RDOB may be explained by this fuel´s negligible sulphur and aromatics contents. Moreover, neat RDOB had a cetane number of 65, compared with the baseline DFO´s 59 (Table 2). Presumably, RDOB contained more paraffins, which increases the cetane number (Laurikko et al. 2014, Heywood 2018). Based on Erman et al. (2020), an elevated cetane number followed by a shortened ignition delay seems to lower the nucleation mode PN at low load. The higher cetane number of RDOB might have promoted the reduction of the number of the finest particles further.

CTO-derived RDOB was also studied as an alternative marine diesel fuel in Paper IV. This paper aimed to evaluate how LFO, RDO, MGO, RME and a naphtha-LFO blend affect the exhaust PN of a high-speed engine. Considering the variation of mean TPN values, no consistent conclusion could be drawn about the differences between fuels with regard to TPN. The sulphur content of MGO was below 100 mg/kg. Thus, MGO contained slightly more sulphur than the other fuels, which showed very low sulphur levels (all < 10 mg/kg). This might explain the slightly higher TPNs detected with MGO at some loads (Aufdenblatten et al. 2002). In the study of Vaaraslahti et al. (2004), however, an increase in the sulphur content to 40 mg/kg did not show any change in the PSD. Overall, the results obtained with circular-economy-based MGO and the renewable naphtha and LFO blend cannot be compared with those of other comparable published studies of these fuels´ effects because such studies are sparse. Consequently, Paper IV´s TPN results are unique and novel information about two realistic alternative fuel options.

Paper V concerned the effects of LFO, MGO and the naphtha-LFO blend on the exhaust PN of a medium-speed engine intended for power plants and marine applications. Each fuel showed a stable TPN level over the extended measurement period of eight minutes. The high-volatility fractions of naphtha most probably promoted air-fuel mixing and a reduction of particulates in the case of the blend. The blend´s lower sulphur content, relative to the baseline LFO, was another possible reason for its lower TPN.

Finally, PN reductions can be improved further by optimising the fuel injection separately for each alternative fuel (Aatola et al. 2008; Bohl et al. 2018). However, in the current study, no engine parameters were optimised for any of the fuels. The individual optimisation of engine parameters to suit fuels must be the next step in order to realise the maximum potential benefits of new renewable fuels.

6 CONCLUSIONS

The results obtained from the studies of Papers I–V allow the following conclusions to be drawn.

1) Circular-economy-based MGO and a blend of renewable naphtha and LFO are potential novel fuel options for medium-speed diesel engines if seeking a notable reduction of PN emissions. The share of up to 26 vol.-% of naphtha in the blend proved to work well in the medium-speed diesel engine.

2) Depending on the load, TPN reductions of 5 to 51% were achieved by fuelling the medium-speed engine with the naphtha-LFO blend instead of neat LFO.

3) Circular-economy-based MGO also reduced the TPN compared with LFO in the medium-speed engine. Reductions of 24 to 44% were recorded within the power output range of 300 to 600 kW.

4) In a high-speed engine, neither the blend of renewable naphtha and LFO (20/80 vol.-%) nor the circular-economy-based MGO reduced TPN relative to the baseline LFO. However, the naphtha blend was quite similar to LFO with regard to TPN.

5) RME and SME reduced the exhaust PN within a particle size range of 70 to 200 nm at the majority of loads in the same high-speed engine. This was most likely due to the high oxygen content of those fuels.

6) TPN, however, was higher with RME and SME than with DFO because the nucleation mode particles increased with methyl esters.

7) RDOA from waste fat, residue or vegetable oil did not bring any clear benefit for the TPN of the same high-speed engine. Results were better than those with DFO at some loads, but worse at other loads.

8) Increasing the share of CTO-derived RDOB in the fuel blend with DFO reduced TPN emissions throughout the entire test cycle of the high-speed engine. TPN with neat RDOB was 33% lower than with fossil DFO.

9) Neat RDOB gave a clear PN reduction at a particle size category of 10 nm with the high-speed engine at low idle. Two of the main reasons for this PN reduction are most probably RDOB´s negligible sulphur and aromatics contents.

10) There was a notable rise in TPN emissions during a 500-hour endurance test run on the other high-speed engine, fuelled by a blend of SME (20 vol.-%) and DFO (80 vol.-%). This was caused by a large increase in nucleation mode particles: PN above 50 nm did not change. The rise in nucleation mode particles seemed not to be combustion-related but associated with the fine copper particles originating from some engine component.

11) Overall, the results provided new information, especially concerning two renewable diesels, renewable naphtha and circular-economy marine gas oil. Each of these offers potential for better fuel sustainability.

Future studies of exhaust PN of non-road diesel engines will entail individual optimisation of the engine parameters to suit each fuel. Extended, endurance-type studies are also required. Thorough analyses of particle composition are needed. Further investigation of the influence of lubricating oil composition is another task, aiming to limit PN emissions caused by oils. Additionally, maintenance procedures and service life of the lubricating oil filter must be examined.

7 SUMMARY

The main goal of this thesis was to investigate how different alternative fuels, originating from either renewable or circular-economy feedstock, affect the exhaust PN in non-road diesel engines. The seven studied alternative fuels included two renewable diesels from different feedstock; circular-economy-based MGO; a blend of renewable naphtha and marine LFO; RME; SME; and a blend of SME and DFO. Two fossil diesels, DFO and LFO, served as baseline fuels. The selection of fuels was primarily based on the demands of the company partners and on the availability of fuels.

Five experimental studies (Papers I–V) were performed in order to achieve the goal. Three different engines were examined at laboratory conditions during the research work. The engines used in Papers I–IV were high-speed, non-road diesel engines while the engine in Paper V was a medium-speed diesel. The engines were not equipped with exhaust gas aftertreatment systems, except in Paper II, where a diesel oxidation catalyst and a urea-based selective catalyst reactor were incorporated into the exhaust pipe.

PN from raw exhaust gas was measured during the research by means of an engine exhaust particle sizer (EEPS 3090, TSI Inc.), assessing particles in a size range of 5.6 to 560 nm. For this dissertation, the TPN was calculated from the original PN recordings in the same size range, applying a time interval of 0.1 s for the processing of PN data.

From the viewpoint of particulate emissions, circular-economy-based MGO and the blend of renewable naphtha and LFO both proved to be potential novel fuel options for the high and medium-speed, non-road diesel engines. The naphtha-LFO blend with 26 vol.-% of naphtha worked well in the medium-speed diesel engine.

Depending on the load, TPN reductions of 5 to 51% were achieved by fuelling the medium-speed engine with the naphtha-LFO blend. Circular-economy-based MGO also reduced the TPN compared with LFO, giving reductions of 24 to 44% within the engine load range of 10 to 100%. These results provide new insights about renewable and recycled fuel options offering a sustainable fuel policy.

This research aimed to also provide valuable information about the use of innovative renewable diesel and its blends in a modern, non-road diesel engine. Increasing the proportion of renewable CTO-derived RDOB in a fuel blend with DFO reduced TPN emissions throughout the entire load-speed range of the engine. Using neat RDOB instead of fossil DFO lowered TPN by 33%. Raising the

proportion of RDOB in the fuel reduced its aromatics content, which most likely contributed to the TPN reductions. The beneficial effect of neat RDOB was also detected with the engine at low idle with zero load, giving a clear reduction of nucleation mode PN. Another renewable diesel, RDOA, did not improve the PN emissions performance of the high-speed engine but, as a whole, the results were quite similar to those with DFO.

When considering the end-users, long-term compliance with PN limits is an important issue. TPN emissions deteriorated notably during a 500-hour endurance test of an engine fuelled by a blend of SME (20 vol.-%) and DFO (80 vol.-%). However, only the nucleation mode particles increased and the reason was, most probably, not related to combustion but to wear of some engine component.

This dissertation presents new scientific conclusions about the effects of renewable and recycled fuels on the exhaust particle numbers in non-road diesel engines. Engine manufacturers, fuel producers and refiners as well as authorities are those most likely to make use of the results and conclusions.

References

Aatola, H., Larmi, M., Sarjovaara, T., & Mikkonen, S. (2008). Hydrotreated Vegetable Oil (HVO) as a Renewable Diesel Fuel: Trade-off between NO_x, Particulate Emission, and Fuel Consumption of a Heavy Duty Engine. *SAE Technical Paper* 2008-01-2500. Available from: https://doi.org/10.4271/2008-01-2500.

Alrefaai, M.M., Peña, G.D.G., Raj, A., Stephen, S., Anjana, T. & Dindi, A. (2018). Impact of dicyclopentadiene addition to diesel on cetane number, sooting propensity, and soot characteristics. *Fuel* 216: 110–120. Available from: https://doi.org/10.1016/j.fuel.2017.11.145.

An, W.J., Pathak, R.K., Lee, B.H. & Pandis, S.N. (2007). Aerosol volatility measurement using an improved thermodenuder: Application to secondary organic aerosol. *Journal of Aerosol Science* 38(3): 305–314. Available from: https://doi.org/10.1016/j.jaerosci.2006.12.002.

Anderson, M., Salo, K. & Fridell, E. (2015). Particle and gaseous emissions from an LNG powered ship. *Environmental Science & Technology* 49(20): 12568–12575. Available from: https://doi.org/10.1021/acs.est.5b02678.

Anderson, J. O., Thundiyil, J. G. & Stolbach A. (2012). Clearing the air: a review of the effects of particulate matter air pollution on human health. *Journal of Medical Toxicology* 8(2), 166–175. Available from: https://doi.org/10.1007/s13181-011-0203-1.

Apte, J.S., Brauer, M., Cohen, A.J., Ezzati, M. & Pope, C.A. (2018). Ambient PM 2.5 reduces global and regional life expectancy. *Environmental Science and Technology Letters* 5(9): 546–551. Available from: https://doi.org/10.1021/acs.estlett.8b00360.

Arnold, F., Pirjola, L., Aufmhoff, H., Schuck, T., Lähde, T. & Hämeri, K. (2006). First gaseous sulphuric acid measurements in automobile exhaust: Implications for volatile nanoparticle formation. *Atmospheric Environment* 40(37): 7079–7105. Available from: http://doi.org/10.1016/j.atmosenv.2006.06.038.

Aufdenblatten, S., Schänzlin, K., Bertola, A., Mohr, M., Przybilla, K. & Lutz, T. (2002). Characterization of particle emissions from modern internal combustion engines. *Motortechnische Zeitschrift* 63(11): 962–974. (In German.)

Bach, F., Tschöke, H. & Simon, H. (2009). Influence of Alternative Fuels on Diesel Engine Aftertreatment. In: 7th International Colloquium Fuels - mineral oil based and alternative fuels 14–15th January, Ostfildern, Germany.

Barrientos, E.J., Maricq, M.M., Boehman, A.L. & Anderson, J.E. (2015). Impact of ester structures on the soot characteristics and soot oxidative reactivity of biodiesel. *SAE Technical Paper* 2015-01-1080. Available from: https://doi.org/10.4271/2015-01-1080.

Biswas, S., Hu, S., Verma, V., Herner, J. D., Robertson, W. H., Ayala, A. & Sioutas, C. (2008). Physical properties of particulate matter (PM) from late model heavy-

duty diesel vehicles operating with advanced PM and NO_x emission control technologies. *Atmospheric Environment* 42(22): 5622–5634. Available from: https://doi.org/10.1016/j.atmosenv.2008.03.007.

Bohl, T., Smallbone, A., Tian, G., & Roskilly, A. P. (2018). Particulate number and NO_x trade-off comparisons between HVO and mineral diesel in HD applications. *Fuel* 215: 90–101. Available from: https://doi.org/10.1016/j.fuel.2017.11.023.

Burel, F., Taccani, R. & Zuliani, N. (2013). Improving sustainability of maritime transport through utilization of Liquefied Natural Gas (LNG) for propulsion. *Energy* 57: 412–420. Available from: https://doi.org/10.1016/j.energy.2013.05.002.

Chu-Van, T., Surawski, N., Ristovski, Z., Yuan, C. S., Stevanovic, S., Rahman, S. A., Hossain, F. M., Guo, Y., Rainey, T. & Brown, R. J. (2020). The effect of diesel fuel sulphur and vanadium on engine performance and emissions. *Fuel* 261: 116437. Available from: https://doi.org/10.1016/j.fuel.2019.116437.

Eastwood, P. (2008). *Particulate Emissions from Vehicles*. Chichester: John Wiley & Sons Ltd. 494 pp. ISBN 978-0-470-72455-2.

EN 14214:2012+A1:2014. (2014). Liquid petroleum products – Fatty acid methyl esters (FAME) for use in diesel engines and heating applications – Requirements and test method. Finnish Petroleum Federation.

Erman, A. G., Hellier, P. & Ladommatos, N. (2020). The impact of ignition delay and further fuel properties on combustion and emissions in a compression ignition engine. *Fuel* 262: 116155. Available from: https://doi.org/10.1016/j.fuel.2019.116155.

EU Regulation 2016/1628. (2016). Regulation of the European Parliament and of the Council on requirements relating to gaseous and particulate pollutant emission limits and type-approval for internal combustion engines for non-road mobile machinery. [online] [cited on 4.6.2019]. Available from: http://data.europa.eu/eli/reg/2016/1628/oj.

Filippo, A.D. & Maricq, M.M. (2008). Diesel nucleation mode particles: Semivolatile or solid?. *Environmental Science and Technology* 42(21): 7957–7962. Available from: https://doi.org/10.1021/es8010332.

Florentinus, A., Hamelinck, C., van den Bos, A., Winkel, R. & Cuijpers, M. (2012). Potential of biofuels for shipping - Final Report. Prepared by Ecofys for European Maritime Safety Agency (EMSA). [online] [cited on 29.8.2019]. Available from: https://www.ecofys.com/files/files/ecofys_2012_potential_of_biofuels_in_shipping_02.pdf.

Giechaskiel, B., Arndt, M., Schindler, W., Bergmann, A., Silvis, W. & Drossinos, Y. (2012). Sampling of non-volatile vehicle exhaust particles: a simplified guide. *SAE International Journal of Engines* 5(2), 379-399.

Giechaskiel, B., Ntziachristos, L., Samaras, Z., Casati, R., Scheer, V. & Vogt, R. (2007). Effect of speed and speed-transition on the formation of nucleation mode

particles from a light duty diesel vehicle. *SAE Technical Paper* 2007-01-1110. Available from: https://doi.org/10.4271/2007-01-1110.

Happonen, M., Lähde, T., Messing, M. E., Sarjovaara, T., Larmi, M., Wallenberg, L. R., Virtanen, A. & Keskinen, J. (2010). The comparison of particle oxidation and surface structure of diesel soot particles between fossil fuel and novel renewable diesel fuel. *Fuel* 89(12): 4008–4013. Available from: https://doi.org/10.1016/j.fuel.2010.06.006.

Heft-Neal, S., Burney, J., Bendavid, E. & Burke, M. (2018). Robust relationship between air quality and infant mortality in Africa. *Nature* 559(7713): 254–258. Available from: https://doi.org/10.1038/s41586-018-0263-3.

Heikkilä, J., Virtanen, A., Rönkkö, T., Keskinen, J., Aakko-Saksa, P. & Murtonen, T. (2009). Nanoparticle emissions from a heavy-duty engine running on alternative diesel fuels. *Environmental Science and Technology* 43(24): 9501–9506. Available from: https://doi.org/10.1021/es9013807.

Hellier, P., Jamil, F., Zaglis-Tyraskis, E., Ala'a, H. A.-M., Al Haj, L. & Ladommatos, N. (2019). Combustion and emissions characteristics of date pit methyl ester in a single cylinder direct injection diesel engine. *Fuel* 243: 162–171. Available from: https://doi.org/10.1016/j.fuel.2019.01.022.

Heywood, J.B. (1988). *Internal Combustion Engine Fundamentals*. New York: McGraw-Hill Inc. 930 pp. ISBN 0-07-028637-X.

Heywood, J.B. (2018). *Internal Combustion Engine Fundamentals*. 2nd Edition. New York: McGraw-Hill Education. 1056 pp. ISBN 978-1-260-11610-6.

Im, U., Brandt, J., Geels, C., Hansen, K.M., Christensen, J.H., Andersen, M.S., Solazzo, E., Kioutsioukis, I., Alyuz, U., Balzarini, A., Baro, R., Bellasio, R., Bianconi, R., Bieser, J., Colette, A., Curci, G., Farrow, A., Flemming, J., Fraser, A., Jimenez-Guerrero, P., Kitwiroon, N., Liang, C.-K., Nopmongcol, U., Pirovano, G., Pozzoli, L., Prank, M., Rose, R., Sokhi, R., Tuccella, P., Unal, A., Garcia Vivanco, M., West, J., Yarwood, G., Hogrefe, C. & Galmarini, S. (2018). Assessment and economic valuation of air pollution impacts on human health over Europe and the United states as calculated by a multi-model ensemble in the framework of AQMEII3. *Atmospheric Chemistry and Physics* 18(8): 5967–5989. Available from: https://doi.org/10.5194/acp-18-5967-2018.

Janssen, N.A., Hoek, G., Simic-Lawson, M., Fischer, P., Van Bree, L., Ten Brink, H., Keuken, M., Atkinson, R.W., Anderson, H.R., Brunekreef, B. & Cassee, F.R. (2011). Black carbon as an additional indicator of the adverse health effects of airborne particles compared with PM_{10} and $PM_{2.5}$. *Environmental Health Perspectives* 119(12): 1691–1699. Available from: https://doi.org/10.1289/ehp.1003369.

Jung, H., Kittelson, D.B. & Zachariah, M.R. (2006). Characteristics of SME biodiesel-fueled diesel particle emissions and the kinetics of oxidation. *Environmental Science and Technology* 40(16): 4949–4955. Available from: https://doi.org/10.1021/es0515452.

Kalghatgi, G. (2018). Is it really the end of internal combustion engines and petroleum in transport?. *Applied Energy* 225: 965–974. Available from: https://doi.org/10.1016/j.apenergy.2018.05.076.

Karagulian, F., Belis, C. A., Dora, C. F. C., Prüss-Ustün, A. M., Bonjour, S., Adair-Rohani, H. & Amann, M. (2015). Contributions to cities' ambient particulate matter (PM): A systematic review of local source contributions at global level. *Atmospheric Environment* 120: 475–483. Available from: https://doi.org/10.1016/j.atmosenv.2015.08.087.

Kittelson, D.B. (1998). Engines and nanoparticles: a review. *Journal of Aerosol Science* 29(5–6): 575–588. Available from: https://doi.org/10.1016/S0021-8502(97)10037-4.

Kittelson, D.B., Arnold, M. & Watts, W.F. (1999). Review of diesel particulate matter sampling methods: Final report. University of Minnesota, Department of Mechanical Engineering Center for Diesel Research, Minneapolis, MN. 64 pp. [online] [cited on 5.6.2019]. Available from: http://www.me.umn.edu/centers/cdr/reports/EPAreport3.pdf.

Kittelson, D.B., Watts, W.F. & Johnson, J. (2002). Diesel aerosol sampling methodology – CRC E-43: Technical summary and conclusions. University of Minnesota, Department of Mechanical Engineering, Minneapolis, MN 55455. 23 pp. [online] [cited on 6.8.2019]. Available from: http://www.nanoparticles.org/pdf/Kittelson-Watts.pdf.

Lapuerta, M., Armas, O. & Rodriguez-Fernandez, J. (2008). Effect of biodiesel fuels on diesel engine emissions. *Progress in Energy and Combustion Science* 34(2): 198–223. Available from: https://doi.org/10.1016/j.pecs.2007.07.001.

Laurikko, J., Nylund, N., Aakko-Saksa, P., Mannonen, S., Vauhkonen, V. & Roslund, P. (2014). Crude tall oil-based renewable diesel in passenger car field test. *SAE Technical Paper* 2014-01-2774. Available from: https://doi.org/10.4271/2014-01-2774.

Li, R., Wang, Z., Ni, P., Zhao, Y., Li, M. & Li, L. (2014). Effects of cetane number improvers on the performance of diesel engine fuelled with methanol/biodiesel blend. *Fuel* 128: 180–187. Available from: https://doi.org/10.1016/j.fuel.2014.03.011.

Lähde, T., Rönkkö, T., Virtanen, A., Solla, A., Kytö, M., Söderström, C. & Keskinen, J. (2010). Dependence between nonvolatile nucleation mode particle and soot number concentrations in an EGR equipped heavy-duty diesel engine exhaust. *Environmental Science and Technology* 44(8): 3175–3180. Available from: https://doi.org/ 10.1021/es903428y.

Lähde, T., Rönkkö, T., Happonen, M., Söderström, C., Virtanen, A., Solla, A., Kytö, M., Rothe, D. & Keskinen, J. (2011). Effect of fuel injection pressure on a heavy-duty diesel engine nonvolatile particle emission. *Environmental Science and Technology* 45(6): 2504–2509. Available from: https://doi.org/10.1021/es103431p.

Mason, B., Bradley, W., Pezouvanis, A. & Ebrahimi, K. (2016). Repeatable steady-state measurement of particulate number emissions in engine experiments. *International Journal of Engine Research* 17(10): 1108–1117. Available from: http://doi.org/10.1177/1468087416643667.

Maricq, M. M. (2014). Examining the relationship between black carbon and soot in flames and engine exhaust. *Aerosol Science and Technology* 48(6): 620–629. Available from: http://doi.org/10.1080/02786826.2014.904961.

Maricq, M. M., Chase, R. E., Xu, N. & Laing, P. M. (2002). The effects of the catalytic converter and fuel sulfur level on motor vehicle particulate matter emissions: light duty diesel vehicles. *Environmental Science and Technology* 36(2): 283–289. Available from: https://doi.org/10.1021/es010962l.

Mathis, U., Mohr, M., Kaegi, R., Bertola, A. & Boulouchos, K. (2005). Influence of diesel engine combustion parameters on primary soot particle diameter. *Environmental Science and Technology* 39(6): 1887–1892. Available from: https://doi.org/10.1021/es049578p.

Mathis, U., Ristimaki, J., Mohr, M., Keskinen, J., Ntziachristos, L., Samaras, Z. & Mikkanen, P. (2004). Sampling conditions for the measurement of nucleation mode particles in the exhaust of a diesel vehicle. *Aerosol Science and Technology* 38(12): 1149–1160. Available from: https://doi.org/10.1080/027868290891497.

Millo, F., Rafigh, M., Andreata, M., Vlachos, T., Arya, P. & Miceli, P. (2017). Impact of high sulfur fuel and de-sulfation process on a close-coupled diesel oxidation catalyst and diesel particulate filter. *Fuel* 198: 58–67. Available from: https://doi.org/10.1016/j.fuel.2017.01.006.

Mollenhauer, K. & Tschöke, H. (2010). *Handbook of Diesel Engines*. Heidelberg, Berlin: Springer-Verlag. 636 pp. ISBN 978-3-540-89082-9.

Nabi, M.N., Brown, R.J., Ristovski, Z. & Hustad, J.E. (2012). A comparative study of the number and mass of fine particles emitted with diesel fuel and marine gas oil (MGO). *Atmospheric Environment* 57: 22–28. Available from: https://doi.org/10.1016/j.atmosenv.2012.04.039.

Nousiainen, P., Niemi, S., Rönkkö, T., Karjalainen, P., Keskinen, J., Kuuluvainen, H., Pirjola, L. & Saveljeff, H. (2013). Effect of injection parameters on exhaust gaseous and nucleation mode particle emissions of a Tier 4i nonroad diesel engine. *SAE Technical Paper* 2013-01-2575. Available from: https://dx.doi.org/10.4271/2013-01-2575.

Ntziachristos, L., Samaras, Z., Pistikopoulos, P., & Kyriakis, N. (2000). Statistical analysis of diesel fuel effects on particle number and mass emissions. *Environmental Science & Technology* 34(24): 5106–5114. Available from: https://doi.org/10.1021/es000074a.

Nyström, R., Sadiktsis, I., Ahmed, T.M., Westerholm, R., Koegler, J.H., Blomberg, A., Sandström, T. & Boman, C. (2016). Physical and chemical properties of RME biodiesel exhaust particles without engine modifications. *Fuel* 186: 261–269. Available from: https://doi.org/10.1016/j.fuel.2016.08.062.

Oberdörster, G., Oberdörster, E. & Oberdörster, J. (2005). Nanotoxicology: an emerging discipline evolving from studies of ultrafine particles. *Environmental Health Perspectives* 113(7): 823–839. Available from: https://doi.org/10.1289/ehp.7339.

Oravisjärvi, K., Pietikäinen, M., Ruuskanen, J., Niemi, S., Laurén, M., Voutilainen, A., Keiski, R. L. & Rautio, A. (2014). Diesel particle composition after exhaust after-treatment of an off-road diesel engine and modeling of deposition into the human lung. *Journal of Aerosol Science* 69: 32–47. Available from: https://doi.org/10.1016/j.jaerosci.2013.11.008.

Petzold, A., Ogren, J. A., Fiebig, M., Laj, P., Li, S.-M., Baltensperger, U., Holzer-Popp, T., Kinne, S., Pappalardo, G., Sugimoto, N., Wehrli, C., Wiedensohler, A. & Zhang, X.-Y. (2013). Recommendations for reporting "black carbon" measurements. *Atmospheric Chemistry and Physics* 13(16): 8365–8379. Available from: http://doi.org/10.5194/acp-13-8365-2013.

Pinzi, S., Rounce, P., Herreros, J. M., Tsolakis, A. & Dorado, M.P. (2013). The effect of biodiesel fatty acid composition on combustion and diesel engine exhaust emissions. *Fuel* 104: 170–182. Available from: https://doi.org/10.1016/j.fuel.2012.08.056.

Quiros, D. C., Hu, S., Hu, S., Lee, E. S., Sardar, S., Wang, X., Olfert, J. S., Jung, H. S., Zhu, Y., & Huai, T. (2015). Particle effective density and mass during steady-state operation of GDI, PFI, and diesel passenger cars. *Journal of Aerosol Science* 83(5): 39–54. Available from: https://doi.org/10.1016/j.jaerosci.2014.12.004.

Rounce, P., Tsolakis, A. & York, A.P.E. (2012). Speciation of particulate matter and hydrocarbon emissions from biodiesel combustion and its reduction by aftertreatment. *Fuel* 96: 90–99. Available from: https://doi.org/10.1016/j.fuel.2011.12.071.

Rönkkö, T., Virtanen, A., Kannosto, J., Keskinen, J., Lappi, M. & Pirjola, L. (2007). Nucleation mode particles with a nonvolatile core in the exhaust of a heavy duty diesel vehicle. *Environmental Science and Technology* 41(18): 6384–6389. Available from: https://doi.org/ 10.1021/es0705339.

Rönkkö, T., Virtanen, A., Vaaraslahti, K., Keskinen, J., Pirjola, L. & Lappi, M. (2006). Effect of dilution conditions and driving parameters on nucleation mode particles in diesel exhaust: Laboratory and on-road study. *Atmospheric Environment* 40(16): 2893–2901. Available from: https://doi.org/10.1016/j.atmosenv.2006.01.002.

Samec, N., Kegl, B. & Dibble, R.W. (2002). Numerical and experimental study of water/oil emulsified fuel combustion in a diesel engine. *Fuel* 81(16): 2035–2044. Available from: https://doi.org/10.1016/S0016-2361(02)00135-7.

SFS-EN 590:2013. (2013). Automotive fuels. Diesel. Requirements and test methods. Finnish Petroleum Federation. 1+13 pp.

Schumacher, L.G., Peterson, C.L. & Van Gerpen, J. (2005). Engine oil analysis of biodiesel-fueled engines. *Applied Engineering in Agriculture* 21(2): 153–158. Available from: https://doi.org/10.13031/2013.18146.

Szybist, J.P., Song, J., Alam, M. & Boehman, A.L. (2007). Biodiesel combustion, emissions and emission control. *Fuel Processing Technology* 88(7): 679–691. Available from: https://doi.org/10.1016/j.fuproc.2006.12.008.

Sirviö, K., Niemi, S., Katila, T., Ovaska, T., Nilsson, O. & Hiltunen, E. (2016). B20 fuel effects on engine lubricating oil properties. In: The 28th CIMAC World Congress on Combustion Engine Technology 6–10th June, Helsinki, Finland; Paper No.: 025, pp. 1–8.

Sirviö, K., Niemi, S., Heikkilä, S., Kiijärvi, J., Hissa, M. & Hiltunen, E. (2019). Feasibility of new liquid fuel blends for medium-speed engines. *Energies* 12(14): 2799. Available from: https://doi.org/10.3390/en12142799.

Srinivasan, K.K., Agarwal, A.K., Krishnan, S.R. & Mulone, V. (2019). Introduction to Advanced Combustion Technologies: The Role of Natural Gas in Future Transportation and Power Generation Systems. In: Srinivasan, K.K., Agarwal, A.K., Krishnan, S.R. & Mulone, V. (Eds.). *Natural Gas Engines*, pp. 1–6. Singapore: Springer Nature. ISBN 978-981-13-3306-4.

Sun, W., Wang, Q., Guo, L., Cheng, P., Li, D. & Yan, Y. (2019). Influence of biodiesel/diesel blends on particle size distribution of CI engine under steady/transient conditions. *Fuel* 245: 336–344. Available from: https://doi.org/10.1016/j.fuel.2019.01.101.

Testo (2016). Testo MD19-3E. User Manual. Version 1.03.

Timonen, H., Karjalainen, P., Aalto, P., Saarikoski, S., Mylläri, F., Karvosenoja, N., Jalava, P., Asmi, E., Aakko-Saksa, P., Saukkonen, N., Laine, T., Saarnio, K., Niemelä, N., Enroth, J., Väkevä, M., Oyola, P., Pagels, J., Ntziachristos, L., Cordero, R., Kuittinen, N., Niemi, J. V. & Rönkkö, T. (in Press). Adaptation of Black Carbon Footprint Concept Would Accelerate Mitigation of Global Warming. *Environmental Science and Technology Viewpoint*, published online on October 16, 2019. Available from: https://doi.org/10.1021/acs.est.9b05586.

Tree, D. R. & Svensson, K. I. (2007). Soot processes in compression ignition engines. *Progress in Energy and Combustion Science* 33(3): 272–309. Available from: https://doi.org/10.1016/j.pecs.2006.03.002.

TSI (2009). Model 3090. Operation and Service Manual of Engine Exhaust Particle Sizer™ Spectrometer. P/N 1980494, Revision F.

Tsolakis, A. (2006). Effects on particle size distribution from the diesel engine operating on RME-biodiesel with EGR. *Energy & Fuels* 20(4): 1418–1424. Available from: https://doi.org/10.1021/ef050385c.

Ushakov, S. & Lefebvre, N. (2019). Assessment of hydrotreated vegetable oil (HVO) applicability as an alternative marine fuel based on its performance and

emissions characteristics. *SAE International Journal of Fuels and Lubricants* 12(2). Available from: https://doi.org/10.4271/04-12-02-0007.

Vaaraslahti, K., Virtanen, A., Ristimäki, J. & Keskinen, J. (2004). Nucleation mode formation in heavy-duty diesel exhaust with and without a particulate filter. *Environmental Science and Technology* 38(18): 4884–4890. Available from: https://doi.org/10.1021/es0353255.

Vaaraslahti, K., Keskinen, J., Giechaskiel, B., Solla, A., Murtonen, T. & Vesala, H. (2005). Effect of lubricant on the formation of heavy-duty diesel exhaust nanoparticles. *Environmental Science and Technology* 39(21): 8497–8504. Available from: https://doi.org/10.1021/es0505503.

Wang, X., Grose, M.A., Caldow, R., Osmondson, B.L., Swanson, J.J., Chow, J.C., Watson, J.G., Kittelson, D.B., Li, Y., Xue, J., Jung, H. & Hu, S. (2016a). Improvement of Engine Exhaust Particle Sizer (EEPS) Size Distribution Measurement – II. Engine Exhaust Aerosols. *Journal of Aerosol Science* 92: 83–94. Available from: https://doi.org/10.1016/j.jaerosci.2015.11.003.

Wang, Z., Li, L., Wang, J. & Reitz, R.D. (2016b). Effect of biodiesel saturation on soot formation in diesel engines. *Fuel* 175: 240–248. Available from: https://doi.org/ 10.1016/j.fuel.2016.02.048.

WHO. (2018). 9 out of 10 people worldwide breathe polluted air, but more countries are taking action. News Release 2.5.2018 [online]. Available from: https://www.who.int/news-room/detail/02-05-2018-9-out-of-10-people-worldwide-breathe-polluted-air-but-more-countries-are-taking-action.

WHO. (2019). Air Pollution. Maps and Databases. WHO Global Ambient Air Quality Database. [online] [cited on 25.6.2019]. Available from: https://www.who.int/airpollution/data/cities/en/.

Wiedensohler, A., Birmili, W., Nowak, A., Sonntag, A., Weinhold, K., Merkel, M., Wehner, B., Tuch, T., Pfeifer, S., Fiebig, M., Fjäraa, A. M., Asmi, E., Sellegri, K., Depuy, R.,Venzac, H., Villani, P., Laj, P., Aalto, P., Ogren, J. A., Swietlicki, E., Williams, P., Roldin, P., Quincey, P., Hüglin, C., Fierz-Schmidhauser, R., Gysel, M., Weingartner, E., Riccobono, F., Santos, S., Grüning, C., Faloon, K., Beddows, D., Harrison, R., Monahan, C., Jennings, S. G., O'Dowd, C. D., Marinoni, A., Horn, H.-G., Keck, L., Jiang, J., Scheckman, J., Mcmurry, P. H., Deng, Z., Zhao, C. S., Moerman, M., Henzing, B., De Leeuw, G., Löschau, G. & Bastian, S. (2012). Mobility particle size spectrometers: harmonization of technical standards and data structure to facilitate high quality long-term observations of atmospheric particle number size distributions. *Atmospheric Measurement Techniques* 5: 657–685. Available from: https://doi.org/10.5194/amt-5-657-2012.

Wiedensohler, A., Wiesner, A., Weinhold, K., Birmili, W., Hermann, M., Merkel, M., Müller, T., Pfeifer, S., Schmidt, A., Tuch, T., Velarde, F., Quincey, P., Seeger, S. & Nowak, A. (2018). Mobility particle size spectrometers: Calibration procedures and measurement uncertainties. *Aerosol Science and Technology* 52(2): 146–164. Available from: https://doi.org/10.1080/02786826.2017.1387229.

Zetterdahl, M., Moldanová, J., Pei, X., Pathak, R.K. & Demirdjian, B. (2016). Impact of the 0.1% fuel sulfur content limit in SECA on particle and gaseous emissions from marine vessels. *Atmospheric Environment* 145: 338–345. Available from: https://doi.org/10.1016/j.atmosenv.2016.09.022.

Zetterdahl, M., Salo, K., Fridell, E. & Sjöblom, J. (2017). Impact of aromatic concentration in marine fuels on particle emissions. *Journal of Marine Science and Application* 16(3): 352–361. Available from: https://doi.org/10.1007/s11804-017-1417-7.

Zhu, L., Cheung, C.S. & Huang, Z. (2016). A comparison of particulate emission for rapeseed oil methyl ester, palm oil methyl ester and soybean oil methyl ester in perspective of their fatty ester composition. *Applied Thermal Engineering* 94: 249–255. Available from: https://doi.org/10.1016/j.applthermaleng.2015.10.132.

Zimmerman, N., Godri Pollitt, K. J., Jeong, C. H., Wang, J. M., Jung, T., Cooper, J. M., Wallace, J. S. & Evans, G. J. (2014). Comparison of three nanoparticle sizing instruments: The influence of particle morphology. *Atmospheric Environment* 86: 140–147. Available from: https://doi.org/10.1016/j.atmosenv.2013.12.023.

Yang, H. H., Chien, S. M., Lo, M. Y., Lan, J. C. W., Lu, W. C. & Ku, Y. Y. (2007). Effects of biodiesel on emissions of regulated air pollutants and polycyclic aromatic hydrocarbons under engine durability testing. *Atmospheric Environment* 41(34): 7232–7240. Available from: https://doi.org/10.1016/j.atmosenv.2007.05.019.

Publications

This doctoral dissertation consists of the following five publications, referred to in the text by their Roman numerals:

I. Ovaska, Teemu; Niemi, Seppo; Sirviö, Katriina; Nilsson, Olav. 2019. Exhaust Particle Number of a Non-Road Diesel Engine Fuelled by Methyl Esters with Different Fatty Acid Compositions. *Agronomy Research*, volume 17, issue Special Issue 1, pages 1165–1180. ISSN: 1406-894X.

II. Ovaska, Teemu; Niemi, Seppo; Katila, Tapani; Nilsson, Olav. 2018. Exhaust Particle Size Distributions of a Non-Road Diesel Engine in an Endurance Test. *Agronomy Research*, volume 16, issue Special Issue 1, pages 1159–1168. ISSN: 1406-894X.

III. Niemi, Seppo; Vauhkonen, Ville; Mannonen, Sari; Ovaska, Teemu; Nilsson, Olav; Sirviö, Katriina; Heikkilä, Sonja; Kiijärvi, Jukka. 2016. Effects of Wood-Based Renewable Diesel Fuel Blends on the Performance and Emissions of a Non-Road Diesel Engine. *Fuel*, volume 186, pages 1–10. ISSN: 0016-2361.

IV. Ovaska, Teemu; Niemi, Seppo; Sirviö, Katriina; Nilsson, Olav; Portin, Kaj; Asplund, Tomas. 2019. Effects of Alternative Marine Diesel Fuels on the Exhaust Particle Size Distributions of an Off-Road Diesel Engine. *Applied Thermal Engineering*, volume 150, pages 1168–1176. ISSN: 1359-4311.

V. Ovaska, Teemu; Niemi, Seppo; Sirviö, Katriina; Heikkilä, Sonja; Portin, Kaj; Asplund, Tomas. 2019. Effect of Alternative Liquid Fuels on the Exhaust Particle Size Distributions of a Medium-Speed Diesel Engine. *Energies*, volume 12, page 2050. ISSN: 1996-1073.

Author´s contribution

Paper I: Ovaska is the main author. Ovaska, Nilsson and Sirviö implemented the engine experiments. Sirviö performed the laboratory analyses. Ovaska analysed the emission data and visualised the results. Ovaska and Niemi wrote the paper.

Paper II: Ovaska is the main author. The research was within a wider context of engine experiments designed by Katila and Niemi. Nilsson and Ovaska carried out the engine experiments. Ovaska analysed the emission data and visualised the results. Ovaska and Niemi wrote the paper.

Paper III: Ovaska is the co-author. The research was part of a wider range of engine experiments designed by Vauhkonen, Mannonen and Niemi. Nilsson, Sirviö, Ovaska and Heikkilä conducted the engine experiments. Ovaska analysed the emission data and visualised the results. Niemi wrote the paper. Kiijärvi was responsible for the layout of the paper.

Paper IV: Ovaska is the main author. The research formed part of a series of engine experiments designed by Portin, Asplund and Niemi. Nilsson, Ovaska and Sirviö conducted the engine experiments. Ovaska and Niemi wrote the paper.

Paper V: Ovaska is the main author. The research was part of a wider range of engine experiments designed by Portin, Asplund and Niemi. Ovaska, Sirviö and Heikkilä carried out the engine experiments. Ovaska and Niemi wrote the paper.

Paper I

Agronomy Research **17**(S1), 1165–1180, 2019
https://doi.org/10.15159/AR.19.089

Exhaust particle number of a non-road diesel engine fuelled by methyl esters with different fatty acid compositions

T. Ovaska*, S. Niemi, K. Sirviö and O. Nilsson

University of Vaasa, School of Technology and Innovations, P.O. Box 700, FI-65101 Vaasa, Finland
*Correspondence: teemu.ovaska@univaasa.fi

Abstract. The main aim of this study was to find out how methyl esters with different fatty acid compositions affect the exhaust particle numbers. Along with fossil diesel fuel oil (DFO) and renewable diesel (HVO), a high-speed non-road diesel engine was fuelled by rapeseed (RME) and soybean (SME) methyl esters. Particle numbers within the size range of 5.6–560 nm were measured by means of an engine exhaust particle sizer (EEPS). The exhaust smoke, gaseous emissions and the basic engine performance were also determined. During the measurements, the 4-cylinder, turbocharged, intercooled engine was run according to the non-road steady cycle. Methyl esters reduced particles within the size range of 70 to 200 nm. For RME and SME, both positive and significant correlations were found between the sum of the particle numbers detected above the size category of 23 nm and methyl palmitate (C16:0), methyl stearate (C18:0) and methyl linoleate (C18:2) contents at 10% load at rated speed. In terms of nitrogen oxide (NO_x) and hydrocarbon (HC) emissions, HVO was beneficial while carbon monoxide (CO) emission was the lowest with DFO. The level in smoke emission was negligible.

Key words: diesel engine, particle number, methyl ester, fatty acid composition.

INTRODUCTION

The European Parliament and of the Council promoted the use of energy from renewable sources by setting the renewable energy directive in 2009. For the transport sector, the sub-target of the directive was that 10% of the fuels are from renewable sources by 2020 (Directive 2009/28/EC). In order to meet this target, the Fatty Acid Methyl Esters (FAME) has been widely used in EU as a blending component with fossil diesel fuel oil (DFO) during the past 10 years. Furthermore, the use of FAME in cultivation, transportation and distribution machineries is seen as an option for the improvement of the life cycle based greenhouse gas (GHG) balances of FAME (Jungmeier et al., 2016).

Diesel engine exhaust particles form the size distribution with two distinctive particle modes; accumulation mode and nucleation mode. The particle mean diameters in nucleation mode are under 50 nm, whereas the mean diameter range in accumulation mode is 50–500 nm (Kittelson, 1998; Rönkkö et al., 2006; Rönkkö et al., 2007; Filippo & Maricq, 2008; Lähde et al., 2010). Nucleation mode includes the particles which are believed to form during dilution when the exhaust gas gets mix up with the ambient air. Accumulation mode is thought to consist mainly of the agglomerated carbon soot

particles which result from the incomplete burning of either the fuel or the lubricating oil remnants inside the cylinder (Kittelson et al., 1999; Rönkkö et al., 2007; Nousiainen et al., 2013). Soot formation can be enhanced by improving soot oxidation (Wang et al., 2016b).

FAME fuels contain fatty acids with different lengths of molecule chains. As the molecule chain shortens, relative amount of oxygen increase in the chain. Soot oxidation improves (Pinzi et al., 2013; Barrientos et al., 2015). Moreover, the different fatty acids have divergent number of carbon–carbon double bonds in the chemical structure of FAME. Saturated fatty acids do not have double bonds while unsaturated have one or more. The less the fraction of unsaturated fatty acids the lower the soot precursors resulted from FAME fuel combustion (Zhu et al., 2016; Wang et al., 2016b).

Schönborn et al. (2009) studied the combustion behaviour of pure individual fatty acid alcohol ester molecules in a single-cylinder research engine. As a one result, particulate mass was detected to increase as the length of ester molecule was increased. They gave reason for the increased mass by means of particle numbers. Unsaturated fatty ester molecules produced more particles in the diameter range of about 40 and 200 nm compared to diesel fuel. In the study of Pinzi et al. (2013), particulate mass was increased as chain length of methyl ester was increased.

This paper presents how methyl esters with different fatty acid compositions affected the exhaust particle numbers. Along with fossil diesel fuel oil (DFO) and renewable diesel (HVO), a high-speed non-road diesel engine was fuelled by rapeseed (RME) and soybean (SME) methyl esters. Alongside the exhaust gas particle number and size distributions, the exhaust smoke, gaseous emissions and basic engine performance were determined. The high-speed off-road diesel engine was driven according to the non-road steady cycle (NRSC). During the experiments, no parameter optimization was applied with the studied fuels.

MATERIALS AND METHODS

The experimental measurements were performed by the University of Vaasa at the engine laboratory of the Technobothnia Research Centre in Vaasa, Finland.

Engine

The 4-cylinder test engine was a turbocharged, intercooled (air-to-water) off-road diesel engine, equipped with a common-rail fuel injection system. The engine had no exhaust gas after treatment. The main engine specification is given in Table 1.

Table 1. Main engine specification

Engine	AGCO POWER 44 AWI
Cylinder number	4
Bore (mm)	108
Stroke (mm)	120
Swept volume (dm^3)	4.4
Rated speed (rpm)	2,200
Rated power (kW)	101
Maximum torque with rated speed (Nm)	455*
Maximum torque with 1,500 rpm (Nm)	583*

*conformable to measured torques obtained with DFO fuel.

Fuels

The effects of rapeseed methyl ester (RME), soybean methyl ester (SME), and hydrotreated vegetable oil (HVO) on the exhaust gas particles were investigated along

with commercial low-sulphur diesel fuel oil (DFO). The fuel specifications are in Table 2. RME and SME fulfilled the requirements of EN14214 standard. DFO was used as the reference fuel, completely fulfilling the fuel standard EN590. For DFO, the lower heating value (MJ L^{-1}) was based on the information received from the fuel supplier. The unit conversion from MJ l^{-1} to MJ kg^{-1} was calculated. The lower heating values of RME, SME and HVO were computed based on the elementary analyses of fuels (Mollenhauer & Schreiner, 2010).

Table 2. Fuel specifications

Parameter	Method	DFO	RME	SME	HVO	Unit
Cetane number	ASTM D6890	-	53.5	47.3	74.7	-
Density (15 °C)	EN ISO 12185	834	883	885	779	kg m^{-3}
Sulfur content	EN ISO 20846	3.6	-	-	< 1	mg kg^{-1}
	ASTM D7039	-	< 2	3	-	mg kg^{-1}
Carbon content	ASTM D5291	-	77.4	77.0	84.2	wt.-%
Hydrogen content	ASTM D5291	-	12.2	11.9	15.1	w.t-%
Nitrogen content	ASTM D5291	-	< 0.2	< 0.2	-	wt.-%
Water content	EN ISO 12937	-	132	353	19	mg kg^{-1}
Kin. viscosity (40 °C)	Fuel supplier's info	-	4.5	4.1	2.9	mm^2 s^{-1}
Lower heating value	Fuel supplier's info	36.0*	-	-	-	MJ L^{-1}
	By calculating	43.2	37.7	37.2	43.8	MJ kg^{-1}

*(Teboil, 2019).

Any parameter optimization was not made with the studied fuels. The engine lubricant was the development product of the supplier. The fatty acid composition of RME and SME were analysed, Table 3.

Table 3. Fatty acid compositions for RME and SME

Methyl ester	RME %	SME %
10:0	< 0.1	-
12:0	-	0.1
14:0	< 0.1	0.1
16:0	4.5	11.2
16:1 cis	0.4	0.1
17:0	< 0.1	0.1
17:1	0.2	0.1
18:0	1.6	4.4
18:1 cis	61	21.8
18:2 konj.	-	< 0.1
18:2 n-6 cis	19.3	52.9
18:3 n-3 cis (ALA)	9.9	7.6
20:0	0.6	0.3
20:1	1.3	0.2
20:2 n-6 cis	0.1	0.1
22:0	0.3	0.3
22:1 n-9 cis	0.3	0.1
24:0	0.1	0.1
24:1	0.2	-
Saturated fatty acids total	7.1	16.7
Monounsaturated fatty acids total	63.3	22.3
Polyunsaturated fatty acids total	29.3	60.5
Iodine number	113.8	130.8

Analytical instruments

The particles from a size range of 5.6 to 560 nm were recorded by using the engine exhaust particle sizer (EEPS). The adopted measurement instruments for gaseous emissions and air mass flow rate are also listed in Table 4.

Before the measurements, the analysers were calibrated manually once a day according to the instructions of the instrument manufacturers. For the EEPS, the sample flow rate was adjusted at 5.0 L min^{-1}, and the 'SOOT' inversion was applied in the data processing (Wang et al., 2016a). The arrangement of the test bench and measurement devices is seen in Fig. 1.

Table 4. Measuring equipment for gaseous emissions and intake air

Parameter	Device	Technology
Particle number and size distribution	TSI EEPS 3090	spectrometer
Hydrocarbons	J.U.M. VE7	HFID
Smoke	AVL 415 S	optical filter
NO_x, CO, CO_2, O_2	TSI CA-6203 CA-CALC	electrochemical
NO_x, λ	WDO UniNO_x sensors	ZrO_2-based multilayer
O_2	Siemens Oxymat 61	paramagnetic
Air mass flow rate	ABB Sensyflow P	thermal mass

During the measurements, the exhaust gas sample was diluted at two stages in order to decrease the particle concentration of the sample for the EEPS. The sample was first diluted with ambient air by means of the porous tube diluter (PTD, Ntziachristos et al., 2004). Then, the sample was led through the secondary dilution, which was performed with Dekati ejector diluter. The total dilution ratio of exhaust sample was determined by simultaneously measuring CO_2 concentration before and after the dilution stages. The particle sampling system was provided by Tampere University. This study was a part of the larger measurement campaigns and emission data acquirement. In the studies of Karjalainen et al. (2014) and Alanen et al. (2017), the above-mentioned dilution devices were also used upstream of the EEPS. However, a thermodenuder was not employed in this study (An et al., 2007).

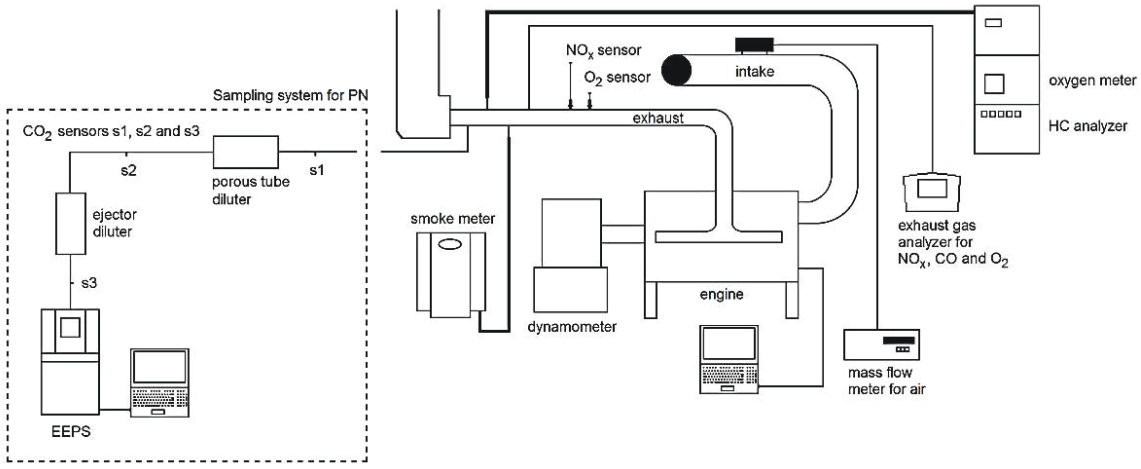

Figure 1. Experimental set-up.

The particle number (PN) was recorded consecutively three times. Each recording was one-minute long. The averaging interval of 2 seconds was used when the data was stored. The uncertainty of the PN measurement was approximated by calculating the standard deviation of the PN averages, taken from each one-minute recording.

Total particle numbers (TPN, from 5.6 to 560 nm) were calculated from the PN recordings by adding up the PN concentrations indicated in the size bins of the EEPS spectrometer during the one averaging interval. For the presented results of this paper, the average of PN sums was calculated. Moreover, the averages of the normalized PN concentrations ($dN/d\log D_p$) were calculated from each bin in order to illustrate the particle size distributions.

Based on the measured CO_2 concentrations before and after the dilution stages, the dilution ratios were calculated both for the porous type diluter (DR_{PTD}) as in (1) and for the ejector diluter ($DR_{ejector}$) as in (2). Then, the total dilution ratio (DR_{tot}) was calculated as in (3).

$$DR_{PTD} = \frac{(CO_2)_{s1} - (CO_2)_{bg}}{(CO_2)_{s2} - (CO_2)_{bg}} \quad (1)$$

$(CO_2)_{s1}$ and $(CO_2)_{s2}$ are the CO_2 concentrations of raw exhaust and diluted exhaust after first dilution stage, respectively. $(CO_2)_{bg}$ is the ambient CO_2 concentration.

$$DR_{ejector} = \frac{(CO_2)_{s2} - (CO_2)_{bg}}{(CO_2)_{s3} - (CO_2)_{bg}} \quad (2)$$

$(CO_2)_{s3}$ is the CO_2 concentration after the dilution stages before the EEPS.

$$DR_{tot} = DR_{PTD} \cdot DR_{ejector} \quad (3)$$

The calculated TPN averages and the averages of the normalized PN concentrations were multiplied by the DR_{tot} of the exhaust sample in order to present the corresponding concentrations in the raw exhaust.

However, no consistent conclusions could be drawn concerning the particle numbers under the size category of 20 nm due to the following reasons. Firstly, mobility particle size spectrometers, as EEPS, have been found to be best for the measurement of the particle numbers within the size range of 20–200 nm (Wiedensohler et al., 2012). Outside this size range, the elevated uncertainties may exist as described by Wiedensohler et al. (2018). Secondly, the nucleation mode formation has been reported to be sensitive not only to the engine parameters (Lähde et al., 2011), fuel and lubricating oil characteristics (Vaaraslahti et al., 2005), and exhaust after-treatment (Maricq et al., 2002), but also to dilution conditions such as dilution ratio, temperature and relative humidity of the dilution air (Mathis et al., 2004). On the other hand, Rönkkö et al. (2007) reported that its formation was insensitive to the fuel sulphur content, dilution air temperature, and relative humidity of ambient air.

The recorded particle numbers below 23 nm were omitted due to the two reasons. The first reason was the uncertainties related to the complex nature of nucleation mode PN and the PN measurement by means of EEPS under the size category of 20 nm. The second reason was the PN legislation which limits the particle number from the size of 23 nm on. Thus, the calculated TPN was divided into two categories depending on how many of the particles out of the average TPN were below or above the size category of 23 nm.

The authors of this paper believe the nucleation mode formation could be avoided if a thermodenuder is employed during the PN measurement (An et al., 2007). According to Vaaraslahti et al. (2004), the nucleation mode evaporates completely when an exhaust sample is heated enough.

The recorded smoke value was the average of three consecutively measured smoke numbers.

The sensor data were collected and the engine control parameters were followed via engine management software, provided by the engine manufacturer. By using the software, the temperatures of cooling water, intake air and exhaust gas plus the pressures of the intake air and exhaust gas were recorded.

Based on the measured hydrocarbon (HC), nitrogen oxides (NO_x) and carbon monoxide (CO) concentrations, the brake specific emissions of HC, NO_x and CO were calculated according to the ISO 8178 standard.

Experimental matrix and running procedure

The measurements were conducted according to the test cycle C1 of the ISO 8178-4 standard, known as the non-road steady cycle (NRSC) (ISO 8178-4:2017, 2017). The rated speed of the engine was 2,200 rpm and the intermediate speed was chosen to be 1,500 rpm. At full load, the maximum torque was 410 nm at rated speed and 525 nm at intermediate speed. The test engine was installed in a test bed and loaded by means of an eddy-current dynamometer of model Horiba WT300.

Each day before the measurements, the intake air temperature was adjusted at 50 °C downstream the charge air cooler when the engine was run at full load at rated speed. The temperature was controlled manually by regulating cooling water flow to the heat exchanger. After this initial adjustment, the temperature was allowed to change with engine load and speed. The engine was then run according to the NRSC cycle for the measurements.

Before the recordings at each load point, it was waited that the engine had stabilized, the criteria being that the temperatures of coolant water, intake air and exhaust were stable. The length of the measurement period was not tied to a certain time apart from the particle mass collection.

All measurement values were recorded once at each load point of the cycle. The particle number and size distribution were recorded continuously at each load point. For each fuel, the engine warm up and measurements were performed in an exactly similar way.

The original target was to keep the engine injection parameters constant for all fuels. Due to the lower heating values, the injection rate had, however, to be raised at full loads when the engine was run with the methyl esters. Pre-, main, and post-injections were used for the fuel injection. The upper limits of the total injection rates were changed in the electronic control unit of the engine by means of the WinEEM4 program.

The control system enabled the shift of injection quantity within the entire full load (ultimate torque) curve, Fig. 2. For RME and SME, the required increases in the injection rates were from 95 mg to 100 mg at 1,400 rpm and at 1,500 rpm. With these increases, a proper shape of the injection rate curve could be maintained. For all fuels, the position of the limited injection was also moved from 2,200 rpm to 2,250 rpm.

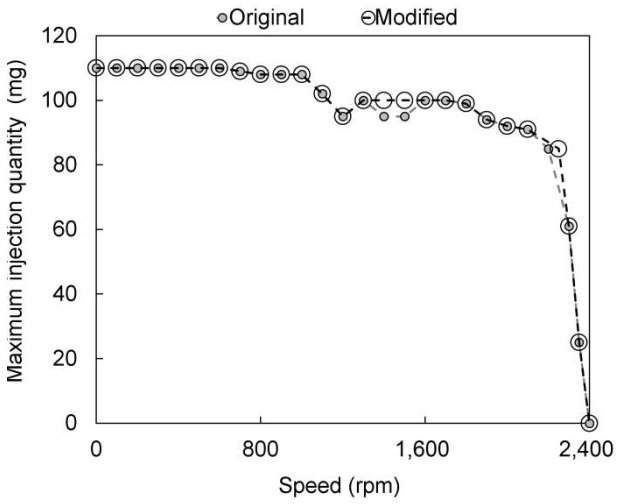

Figure 2. Upper limits of total injection rates at engine operation area.

Fig. 3, a and 3, b show the shares of the pre-, main, and post-injection rates at the load points of the NRSC cycle. For the methyl

esters, the main injection rates were higher than for DFO or HVO since the lower heating value of the esters were lower than those of DFO and HVO.

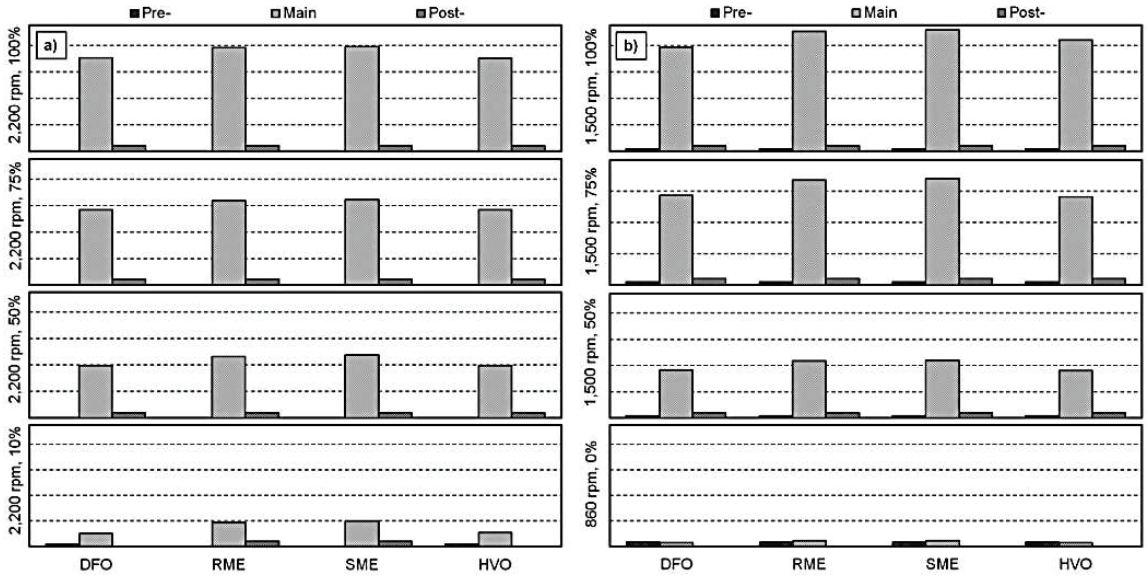

Figure 3. The shares of the pre-, main, and post-injection rates a) at 2,200 rpm and b) at 1,500 rpm and at idle.

RESULTS AND DISCUSSION

Particle size distributions

Due to the uncertainties related to the particle number measurement under the size category of 20 nm and the legislative limitation of PN from the size of 23 nm on, Figs. 4–6 illustrate the detected size distributions between 23 nm and 560 nm. Irrespective of fuel, the detected particles larger than 200 nm accounted for less than 1% of the particles larger than 23 nm in this study. Below, the distributions are examined more thoroughly at certain loads.

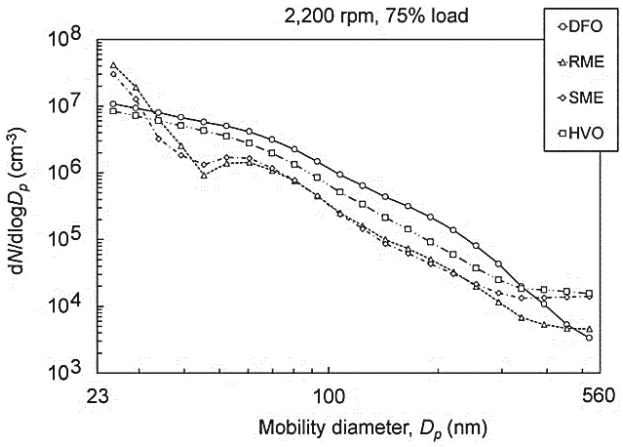

Figure 4. Exhaust particle size distributions from 23 to 560 nm at 75% load at rated speed for different fuels.

Fig. 4 shows the particle size distributions at 75% load at rated speed. Considering the particles above the size category of 23 nm, the detected distributions were quite similar for, on one hand, the methyl esters and, on the other hand, for DFO and HVO. The methyl esters produced less particles above 40 nm compared to DFO and HVO.

For 10% load, the size distributions from 23 to 560 nm are illustrated in Fig. 5. Now, the lowest PN was recorded with HVO and the highest with the methyl esters within the entire size range. The esters emitted considerably higher particle numbers than HVO and DFO.

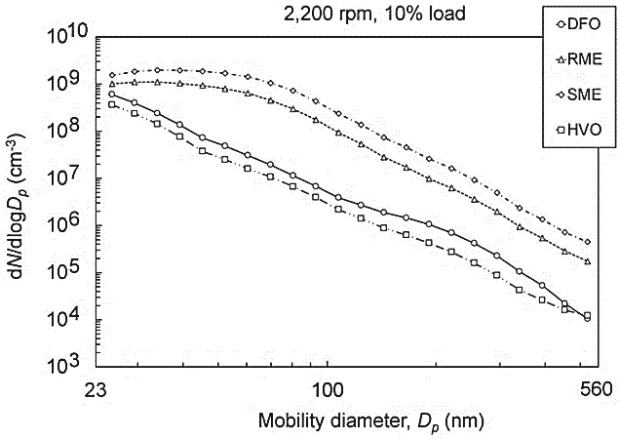

Figure 5. Exhaust particle size distributions from 23 to 560 nm at 10% load at rated speed for different fuels.

At idle (Fig. 6), HVO emitted the lowest while the methyl esters the highest PN below the size of 70 nm. The change in order of the fuels was detected above 100 nm. With the methyl esters, the lowest PN was detected from the size of 100 nm on. HVO was particularly favourable within the range of, say, below 50 nm.

The physical properties of the liquid fuel tend to control fuel spray characteristics while the fuel composition determines the pathways of chemical reactions during combustion (Eastwood, 2008). Besides the fuel sulphur content, particle formation is also influenced by other fuel characteristics such as the fuel density (Szybist et al., 2007; Bach et al., 2009), viscosity (Mathis et al., 2005; Tsolakis, 2006), cetane number (Li et al., 2014; Alrefaai et al., 2018), and the water content of fuel (Samec et al., 2002).

The current test fuels were practically free of sulphur. Therefore, the effects of sulphur could be assumed as negligible although lube oil contained sulphur. The lube oil consumption is, however, so small that the effects of sulphur compounds were assessed negligible.

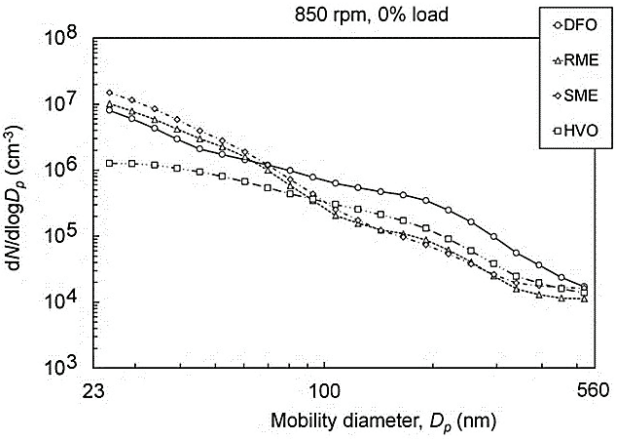

Figure 6. Exhaust particle size distributions from 23 to 560 nm at idle for different fuels.

Fuel density, viscosity, and compressibility determine the start of injection. After the injection has started, an increased cetane number leads to a shortened ignition delay plus advanced combustion. (Kegl et al., 2013). Higher fuel density and viscosity lead to an advanced start of injection. This may be followed by incomplete combustion due to poor fuel atomization. Thus, the soot emission will increase (Nabi et al., 2012).

However, the higher the water concentration in the fuel jet, the more heat is needed to vaporize the water bound by fuel. The heat absorption by water vaporization lowers the surrounding intake air temperature in the engine cylinder. As a consequence, the ignition delay period extends and thus, combustion period shortens (Samec et al., 2002;

Armas et al., 2005). This lowers the peak temperatures in combustion region due to an increase in specific heat of the air-fuel mixture around the propagating flame across the cylinder (Bedford et al., 2000). Furthermore, the vaporization of water releases oxygen which promotes soot oxidation. In this study, however, the water content of both methyl esters was low, and for DFO and HVO, negligible.

At several loads, however, the methyl esters reduced the PN within the size range of 100 to 300 nm most likely due to oxygen bounded in mono-alkyl-ester molecules (Yang et al., 2007; Lapuerta et al., 2008). More complete combustion was enabled and more effective soot oxidation was promoted during the methyl ester usage compared with DFO or HVO.

Earlier studies have also reported how FAMEs, either as neat or as blending components, had a similar decreasing effect on the number of accumulation mode particles (Jung et al., 2006; Heikkilä et al., 2009; Rounce et al., 2012). Moreover, in the study of Hellier et al. (2019), waste date pit methyl ester led to the reduced PN within the size range of 100 to 200 nm compared to fossil diesel. However, they did not detect the corresponding PN reduction with RME or SME.

Above the particle size of 23 nm at 10% load at rated speed and under 70 nm at low idle, HVO showed the most favourable PN results. This was assumed to be caused by the low sulphur content when compared to DFO, and the high cetane number when compared to the methyl esters.

Share and number of particles above 23 nm

Table 5 shows the calculated percentage shares of the particles above the size of 23 nm. At several loads, the share of the particles above 23 nm was below 10%. Irrespective of fuel, the shares greater than 10% were detected at 10% load at rated speed, and at half load at intermediate speed. Furthermore, the share of the particles above 23 nm was above 10% with HVO at full load at rated speed, with DFO at 75% load at intermediate speed, and with RME and SME at idle.

Table 5. The share of particles larger than 23 nm out of the TPN for all fuels at different loads

Speed	Rated				Intermediate			Idle
Load (%)	100	75	50	10	100	75	50	0
PN > 23 nm (%)								
DFO	4.7	5.9	5.8	20	2.5	16	52	2.8
RME	6.9	2.2	6.3	75	2.6	1.9	46	15
SME	1.5	0.9	1.4	83	1.1	0.5	45	11
HVO	16	3.0	2.8	12	1.0	2.9	48	9.4

Fig. 7 presents the sum of detected PN above 23 nm at rated speed. At full load, DFO emitted the lowest PN sum whereas HVO the highest. From 75% to 10% load, HVO emitted the lowest PN sum. The highest PN sum was then detected with either of the methyl esters.

At full load at intermediate speed, DFO emitted the lowest PN sum whereas RME the highest, Fig. 8. But at 75% load, the PN sum was the lowest with SME and the highest with DFO. The sum of detected PN above 23 nm was not varied as much at half load as at the other loads.

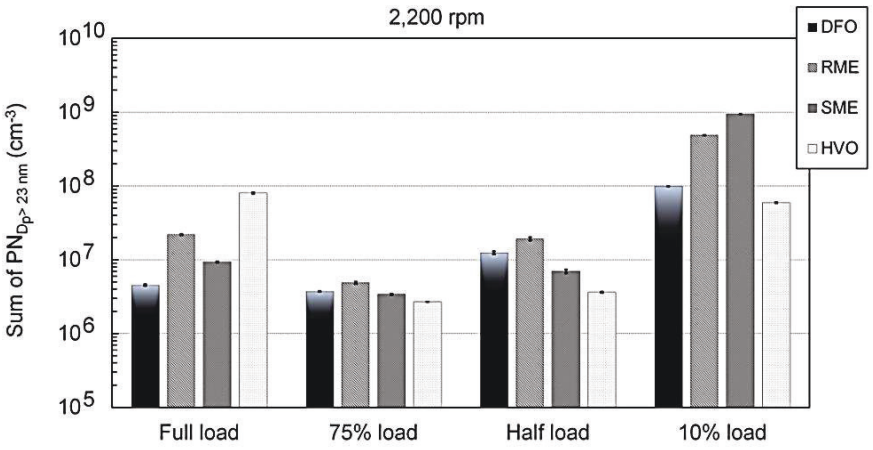

Figure 7. Sum of detected PN above 23 nm at rated speed.

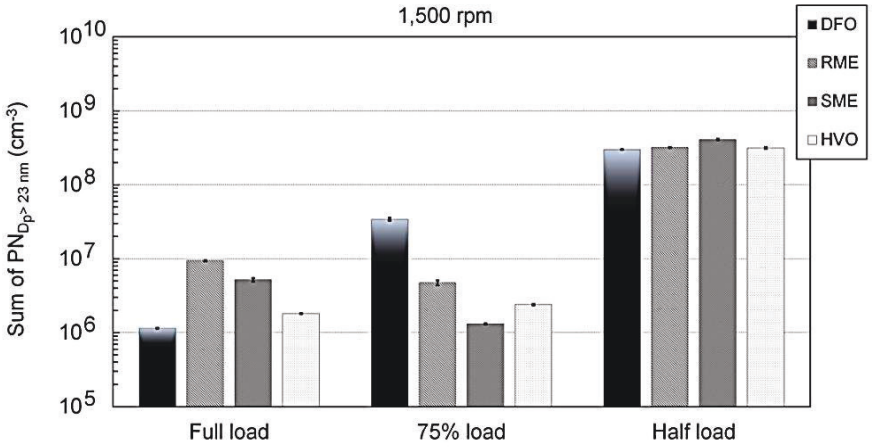

Figure 8. Sum of detected PN above 23 nm at intermediate speed.

For DFO, RME and SME, the sums of detected PN of above 23 nm were compared with the fatty acid compositions of RME and SME. DFO was selected for the comparison, as it did not contain fatty acids. Pearson correlations were calculated in order to find out measures of the strengths of relationships between the percentage shares of fatty acids and the sum of detected PN of above 23 nm. All analysed fatty acids, presented in Table 3, were considered. Moreover, the statistical significance of the correlation was assessed by using the Student's *t-test* under the null hypothesis. Significant correlations were only found between the shares of methyl palmitate (C16:0), methyl stearate (C18:0), methyl linoleate (C18:2), the saturated and the polyunsaturated fatty acids and the sum of detected PN of above 23 nm at 10% load at rated speed, Fig. 9. In this study, significant correlations did not exist at the other load points.

In general, the higher share of C16:0, C18:0, C18:2, the saturated and the polyunsaturated fatty acids, the more particles were detected above the size category of 23 nm. All correlations were both positive and significant at the confidence level of 93%. For the presented interdependences, the values of squared correlation factors were between 0.99–1.0. The calculated significance levels (*p*-values) were between

0.019–0.069. The least squares method was used to the illustrated linear fittings between the data points, Fig. 9.

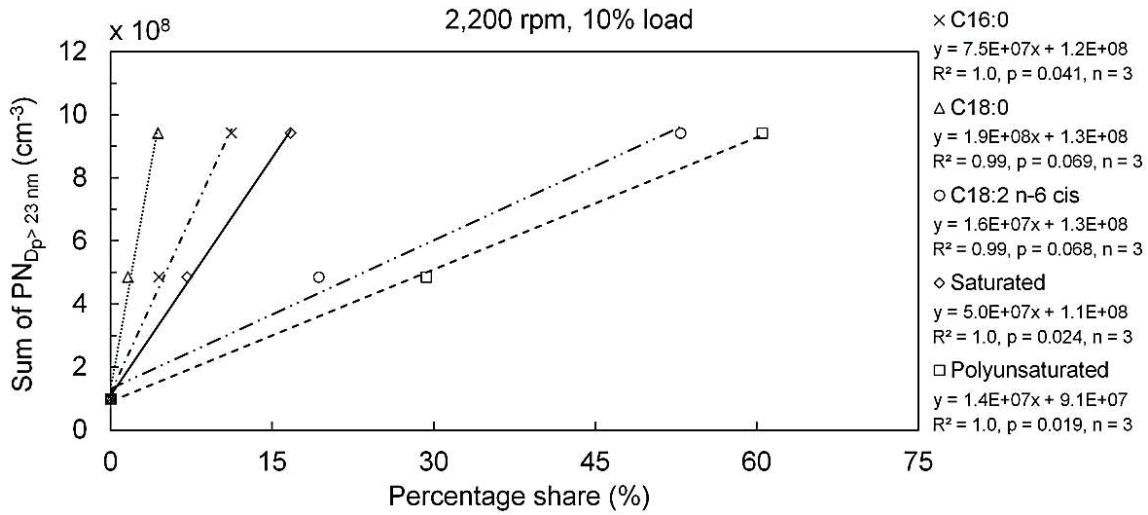

Figure 9. Sum of detected PN above 23 nm of DFO, RME and SME versus the percentage shares of C16:0, C18:0, C18:2), the saturated and the polyunsaturated fatty acids at 10% load at rated speed.

Bünger et al. (2016) found a very strong correlation between polyunsaturated fatty acids and particle mass. They fuelled a heavy-duty diesel engine with four different vegetable oils made from coconut, linseed, palm tree, and rapeseed.

Gaseous emissions and smoke

Generally, HVO was beneficial in terms of hydrocarbon (HC) and nitrogen oxide (NO_x) emissions, Table 6. Carbon monoxide (CO) emission was the lowest with DFO. The combined HC emission varied between 0.13–0.52 g kWh^{-1}. The smallest emissions, calculated all along the whole cycle, were created when HVO was used. The greatest emissions were emitted by SME.

Table 6. Cycle-weighted brake specific emissions of HC, NO_x and CO and smoke number ranges from lowest to highest within the NRSC cycle with different fuels

	HC (g kWh^{-1})	NO_x (g kWh^{-1})	CO (g kWh^{-1})	Smoke (FSN)
DFO	0.19	8.8	0.61	0.006–0.062
RME	0.38	10.0	1.55	0.005–0.012
SME	0.52	10.0	2.05	0.006–0.019
HVO	0.13	8.4	1.34	0.011–0.032

In the study of Niemi et al. (2016), the experimental setup was exactly the same when only the HC measurement is considered. For comparison, the cycle-weighted brake specific emission of HC was then 0.18 g. kWh^{-1} when DFO was used as fuel.

The less unburned HC available after fuel combustion, the smaller the likelihood that gaseous HC species affect the nanoparticle growth by condensation during the exhaust gas dilution and cooling processes (Kittelson, 1998; Khalek et al., 2000; Northrop et al., 2011).

Combined NO_x emissions varied between 8.6–10. g kWh^{-1}. The smallest NO_x emissions were created when HVO was used. The greatest NO_x emissions were emitted by RME. The difference between RME and SME was negligible. The combined CO emission varied between 0.61–2.04 g kWh^{-1}. The greatest emissions were produced by SME.

The level in smoke emission was negligible. If the test engine were a part of a typical agricultural powertrain instead of the laboratory use, it would have been equipped with an SCR catalyst. Therefore, the test engine had been tuned to the high NO_x, which caused, most likely, a decreasing effect on smoke.

Performance

The fuel conversion efficiency of the engine is presented in Figs 10 and 11 for the studied fuels at the speeds of 2,200 rpm and 1,500 rpm. The efficiencies were almost equal with the fuels.

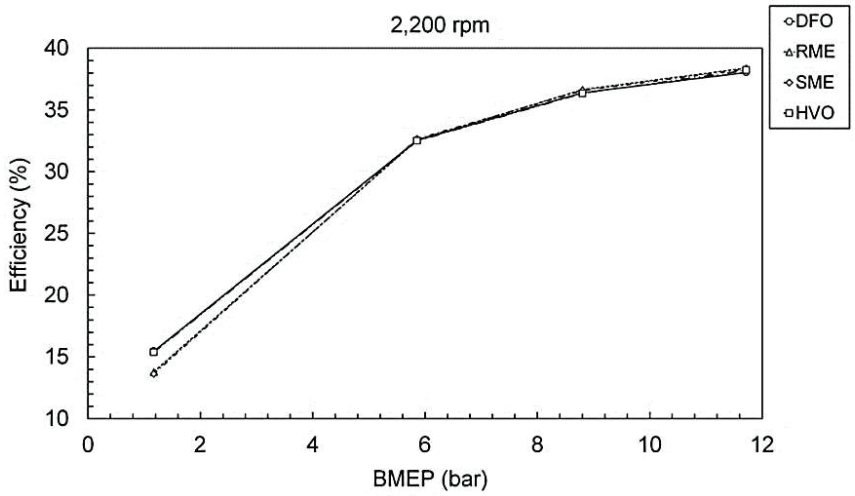

Figure 10. Engine efficiency against engine load at 2,200 rpm with the studied fuels.

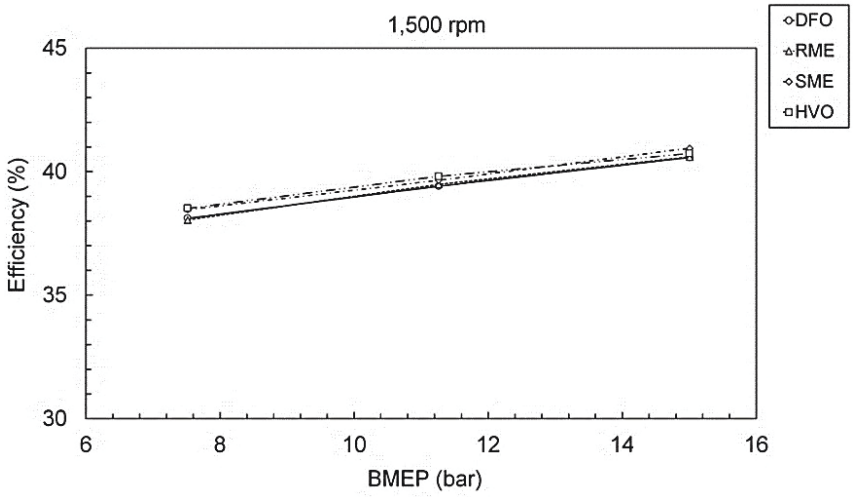

Figure 11. Engine efficiency against engine load at 1,500 rpm with the studied fuels.

CONCLUSIONS

This study focused on the determination of particle number emissions of a high-speed non-road diesel engine. The engine was driven with three bio-based fuels, RME, SME and HVO. DFO formed the baseline fuel. Based on the obtained results, the following conclusions could be drawn:

- Except at 10% load at rated speed, DFO or HVO produced the lowest particle numbers under the size of 30 nm.
- Except at 10% load at rated speed and at half load at intermediate speed, the methyl esters reduced the particle numbers within the size range of 100 to 300 nm most likely due to oxygen bounded in mono-alkyl-ester molecules.
- HVO emitted the least particles above the particle size of 23 nm at 10% load at rated speed and under 70 nm at low idle; this was assumed to be caused by the low sulphur content when compared to DFO, and the high cetane number when compared to the methyl esters.
- In case of RME and SME, both positive and significant correlations were found between the sum of the particle numbers detected above the size category of 23 nm and methyl palmitate (C16:0), methyl stearate (C18:0) and methyl linoleate (C18:2) contents at 10% load at rated speed.
- HVO was beneficial in terms of nitrogen oxide (NO_x) and hydrocarbon (HC) emissions.
- Carbon monoxide (CO) emission was the lowest with DFO.
- The level in smoke emission was negligible.

ACKNOWLEDGEMENTS. This study was one part of the national research project Trends in real-world particle emissions of diesel and gasoline vehicles (TREAM). The authors wish to thank Business Finland (former Tekes – the Finnish Funding Agency for Innovation) for the financial support of the program. AGCO Power placed the experimental engine at our disposal and the other industrial partners Dinex Ecocat Ltd, Neste, MAN and Nanol Technologies also funded the project. Our warmest thanks to all these companies. The Novia University of Applied Sciences allowed us to use the engine laboratory for this study. The authors wish to thank Dr. Jonas Waller, Mr. Holger Sved and Mr. John Dahlbacka for this possibility. The Faculty of Technology at the University of Vaasa granted the working time necessary for rendering this work into the published form. The authors wish to thank the Dean of the Faculty, Professor Erkki Antila, and Professor Timo Vekara.

REFERENCES

Alanen, J., Simonen, P., Saarikoski, S., Timonen, H., Kangasniemi, O., Saukko, E. & Keskinen, J. 2017. Comparison of primary and secondary particle formation from natural gas engine exhaust and of their volatility characteristics. *Atmos. Chem. Phys.* **17**(14), 8739–8755.

Alrefaai, M.M., Peña, G.D.G., Raj, A., Stephen, S., Anjana, T. & Dindi, A. 2018. Impact of dicyclopentadiene addition to diesel on cetane number, sooting propensity, and soot characteristics. *Fuel* **216**, 110–120.

An, W.J., Pathak, R.K., Lee, B.H. & Pandis, S.N. 2007. Aerosol volatility measurement using an improved thermodenuder: Application to secondary organic aerosol. *J. Aerosol Sci.* **38**(3), 305–314.

Armas, O., Ballesteros, R., Martos, F.J. & Agudelo, J.R. 2005. Characterization of light duty diesel engine pollutant emissions using water-emulsified fuel. *Fuel* **84**(7–8), 1011–1018.

Bach, F., Tschöke, H. & Simon, H. 2009. Influence of Alternative Fuels on Diesel Engine Aftertreatment. In: 7th International Colloquium Fuels - mineral oil based and alternative fuels 14–15th January, Ostfildern, Germany.

Barrientos, E.J., Maricq, M.M., Boehman, A.L. & Anderson, J.E. 2015. Impact of ester structures on the soot characteristics and soot oxidative reactivity of biodiesel. *SAE Tech. Pap.* 2015-01-1080.

Bedford, F., Rutland, C., Dittrich, P., Raab, A. & Wirbeleit, F. 2000. Effects of direct water injection on DI diesel engine combustion. *SAE Tech. Pap.* 2000-01-2938.

Bünger, J., Bünger, J.F., Krahl, J., Munack, A., Schröder, O., Brüning, T., Hallier, E. & Westphal, G.A. 2016. Combusting vegetable oils in diesel engines: the impact of unsaturated fatty acids on particle emissions and mutagenic effects of the exhaust. *Arch. toxicol.* **90**(6), 1471–1479.

Eastwood, P. 2008. Particulate Emissions from Vehicles. Chichester: John Wiley & Sons Ltd. 494 p. ISBN 978-0-470-72455-2.

Filippo, A.D. & Maricq, M.M. 2008. Diesel nucleation mode particles: Semivolatile or solid?. *Environ. Sci. Technol.* **42**(21), 7957–7962.

Heikkilä, J., Virtanen, A., Rönkkö, T., Keskinen, J., Aakko-Saksa, P. & Murtonen, T. 2009. Nanoparticle emissions from a heavy-duty engine running on alternative diesel fuels. *Environ. Sci. Technol.* **43**(24), 9501–9506.

Hellier, P., Jamil, F., Zaglis-Tyraskis, E., Ala'a, H., Al Haj, L. & Ladommatos, N. 2019. Combustion and emissions characteristics of date pit methyl ester in a single cylinder direct injection diesel engine. *Fuel* **243**, 162–171.

ISO 8178-4:2017. 2017. Reciprocating internal combustion engines. Exhaust emission measurement. Part 4: Steady-state and transient test cycles for different engine applications. 237 pp.

Karjalainen, P., Pirjola, L., Heikkilä, J., Lähde, T., Tzamkiozis, T., Ntziachristos, L., Keskinen, J. & Rönkkö, T. 2014. Exhaust particles of modern gasoline vehicles: A laboratory and an on-road study. *Atmos. Environ.* **97**, 262–270.

Kegl, B., Kegl, M. & Pehan, S. 2013. Green diesel engine. Biodiesel usage in diesel engines. London: Springer-Verlag. 263 p. ISBN 978-1-4471-5324-5.

Khalek, I.A., Kittelson, D.B. & Brear, F. 2000. Nanoparticle growth during dilution and cooling of diesel exhaust: Experimental investigation and theoretical assessment. *SAE Tech. Pap.* 2000-01-0515.

Kittelson, D.B. 1998. Engines and nanoparticles: a review. *J. Aerosol Sci.* **29**(5–6), 575–588.

Kittelson, D.B., Arnold, M. & Watts, W.F. 1999. Review of diesel particulate matter sampling methods: Final Report. University of Minnesota, Minneapolis, MN, 63.

Jung, H., Kittelson, D.B. & Zachariah, M.R. 2006. Characteristics of SME biodiesel-fueled diesel particle emissions and the kinetics of oxidation. *Environ. Sci. Technol.* **40**(16), 4949–4955.

Jungmeier, G., Pucker, J., Ernst, M., Haselbacher, P., Lesschen, J.P., Kraft, A., Schulzke, T. & van Loo, E.N. 2016. Improving the sustainability of fatty acid methyl esters (Fame–biodiesel)–assessment of options for industry and agriculture. In: The 24th European Biomass Conference and Exhibition, 6–9 June 2016, Amsterdam, The Netherlands.

Lapuerta, M., Armas, O. & Rodriguez-Fernandez, J. 2008. Effect of biodiesel fuels on diesel engine emissions. *Progr. Energy Combust. Sci.* **34**(2), 198–223.

Li, R., Wang, Z., Ni, P., Zhao, Y., Li, M. & Li, L. 2014. Effects of cetane number improvers on the performance of diesel engine fuelled with methanol/biodiesel blend. *Fuel* **128**, 180–187.

Lähde, T., Rönkkö, T., Happonen, M., Söderström, C., Virtanen, A., Solla, A., Kytö, M., Rothe, D. & Keskinen, J. 2011. Effect of fuel injection pressure on a heavy-duty diesel engine nonvolatile particle emission. *Environ. Sci. Technol.* **45**(6), 2504–2509.

Lähde, T., Rönkkö, T., Virtanen, A., Solla, A., Kytö, M., Söderström, C. & Keskinen, J. 2010. Dependence between nonvolatile nucleation mode particle and soot number concentrations in an EGR equipped heavy-duty diesel engine exhaust. Environ. Sci. Technol. 44(8), 3175–3180.

Maricq, M.M., Chase, R.E., Xu, N. & Laing, P.M. 2002. The effects of the catalytic converter and fuel sulfur level on motor vehicle particulate matter emissions: light duty diesel vehicles. *Environ. Sci. Technol.* **36**(2), 283–289.

Mathis, U., Mohr, M., Kaegi, R., Bertola, A. & Boulouchos, K. 2005. Influence of diesel engine combustion parameters on primary soot particle diameter. *Environ. Sci. Technol.* **39**(6), 1887–1892.

Mathis, U., Ristimaki, J., Mohr, M., Keskinen, J., Ntziachristos, L., Samaras, Z. & Mikkanen, P. 2004. Sampling conditions for the measurement of nucleation mode particles in the exhaust of a diesel vehicle. *Aerosol Sci. Technol.* **38**(12), 1149–1160.

Mollenhauer, K. & Schreiner, K. 2010. History and fundamental principles of the diesel engine. In: K. Mollenhauer & H. Tschöke (Eds.), Handbook of diesel engines, pp. 3–30. Heidelberg, Berlin: Springer-Verlag. ISBN 978-3-540-89082-9.

Nabi, M.N., Brown, R.J., Ristovski, Z. & Hustad, J.E. 2012. A comparative study of the number and mass of fine particles emitted with diesel fuel and marine gas oil (MGO). *Atmos. Environ.* **57**, 22–28.

Niemi, S., Vauhkonen, V., Mannonen, S., Ovaska, T., Nilsson, O., Sirviö, K., Heikkilä, S. & Kiijärvi, J. 2016. Effects of wood-based renewable diesel fuel blends on the performance and emissions of a non-road diesel engine. *Fuel* **186**, 1–10.

Northrop, W.F., Madathil, P.V., Bohac, S.V., Assanis, D.N. 2011. Condensational Growth of Particulate Matter from Partially Premixed Low Temperature Combustion of Biodiesel in a Compression Ignition Engine. *Aerosol Sci. Technol.* **45**, 26–36.

Nousiainen, P., Niemi, S., Rönkkö, T., Karjalainen, P., Keskinen, J., Kuuluvainen, H., Pirjola, L. & Saveljeff, H. 2013. Effect of injection parameters on exhaust gaseous and nucleation mode particle emissions of a Tier 4i nonroad diesel engine. *SAE Tech. Pap.* 2013-01-2575.

Ntziachristos, L., Giechaskiel, B., Pistikopoulos, P., Samaras, Z., Mathis, U., Mohr, M., Ristimäki, J., Keskinen, J., Mikkanen, P., Casati, R., Scheer, V. & Vogt, R. 2004. Performance evaluation of a novel sampling and measurement system for exhaust particle characterization. *SAE Tech. Pap.* 2004-01-1439.

Pinzi, S., Rounce, P., Herreros, J.M., Tsolakis, A. & Dorado, M.P. 2013. The effect of biodiesel fatty acid composition on combustion and diesel engine exhaust emissions. Fuel 104, 170–182.

Rounce, P., Tsolakis, A. & York, A.P.E. 2012. Speciation of particulate matter and hydrocarbon emissions from biodiesel combustion and its reduction by aftertreatment. Fuel **96**, 90–99.

Rönkkö, T., Virtanen, A., Vaaraslahti, K., Keskinen, J., Pirjola, L. & Lappi, M. 2006. Effect of dilution conditions and driving parameters on nucleation mode particles in diesel exhaust: Laboratory and on-road study. *Atmos. Environ.* **40**(16), 2893–2901.

Rönkkö, T., Virtanen, A., Kannosto, J., Keskinen, J., Lappi, M. & Pirjola, L. 2007. Nucleation mode particles with a nonvolatile core in the exhaust of a heavy duty diesel vehicle. *Environ. Sci. Technol.* **41**(18), 6384–6389.

Samec, N., Kegl, B. & Dibble, R.W. 2002. Numerical and experimental study of water/oil emulsified fuel combustion in a diesel engine. *Fuel* **81**(16), 2035–2044.

Schönborn, A., Ladommatos, N., Williams, J., Allan, R. & Rogerson, J. 2009. The influence of molecular structure of fatty acid monoalkyl esters on diesel combustion. *Combustion and flame* **156**(7), 1396–1412.

Teboil. 2019. Product data - summer quality. Helsinki. Available from: https://www.teboil.fi /globalassets/tuotetiedotteet/motor_lammitys-kl_2019.pdf.

Tsolakis, A. 2006. Effects on particle size distribution from the diesel engine operating on RME-biodiesel with EGR. *Energy & Fuels* **20**(4), 1418–1424.

Szybist, J.P., Song, J., Alam, M. & Boehman, A.L. 2007. Biodiesel combustion, emissions and emission control. *Fuel Process. Technol.* **88**(7), 679–691.

Vaaraslahti, K., Virtanen, A., Ristimäki, J. & Keskinen, J. 2004. Nucleation mode formation in heavy-duty diesel exhaust with and without a particulate filter. *Environ. Sci. Technol.* **38**(18), 4884–4890.

Vaaraslahti, K., Keskinen, J., Giechaskiel, B., Solla, A., Murtonen, T. & Vesala, H. 2005. Effect of lubricant on the formation of heavy-duty diesel exhaust nanoparticles. *Environ. Sci. Technol.* **39**(21), 8497–8504.

Wang, X., Grose, M.A., Caldow, R., Osmondson, B.L., Swanson, J.J., Chow, J.C., Watson, J.G., Kittelson, D.B., Li, Y., Xue, J., Jung, H. & Hu, S. 2016a. Improvement of Engine Exhaust Particle Sizer (EEPS) Size Distribution Measurement – II. Engine Exhaust Particles. *J. Aerosol Sci.* **92**, 83–94.

Wang, Z., Li, L., Wang, J. & Reitz, R.D. 2016b. Effect of biodiesel saturation on soot formation in diesel engines. *Fuel* **175**, 240–248.

Wiedensohler, A., Birmili, W., Nowak, A., Sonntag, A., Weinhold, K., Merkel, M., Wehner, B., Tuch, T., Pfeifer, S., Fiebig, M., Fjäraa, A.M., Asmi, E., Sellegri, K., Depuy, R.,Venzac, H., Villani, P., Laj, P., Aalto, P., Ogren, J.A., Swietlicki, E., Williams, P., Roldin, P., Quincey, P., Hüglin, C., Fierz-Schmidhauser, R., Gysel, M., Weingartner, E., Riccobono, F., Santos, S., Grüning, C., Faloon, K., Beddows, D., Harrison, R., Monahan, C., Jennings, S.G., O'Dowd, C.D., Marinoni, A., Horn, H.-G., Keck, L., Jiang, J., Scheckman, J., Mcmurry, P.H., Deng, Z., Zhao, C.S., Moerman, M., Henzing, B., De Leeuw, G., Löschau, G., Bastian, S. 2012. Mobility particle size spectrometers: harmonization of technical standards and data structure to facilitate high quality long-term observations of atmospheric particle number size distributions. *Atmos. Meas. Tech.* **5**, 657–685.

Wiedensohler, A., Wiesner, A., Weinhold, K., Birmili, W., Hermann, M., Merkel, M., Müller, T., Pfeifer, S., Schmidt, A., Tuch, T., Velarde, F., Quincey, P., Seeger, S. & Nowak, A. 2018. Mobility particle size spectrometers: Calibration procedures and measurement uncertainties. *Aerosol Sci. Technol.* **52**(2), 146–164.

Zhu, L., Cheung, C.S. & Huang, Z. 2016. A comparison of particulate emission for rapeseed oil methyl ester, palm oil methyl ester and soybean oil methyl ester in perspective of their fatty ester composition. *Appl. Therm. Eng.* **94**, 249–255.

Yang, H.H., Chien, S.M., Lo, M.Y., Lan, J.C. W., Lu, W.C. & Ku, Y.Y. 2007. Effects of biodiesel on emissions of regulated air pollutants and polycyclic aromatic hydrocarbons under engine durability testing. *Atmos. Environ.* **41**(34), 7232–7240.

Paper II

Agronomy Research **16**(S1), 1159–1168, 2018
https://doi.org/10.15159/AR.18.087

Exhaust particle size distributions of a non-road diesel engine in an endurance test

T. Ovaska[1,*], S. Niemi[1], T. Katila[2] and O. Nilsson[1]

[1]University of Vaasa, School of Technology and Innovations, P.O. Box 700, FI-65101 Vaasa, Finland
[2]AGCO Power Oy, Linnavuorentie 8–10, FI37240 Linnavuori, Nokia, Finland
[*]Correspondence: teemu.ovaska@uva.fi

Abstract. The main objective of this study was to find out how the non-road diesel engine running period of 500 hours affects the exhaust particle size distribution. By means of an engine exhaust particle sizer (EEPS), particle number was measured before the endurance test and after 250 and 500 hours of engine operation. The size distributions were determined at full and 75% loads both at rated and at intermediate speeds. The soot, gaseous emissions and the basic engine performance were also determined and lubricating oil was analysed a few times during the running period. A blend of low-sulphur fossil diesel and soybean methyl ester (B20) was used as fuel in the 4-cylinder, turbocharged, intercooled engine which was equipped with a diesel oxidation catalyst (DOC) and a selective catalytic reduction (SCR) system. All emissions were measured downstream the catalysts. During the 500 hours of operation, the particle number increased considerably within an approximate size range of 7 to 30 nm. Between the initial and final measurements, no notable differences were observed in the particle number emissions within a particle size range of 50 to 200 nm. The copper content of lubricating oil also increased significantly during the 500 hours' experiment. One possible reason for the substantial increase in the nucleation mode particle number was assumed to be copper, which is one of the metallic elements originating from engine wear. The engine efficiency was almost equal, and the differences both in smoke and hydrocarbon emission were negligible throughout the 500 hours' experiment.

Key words: particle number, exhaust aftertreatment, B20, blend fuel, soybean methyl ester.

INTRODUCTION

Some of the combustion products of diesel engines have long been recognized as harmful pollutant emissions that affect the air quality, human health, and climate change. Both the gaseous and particulate emissions are regulated worldwide.

The emission legislation has been met by exploiting different engine design, aftertreatment system, and fuel technologies. All these technologies are needed gradually during 2019–2020 when the new emission stage (Stage V), regulated by the European Commission and the Council, comes into force. The regulation also limits the particle number (PN) emissions of the non-road diesel engines. (EU Regulation 2016/1628). The new PN limitation enforces the usage of diesel particulate filters (DPF) along with the possible catalyst devices in the near future.

Diesel engine exhaust contains non-volatile particles which form the size distribution with two distinctive particle modes; soot mode and core (nucleation) mode. (Kittelson, 1998; Rönkkö et al., 2006; Filippo & Maricq, 2008; Lähde et al., 2010). The formation of the core mode particles is considered to initiate in the cylinder. Soot particles are formed in the cylinder, when either the fuel or the remnants of lubricating oil do not burn completely during combustion. The particle mean diameters in nucleation mode are under 40 nm, whereas the mean diameter range in soot mode is 20–100 nm.

The particles with mean diameters of less than 2.5 µm or 10 µm are often reported to be adverse to human health. In addition, the concentrations of black carbon and nanosized particles < 100 nm may cause health risks. (Oberdörster et al., 2005; Janssen et al., 2011). The smallest particles can deposit onto the lungs and may penetrate into the cardiovascular and even cerebrovascular system via respiratory organs. (Anderson et al., 2012; Oravisjärvi et al., 2014).

Reliable operation of a diesel engine is ensured when the engine is capable of running without failures. When the engine is run with the same fuel in the constant ambient conditions, one can assume that heterogeneous air/fuel mixture preparation during the ignition delay, fuel ignition quality, residence time at different combustion temperatures, and expansion duration are equal. Therefore, the emission formation mechanisms and the resultant concentrations of the different emission species in the exhaust will be the same.

However, mechanical wear of the engine also affects the non-volatile particle number of diesel exhaust in long-term use. The wear metals, such as Fe, Al, Cu, Zn, Co, and Ni, are found among the exhaust particle ash content. (Agarwal, 2005; Dwivedi et al., 2006; Sarvi et al., 2011; Sharma & Murugan, 2017).

This study examined how the non-road diesel engine running period of 500 hours affects the exhaust particle size distribution. A blend of low-sulphur fossil diesel and soybean methyl ester (B20) was used as fuel in the high-speed non-road engine which was equipped with a diesel oxidation catalyst (DOC) and a selective catalytic reduction (SCR) system. The particle number were measured before the endurance test and after 250 and 500 hours of engine operation at full and 75% loads both at rated and at intermediate speeds. The soot, gaseous emissions and the basic engine performance were determined as well. During the experiments, the engine control parameters were kept constant.

MATERIALS AND METHODS

The experimental measurements were performed by the University of Vaasa (UV) at the internal combustion engine (ICE) laboratory of the Technobothnia Research Centre in Vaasa, Finland.

Engine

The test engine was a 4-cylinder non-road diesel engine equipped with a common-rail injection system. The new, turbocharged, intercooled engine was equipped with a DOC and a urea-based SCR system. During all the measurements, emissions were recorded downstream the catalysts.

The test engine was installed in a test bed and loaded by means of an eddy-current dynamometer of model Horiba WT300. The main engine specification is given in Table 1.

Fuel and lubricating oil

Fuel used during the endurance test was a blend of low-sulphur fossil diesel and soybean methyl ester (B20). The fuel consisted of 20 vol.-% soybean methyl ester (SME) and of 80 vol.-% commercial low-sulphur diesel fuel oil (DFO).

Table 1. Main engine specification

Engine	AGCO POWER 49 AWI
Cylinder number	4
Bore (mm)	108
Stroke (mm)	134
Swept volume (dm^3)	4.9
Rated speed (rpm)	2,100
Rated power (kW)	103
Maximum torque with rated speed (Nm)	462*
Maximum torque with 1,500 rpm (Nm)	583*

*conformable to measured torques obtained with B20 fuel.

The commercially available Valtra Engine CR-4, 10W-40 (ACEA E9, API CJ-4) was used as lubricating oil in the engine. Lubricating oil was analysed after the operating hours of 0, 207, 357 and 553. The analysing results of the lubricating oil have been reported earlier by Sirviö et al. (2016).

Analytical instruments

The adopted measurement instruments are listed in Table 2. Before the measurements, the analysers were calibrated manually once a day according to the instructions of the instrument manufacturers. The arrangement of the test bench and measurement devices is seen in Fig. 1 in which temperature sensors are abbreviated to TS.

During the measurements, the particles from a size range of 5.6 to 560 nm were recorded by using the engine exhaust particle sizer (EEPS), for which the sample flow rate was adjusted at 5.0 L min^{-1}. The 'SOOT' inversion was applied in the EEPS data processing. The exhaust sample was first diluted with ambient air by means of a rotating disc diluter (RDD) (model MD19-E3, Matter Engineering AG). The dilution ratio used in the RDD was constant 60 during the measurements. The exhaust aerosol sample was conducted to the RDD and a dilution air was kept at 150 °C. The diluted sample (5 L min^{-1}) was further diluted by purified air with a dilution ratio of 2. Thus, the total dilution ratio used in particle size distribution measurements was 120. In this way, mainly the non-volatile particle fraction 150°C is measured by the EEPS.

Three-minute stable time intervals were chosen for the results recordings of the particle number (PN) and particle size distributions. The average values, calculated from the recordings, were multiplied by the dilution ratio of the exhaust sample.

The recorded smoke value was the average of three consecutively measured smoke numbers.

Table 2. Measuring equipment

Parameter	Device	Technology
Particle number and size distribution	TSI EEPS 3090	spectrometer
Hydrocarbons	J.U.M. VE7	HFID
Smoke	AVL 415 S	optical filter
NO_x	Eco Physics CLD 822 M h	chemiluminescence
NO_x, λ	WDO UniNO_x sensors	ZrO_2-based multilayer
O_2	Siemens Oxymat 61	paramagnetic
Air mass flow rate	ABB Sensyflow P	thermal mass

The sensor data were collected by means of software, made in the LabVIEW system-design platform. In addition to the gaseous emissions, the systems recorded the temperatures of cooling water, intake air and exhaust gas plus the pressures of the intake air and exhaust gas. The engine control parameters were followed via WinEEM4 engine management software, provided by the engine manufacturer.

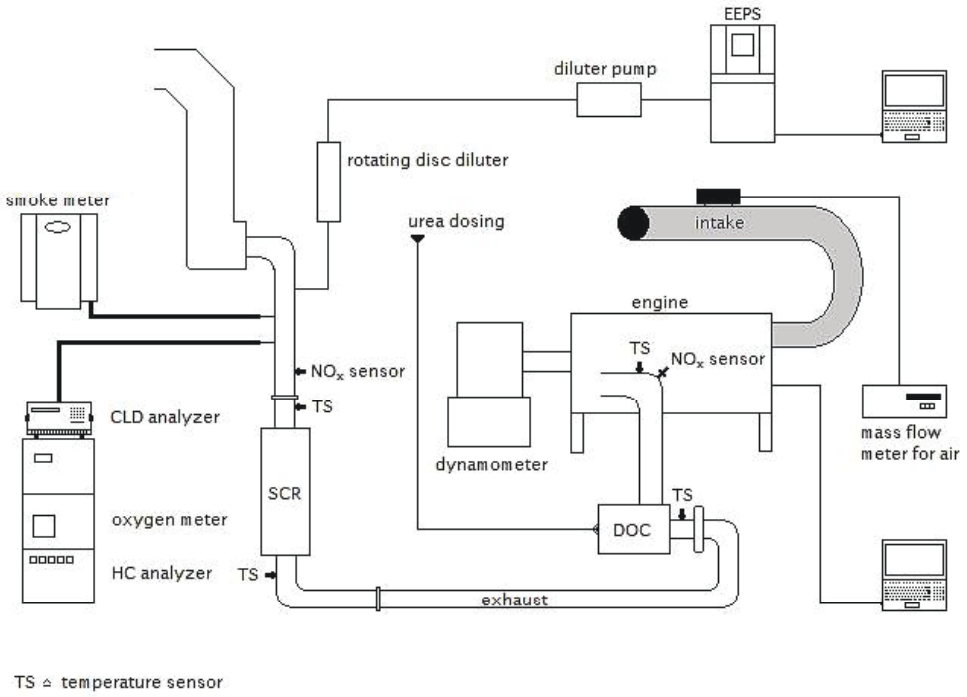

Figure 1. Experimental set-up.

Based on the measured hydrocarbon (HC) concentrations, the brake specific emissions of HC were calculated according to the ISO 8178 standard.

Experimental matrix and running procedure

Before the endurance test of 500 running hours, the baseline performance and emissions measurements were performed with a new engine installation. Thereafter, the engine was daily operated according to a defined running procedure consisting of sequential load points which were supposed to represent the actual use of the engine as

accurately as possible. After 250 hours of engine operation, the performance and emissions measurements were repeated, as they were after 500 hours.

The measurements were conducted at full and 75% loads both at rated and at intermediate speeds. The rated engine speed was 2,100 rpm and the intermediate speed 1,500 rpm.

Before the measurements, the intake air temperature was adjusted at 50 °C downstream the charge air cooler when the engine was run at full load at rated speed. The temperature was controlled manually by regulating cooling water flow to the heat exchanger. After this initial adjustment, the temperature was allowed to change with engine load and speed.

During the measurements, the engine was run with urea dosing, the alpha ratio being 0.95.

Before the recordings at each load point, it was waited that the engine had stabilized, the criteria being that the temperatures of coolant water, intake air and exhaust were stable. The length of the measurement period was not tied to a certain time.

All measurement values were recorded once at each load point.

Daily operation

The daily running cycle between the measurements is given in Table 3. The engine was run by an autopilot-system which was implemented into the LabVIEW platform. The autopilot system made it possible to regulate the dynamometer automatically.

Table 3. Daily cycle of the endurance test

Point	Speed (rpm)	Load (%)	Torque (Nm)	Duration (min)
1	1,000	0	0	15
2	1,300	14	75	15
3	1,600	21	123	15
4	1,800	29	175	30
5	2,000	40	214	15
6	2,100	51	236	15
7	1,900	60	346	15
8	1,700	49	293	15
9	1,500	30	175	30
10	1,200	25	127	15

RESULTS AND DISCUSSION

Particle size distributions

Generally, the PN increased considerably within an approximate size range of 7 to 30 nm during the 500 hours of engine operation. Between the initial and final measurements, no notable differences were, however, observed in the PN emissions within a particle size range of 50 to 200 nm.

Fig. 2 shows the particle size distributions at full and 75% loads both at rated and intermediate speeds. For both speeds and loads, a bimodal shape was detected for the distributions. One peak was detected at a particle size of ca. 10 nm and the other at ca. 32–60 nm. At the initial measurements, the lowest quantity of particles was observed within the size ranges of 7–15 nm and 24–86 nm regardless of the engine speed or load.

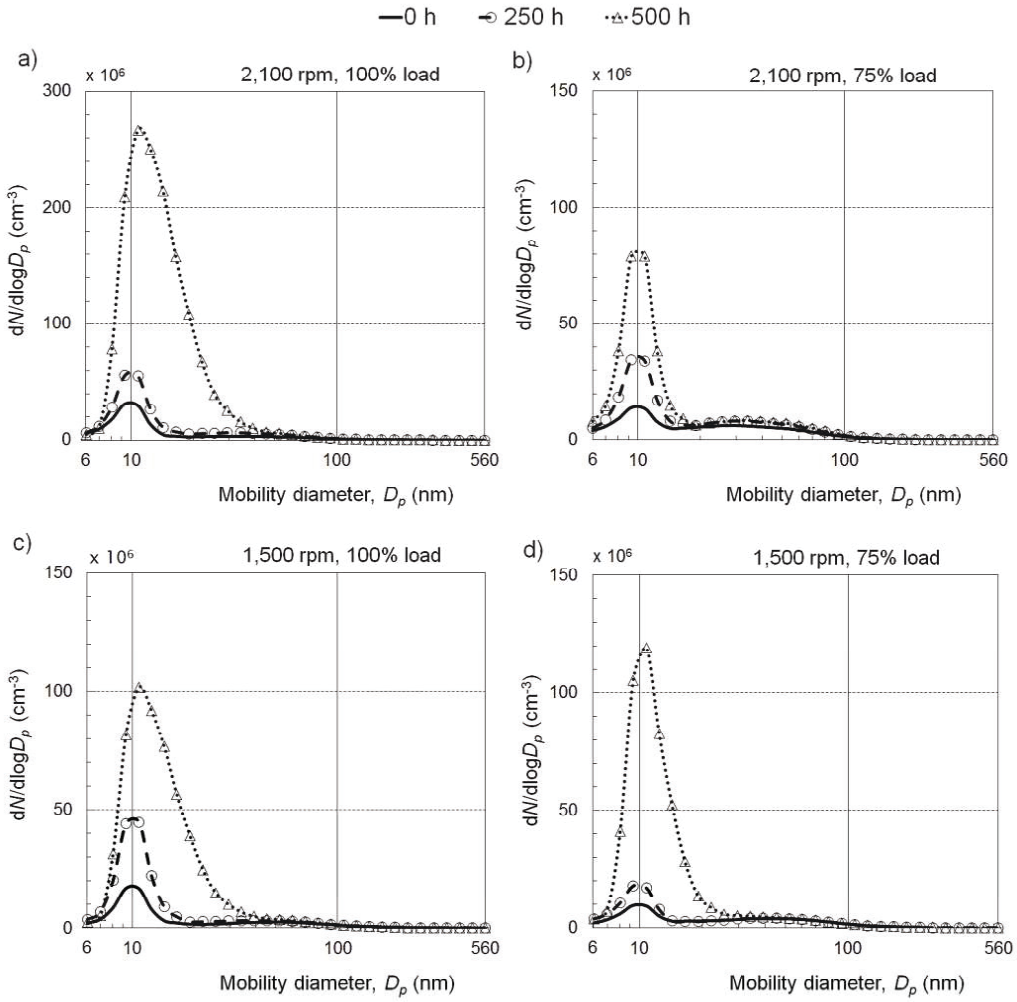

Figure 2. Effect of running period of 500 hours on the exhaust particle size distribution a) at full and b) 75% load at rated speed, and c) at full and d) 75% load at intermediate speed.

After 250 hours' operation, the number of particles under 154 nm increased compared to the baseline apart from at intermediate speed at 75% load where the PN between 86–200 nm decreased. The greatest PN was detected at the size category of 10 nm. At rated speed, the PN was here 1.9-fold at full load and 2.5-fold at 75% load compared to the baseline. At intermediate speed at full and 75% load, the PN was 2.7-fold and 1.8-fold, respectively, at this size category.

After the 500 hours' operation, the PN increased within the size range of 7–200 nm compared to baseline. The highest particle numbers of this study were recorded within the size range of 8–42 nm. The PN peaked again at the size category of 10 nm. Now, at rated speed, the PN was 9.0-fold at full load and 5.9-fold at 75% load compared to the baseline. At intermediate speed at full and 75% load, the PN was 6.1-fold and 13-fold, respectively.

Usually, the initiation of the nucleation is assumed to be sulphur driven. First, when sulphur from fuel and lubricating oil burn in the cylinder, sulphur dioxide is formed. In

the oxidation catalyst, sulphur dioxide of exhaust gas can be converted to sulphur trioxide under high exhaust temperatures. (Giechaskiel et al., 2007) Thus, the nucleation mode of particles downstream the SCR catalyst may be caused by sulphuric acid originating from reaction between sulphur trioxide and water vapor (Vaaraslahti et al., 2004; Arnold et al., 2006; Rönkkö et al, 2007; Biswas et al., 2008). However, the sulphur content of fuel or lubricating oil were not observed to change during the study.

Sirviö et al. (2016) observed that the copper concentration in lubricating oil increased significantly from 49 to 420 ppm between the oil analysis hours of 357 and 553. Copper is one of the metallic elements originating from engine wear. However, the contents of other wear metals, such as lead, did not increase, as would have been probable in the case of damage in bearings or other engine parts (Sirviö et al. 2016).

Schumacher et al. (2005) fuelled an on-road truck diesel engine with the different blends of hydrogenated soybean ethyl-ester. During the first 50,000 miles of operation, 2–3 lubrication oil samples were taken. The samples contained the high levels of copper which were suggested to originate from a copper oil cooler.

For this paper, one possible reason for the substantial increase in the nucleation mode particle number was assumed to be copper which originated from the break-in of a new oil cooler.

Fig. 3 illustrates the effect of the operation time on the measured total particle number (TPN, from 6 to 560 nm), where linear interdependences are presented by using the PN data from each load point.

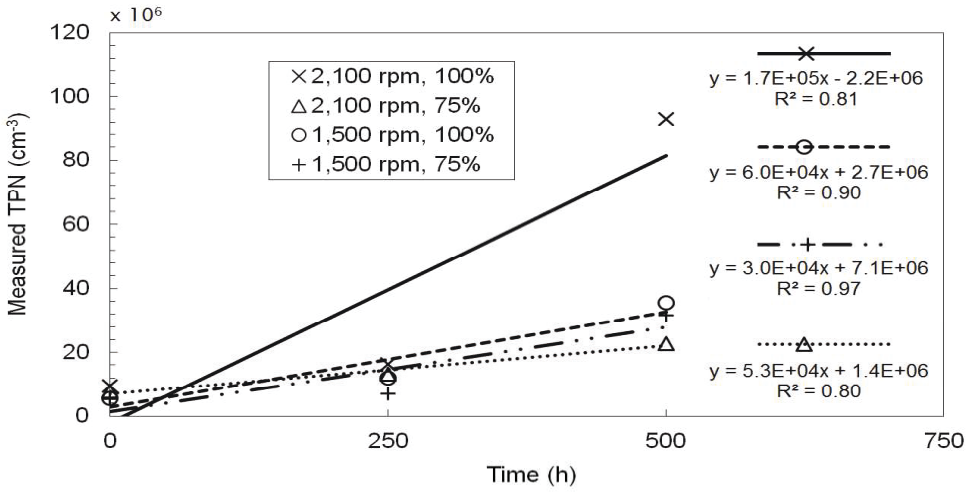

Figure 3. Measured TPN as a function of the operation time.

All correlations were positive irrespective of the engine speed or load. For the presented interdependences, the values of squared correlation factors were between 0.80–0.97.

In general, the total particle numbers were the smallest at the initial measurement and far the highest after 500 hours of engine operation. The least TPN were detected always at intermediate speed at 75% load, whereas the highest TPN were recorded every time at rated power.

HC emissions and smoke

The brake specific HC emission was minor throughout the 500 hours of engine operation, Fig. 4. At rated speed, the HC emission varied from 0.01 to 0.02 g kWh^{-1}, and at intermediate speed from 0.006 to 0.009 g kWh^{-1}. The engine was equipped with a DOC, which reduce the HC concentration of exhaust by promoting the chemical oxidation of HC. Therefore, the HC emission was almost negligible at both loads and speeds.

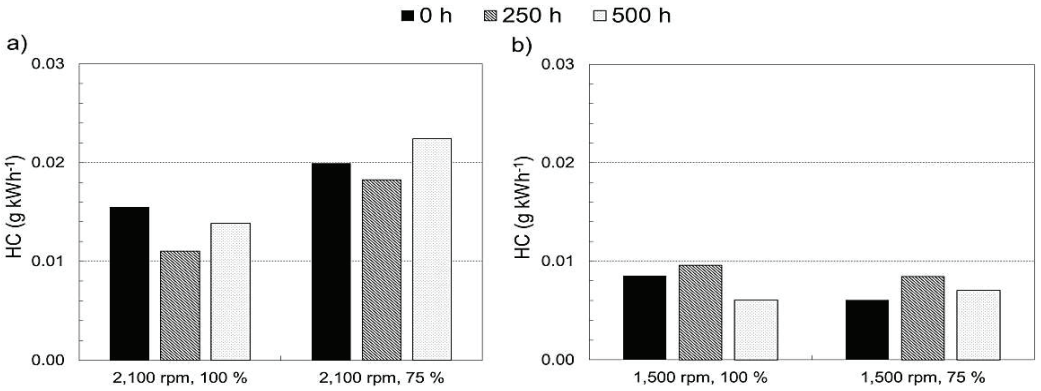

Figure 4. Brake specific HC emissions a) at full and 75% load at rated speed, and b) at full and 75% load at intermediate speed.

Fig. 5 depicts the smoke emissions. Both at rated and at intermediate speed, the smoke was very low, the FSN readings varying from 0.020 to 0.064. No reliable conclusion can be drawn from the smoke emission.

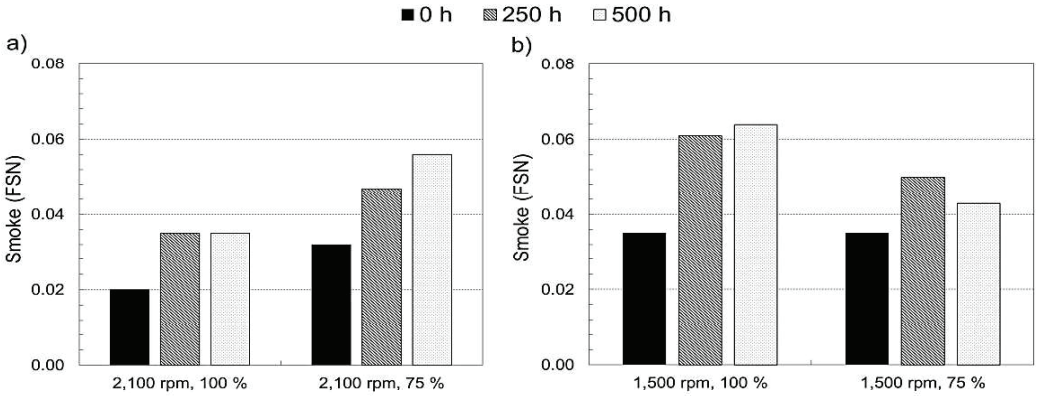

Figure 5. Exhaust smoke a) at full and 75% load at rated speed, and b) at full and 75% load at intermediate speed.

When comparing either the HC or smoke emissions, the differences were negligible, and no clear trend was detected during the 500 hours' operation. The notable increase of PN within an approximate size range of 7 to 30 nm during the 500 hours of engine operation cannot be explained by means of the HC or the smoke emissions.

Performance

The engine efficiency was almost constant at all loads, Fig. 6. At different load points, the efficiencies varied only by 0 to 0.3 percentage points.

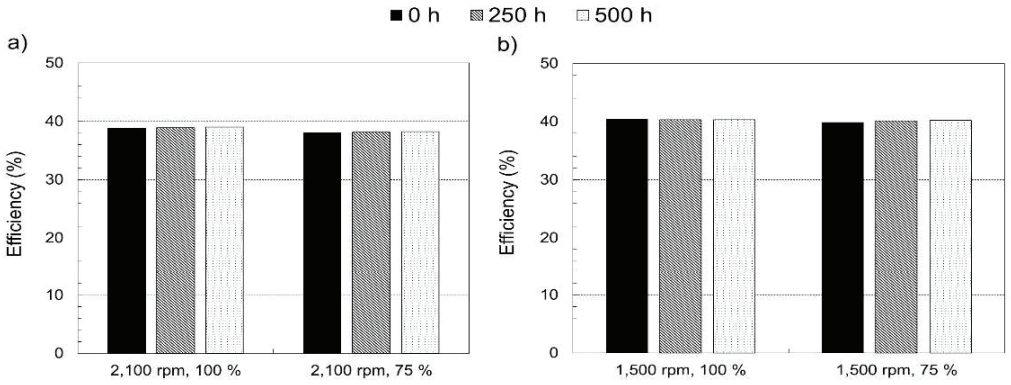

Figure 6. Engine fuel conversion efficiency a) at full and 75% load at rated speed, and b) at full and 75% load at intermediate speed.

CONCLUSIONS

1. During the 500 hours of engine operation, the particle number increased considerably within an approximate size range of 7 to 30 nm
2. No notable differences were observed in the particle number emissions within a particle size range of 50 to 200 nm
3. The correlations between the measured TPN and operation time were positive irrespective of the engine speed or load
4. The engine efficiency remained almost constant, and the changes both in smoke and hydrocarbon emissions were negligible.

The regular change interval for the lubricating oil filter of the non-road diesel engine used in the current study is 500 hours. As a next study, the experiment period could be extended to 1000 hours. Then, the main interest would be the effect of the extended period on the particle number and size distribution, after the oil filter change.

ACKNOWLEDGEMENTS. The Novia University of Applied Sciences allowed us to use the engine laboratory for this study. The authors wish to thank Dr. Jonas Waller, Mr. Holger Sved and Mr. John Dahlbacka for this possibility. In addition, the authors wish to thank Ms. Katriina Sirviö for her assistance during the measurement campaigns and Mr. Tobias Eriksson for operating the engine daily. The authors also thank Mr. Toomas Karhu from Turku University of Applied Sciences for his assistance during the measurements after 500 hours of engine operation.

REFERENCES

Agarwal, A.K. 2005. Experimental investigations of the effect of biodiesel utilization on lubricating oil tribology in diesel engines. *Proc. Inst. Mech. Eng. Part D: J. Automobile Eng.* **219**(5), 703–713.

Anderson, J.O., Thundiyil, J.G. & Stolbach, A. 2012. Clearing the air: a review of the effects of particulate matter air pollution on human health. *J. Med. Toxicol.* **8**(2), 166–175.

Arnold, F., Pirjola, L., Aufmhoff, H., Schuck, T., Lähde, T. & Hämeri, K. 2006. First gaseous sulphuric acid measurements in automobile exhaust: Implications for volatile nanoparticle formation. *Atmos. Environ* **40**(37), 7079–7105.

Biswas, S., Hu, S., Verma, V., Herner, J.D., Robertson, W.H., Ayala, A. & Sioutas, C. 2008. Physical properties of particulate matter (PM) from late model heavy-duty diesel vehicles operating with advanced PM and NO_x emission control technologies. *Atmos. Environ.* **42**(22), 5622–5634.

Dwivedi, D., Agarwal, A.K. & Sharma, M. 2006. Particulate emission characterization of a biodiesel vs diesel-fuelled compression ignition transport engine: A comparative study. *Atmos. Environ* **40**(29), 5586–5595.

EU Regulation 2016/1628. 2016. Regulation of the European Parliament and of the Council on requirements relating to gaseous and particulate pollutant emission limits and type-approval for internal combustion engines for non-road mobile machinery. Accessed 26.1.2018.

Filippo, A.D. & Maricq, M.M. 2008. Diesel nucleation mode particles: Semivolatile or solid?. *Environ. Sci. Technol.* **42**(21), 7957–7962.

Giechaskiel, B., Ntziachristos, L., Samaras, Z., Casati, R., Scheer, V. & Vogt, R. 2007. Effect of speed and speed-transition on the formation of nucleation mode particles from a light duty diesel vehicle. *SAE Tech. Pap.* 2007-01-1110.

Janssen, N.A., Hoek, G., Simic-Lawson, M., Fischer, P., Van Bree, L., Ten Brink, H., Keuken, M., Atkinson, R.W., Anderson, H.R., Brunekreef, B. & Cassee, F.R. 2011. Black carbon as an additional indicator of the adverse health effects of airborne particles compared with PM10 and PM2. 5. *Environ. Health Perspect.* **119**(12), 1691.

Kittelson, D.B. 1998. Engines and nanoparticles: a review. *J. Aerosol Sci.* **29**(5–6), 575–588.

Lähde, T., Rönkkö, T., Virtanen, A., Solla, A., Kytö, M., Söderström, C. & Keskinen, J. 2010. Dependence between nonvolatile nucleation mode particle and soot number concentrations in an EGR equipped heavy-duty diesel engine exhaust. *Environ. Sci. Technol.* **44**(8), 3175–3180.

Oberdörster, G., Oberdörster, E. & Oberdörster, J. 2005. Nanotoxicology: an emerging discipline evolving from studies of ultrafine particles. *Environ. Health Perspect.* **113**(7), 823.

Oravisjärvi, K., Pietikäinen, M., Ruuskanen, J., Niemi, S., Laurén, M., Voutilainen, A., Keiski, R.L. & Rautio, A. 2014. Diesel particle composition after exhaust after-treatment of an off-road diesel engine and modeling of deposition into the human lung. *J. Aerosol Sci.* **69**, 32–47.

Rönkkö, T., Virtanen, A., Vaaraslahti, K., Keskinen, J., Pirjola, L. & Lappi, M. 2006. Effect of dilution conditions and driving parameters on nucleation mode particles in diesel exhaust: Laboratory and on-road study. *Atmos. Environ* **40**(16), 2893–2901.

Rönkkö, T., Virtanen, A., Kannosto, J., Keskinen, J., Lappi, M. & Pirjola, L. 2007. Nucleation mode particles with a nonvolatile core in the exhaust of a heavy duty diesel vehicle. *Environ. Sci. Technol.* **41**(18), 6384–6389.

Sarvi, A., Lyyränen, J., Jokiniemi, J. & Zevenhoven, R. 2011. Particulate emissions from large-scale medium-speed diesel engines: 2. Chemical composition. *Fuel Process. Technol.* **92**(10), 2116–2122.

Schumacher, L.G., Peterson, C.L. & Van Gerpen, J. 2005. Engine oil analysis of biodiesel-fueled engines. *Appl. Eng. Agric.* **21**(2), 153–158.

Sharma, A. & Murugan, S. 2017. Durability analysis of a single cylinder DI diesel engine operating with a non-petroleum fuel. *Fuel* **191**, 393–402.

Sirviö, K., Niemi, S., Katila, T., Ovaska, T., Nilsson, O. & Hiltunen, E. 2016. B20 fuel effects on engine lubricating oil properties. In: *The 28th CIMAC World Congress on Combustion Engine Technology* Helsinki, Finland, Paper No.: 025, pp. 1–8.

Vaaraslahti, K., Virtanen, A., Ristimäki, J. & Keskinen, J. 2004. Nucleation mode formation in heavy-duty diesel exhaust with and without a particulate filter. *Environ. Sci. Technol.* **38**(18), 4884–4890.

Paper III

Fuel 186 (2016) 1–10

Contents lists available at ScienceDirect

Fuel

journal homepage: www.elsevier.com/locate/fuel

Full Length Article

Effects of wood-based renewable diesel fuel blends on the performance and emissions of a non-road diesel engine

Seppo Niemi [a,*], Ville Vauhkonen [b], Sari Mannonen [c], Teemu Ovaska [a], Olav Nilsson [a], Katriina Sirviö [a], Sonja Heikkilä [a], Jukka Kiijärvi [a]

[a] University of Vaasa, PO Box 700, FI65101 Vaasa, Finland
[b] UPM-Kymmene Corporation, Biofuels R & D, Paloasemantie 19, FI53200 Lappeenranta, Finland
[c] UPM-Kymmene Corporation, UPM Biofuels, Alvar Aallonkatu 1, FI00101 Helsinki, Finland

ARTICLE INFO

Article history:
Received 16 June 2016
Received in revised form 10 August 2016
Accepted 11 August 2016
Available online 18 August 2016

Keywords:
Renewable fuel
Renewable diesel
Biofuel
Fuel blends
Non-road diesel engine
Exhaust emissions
Biorefinery

ABSTRACT

Renewable fuels form an essential means to reduce greenhouse gas (GHG) emissions emitted by vehicles and non-road machines. Due to the limited production so far, different blends of renewable fuels in fossil fuels are a realistic way to implement the increasing use of renewable fuels. In addition to significant GHG emissions reduction, further benefits can be achieved when high quality renewable fuels are utilized as blending components since the pollutant exhaust emissions, such as unburned hydrocarbons (HC), carbon monoxide (CO), particulate matter mass (PM) and particle number (PN), may also decrease. A global Finnish forestry company has developed an innovative production process from crude tall oil (CTO), a wood-based residue of pulp making process, to renewable diesel. The fuel properties correspond to those of the traditional fossil fuels but the GHG emissions are reduced significantly.

1. Introduction

The environmental concerns about global warming, gradual reduction of crude oil reserves and stringent emissions legislation have led to the search for alternative fuels for internal combustion (IC) engines. The volatility of conventional fuel prices and increasing global demand for transport energy strongly support this goal. Renewable fuels have the potential to become the sustainable energy source option for various IC engine solutions. Nevertheless, the fuels can only be sustainable if both production and combustion are favorable in ecological terms. Bio and circular economy produce various residues, wastes and secondary materials as potential feedstock for liquid and gaseous fuel production. One of the long-term objectives is to replace large amounts of fossil and first generation renewable fuels with liquids and gases produced from low-value side-products or wastes, lignocellulosic feedstock, agricultural and forestry residues or wastes, or energy crops. [1–4]. The goal is precisely supported by the European Union's commitment to increase the use of renewable energy. In the 2020 and 2030 climate-energy packages, the EU committed to reduce GHG emissions by 20% by 2020 and 40% by 2030, with respect to 1990, and to achieve a share of renewable energy sources 20% by 2020 and at least 27% by 2030. By 2050, the renewable shares may further increase to 40–60%. [5]. Due to the upcoming variety of new fuels and projected increase in the diversification of fuels, quality, usability and other fuel aspects are of increasing importance [6,7].

Generally, the second and third generation renewable fuels are considered more sustainable than the first generation fuels because they generate higher levels of greenhouse gas emission (GHG) reduction and the feedstock does not compete with food production or increase land use. The demand for advanced renewable fuels will increase significantly in the coming years as the EU's target cannot be reached with the current first generation biofuels alone.

Renewable fuels tackle oil dependence, one of the most serious issues affecting energy supply security that many countries face. In compression-ignition engines, the most commonly liquid renewable fuel has been biodiesel or Fatty Acid Methyl Ester (FAME) that is still used in large amounts as a blending component in fossil diesel fuel oil (DF) [8,9]. Some FAME fuels are, however, manufactured from agricultural crops, and thus the fuel production competes with food production, increases land use, and does not fulfill the

* Corresponding author.
E-mail address: seppo.niemi@uva.fi (S. Niemi).

http://dx.doi.org/10.1016/j.fuel.2016.08.048
0016-2361/

high sustainability requirements. Therefore, advanced biofuels produced from non-food feedstock, e.g. wastes, agricultural and forestry residues, energy crops or algae are the preferred choice [10].

In Finland, high-quality liquid fuels are manufactured from various wastes, e.g., animal fats, residues of the forest industry, and wastes from the food industry for vehicle, non-road and generating set use [11]. A global Finnish forestry company produces renewable diesel in commercial scale through an innovative production process from crude tall oil (CTO), a wood-based residue of their own pulp making process. The fuel properties correspond to those of the traditional fossil fuels but the GHG emissions are reduced significantly, up to 80%. CTO as feedstock does not compete with food chain, and there is no indirect land use change.

The suitability of this Finnish CTO renewable fuel has earlier been studied particularly in light-duty and passenger car vehicles [12–14]. In the present study, CTO renewable diesel was investigated in a turbo-charged, intercooled common-rail non-road diesel engine. Considering the total demand of engine fuels and current supply of renewable fuels [15], it is realistic to concentrate on the blends of fossil and renewable fuels. In the present study, the renewable fuel was, however, also studied in neat form. As the baseline fossil fuel, regular low-sulfur Finnish DF was used.

The main aim of the present work was to study how different blends of the CTO renewable diesel (HB) in commercial low-sulfur diesel fuel oil (DF) affect the performance and exhaust emissions of a modern common-rail non-road diesel engine. Neat HB was also studied. Below, the following acronyms are adopted for different fuels and their blends: DF for baseline fossil fuel; HB10 for the blend containing 10 vol.% of HB and 90% of DF; HB20 for the blend of 20 vol.% of HB; HB50 for the blend of 50 vol.% of HB; and HB100 for neat renewable diesel or HB. During the experiments, no modifications were made to the engine components, and the control settings and engine performance were kept constant.

2. Experimental setup

The engine experiments were conducted by the University of Vaasa (UV) at the Internal Combustion Engine (ICE) laboratory of the Technobothnia Research Centre in Vaasa, Finland.

2.1. Fuels

2.1.1. Renewable fuel production and properties

Europe is the most forest-rich region in the world with 1.02 billion hectares of forest amounting 25 percent of the global forest resources [16].

Over the last 20 years, the forest area has expanded in all European regions gaining 0.8 million hectares yearly. Forest growth in the European Union is larger than the current utilization. Wood based renewable fuels are therefore one of the few alternatives to fulfill the set targets of energy security, environmental impact, sustainability, and availability of biomass resources. The focus of current development is on transportation renewable fuels, but in the long run it also opens a possibility for non-road machines, aviation, maritime transportation and power generation fuels.

In the production of the investigated wood-based renewable diesel, crude tall oil (CTO) is used as a feedstock. CTO is a residue of chemical pulping process that contains natural extractive components of wood. CTO is a mixture of 36–58% fatty acids, 10–42% of rosin acids and 10–38% sterols and neutral substances. However, its composition depends on tree species, time of the year, growing cycle and age of the tree, conditions of pulping, and the geographic location. CTO renewable diesel was produced via hydrotreatment in the UPM biorefinery in Lappeenranta.

2.1.2. Studied fuels

In the present engine experiments, commercial Finnish low-sulfur diesel fuel oil (DF) was adopted as the baseline fuel. The CTO derived renewable diesel, UPM BioVerno (HB) was then blended with DF to form blends containing 10, 20 and 50% (V/V) renewable fuel. Neat HB was also studied (HB100). Table 1 depicts the fuel specifications and also lists the limits given in Standard EN590.

As shown, the fuels mainly fulfilled the requirements of the EN590. For HB100, the density 814 kg/m^3 was slightly lower than defined in EN590 (820 kg/m^3). The oxidation stability of HB10 (20 h) was just at the given minimum limit. The polyaromatic hydrocarbon and sulfur contents of HB100 and the blends were lower than those of DF.

2.2. Engine

In the study, a four-cylinder, common-rail diesel engine was examined. The turbocharged, intercooled engine was an AGCO POWER 44 AWI. The engine had been tuned for high NO_x and the use of an SCR catalyst. No exhaust gas after-treatment system was, however, adopted for the current study meaning that engine-out raw emissions were recorded during all measurements. The engine was loaded by means of a Horiba eddy-current dynamometer WT300. The main specification of the test engine is given in Table 2.

2.3. Analytical instruments

The measurement devices adopted for the measurements are presented in Table 3. The arrangement of the test bench and measurement devices are seen in Fig. 1.

The sensor data was collected by software, made in the LabVIEW system-design platform. The recorded quantities were the engine speed and torque, regulated gaseous exhaust emissions, smoke, exhaust particle size distributions, and three unregulated exhaust compounds, namely formaldehyde, methane and nitrous oxide. Several fluid temperatures as well as fluid pressures were recorded. The cylinder pressure was also measured and heat release rates were calculated. The particle mass emissions were omitted since the modern engine emitted too small particle mass amounts for accurate comparison. The engine control functions were followed via a WinEEM4 program, provided by the engine manufacturer.

For the EEPS, the sample flow rate was adjusted at 5.0 dm^3/min. The exhaust sample was diluted with a rotating disc diluter of the raw gas (model MD19-E3, Matter Engineering AG). The dilution ratio was constant (122) during the measurements. For recording of the particulate number and size distributions, three-minute time intervals were chosen during which the total particle concentration was as stable as possible. The average values were calculated from the measured particle numbers during these three-minute time intervals and multiplied by the dilution ratio of the exhaust gas sample. The calculated particle numbers were presented as a function of the particles electrical mobility diameter in the logarithmic scale. The recorded smoke value was the average of five consecutively measured smoke numbers. Based on the measured concentrations of gaseous emissions, the brake specific emissions results were calculated according to the ISO 8178 standard [17].

Table 1
Fuel specifications.

Parameter	Method	DF	HB10	HB20	HB50	HB100	Unit	EN 590:2014-04	
								Min.	Max.
Cetane number (DCN)	DIN EN 15195	59	60	61	65	65	–	51	–
Cetane index	DIN EN ISO 4264	52	53	55	60	69	–	46	–
Density (15 °C)	DIN EN ISO 12185	841	839	835	828	814	kg/m^3	820	845
PAH content	DIN EN 12916	4.4	4.0	3.4	2.4	0.2	% (m/m)	–	8
Sulfur content	DIN EN ISO 20884	8	7	6	<5 (4.6)	<5 (<1)	mg/kg	–	10
Flash point	DIN EN ISO 2719	77	74	73	74	78	°C	>55	–
Carbon residue (10% Dist.)	DIN EN ISO 10370	<0.10	<0.10	<0.10	<0.10	<0.10	% (m/m)	–	0.3
Ash content (775 °C)	DIN EN ISO 6245	<0.005	<0.005	<0.005	<0.005	<0.005	% (m/m)	–	0.01
Water content	DIN EN ISO 12937	30	<30	<30	<30	<30	mg/kg	–	200
Total contamination	DIN EN 12662:1998	3	6	4	6	7	mg/kg	–	24
Copper strip corrosion	DIN EN ISO 2160	1	1	1	1	1	Corr°	–	1
FAME content	DIN EN 14078	⩽ 0.2	⩽ 0.2	⩽ 0.2	⩽ 0.2	⩽ 0.2	% (V/V)	–	7
Oxidation stability	DIN EN ISO 12205	3	2	3	2	<1	g/m^3	–	25
Filterable insolubles		3	2	3	2	<1	g/m^3	–	–
Adherent insolubles		<1	<1	<1	<1	<1	g/m^3	–	–
Oxidation stability	DIN EN 15751	25	20	21	25	32	h	20	–
HFRR (Lubricity)	DIN EN ISO 12156-1	354	412	342	324	228	µm	–	460
Kin. viscosity (40 °C)	DIN EN ISO 3104	3.0	3.0	3.1	3.2	3.5	mm^2/s	2	4.5
% (V/V) recovery at 250 °C	DIN EN ISO 3405	32	33	29	27	20	% (V/V)	–	<65
% (V/V) recovery at 350 °C		94	95	94	94	94	% (V/V)	85	–

Table 2
Test engine specification.

Engine	AGCO POWER 44 AWI
Cylinder number	4
Bore (mm)	108
Stroke (mm)	120
Swept volume (dm)^3	4.4
Rated speed (1/min)	2200
Rated power (kW)	101
Maximum torque at rated speed (Nm)	455
Maximum torque at 1500 1/min (Nm)	583

Table 3
Analytical instruments.

Parameter	Device	Technology
NO_x	Eco Physics CLD 822 M hr	Chemiluminescence
NO_x, λ	WDO UniNO_x sensors	
CO, CO_2	Siemens Ultramat 6	NDIR
Hydrocarbons	J.U.M. VE7	HFID
O_2	Siemens Oxymat 61	Paramagnetic
Particle number and size distribution	TSI EEPS 3090	Spectrometer
Smoke	AVL 415 S	Optical filter
Unregulated gaseous emissions	Gasmet DX4000	FTIR
Cylinder pressure, heat release	Kistler KiBox®	
Air mass flow rate	ABB Sensyflow P	Thermal mass

2.4. Experimental matrix and measurement procedure

The performance and emissions measurements were conducted according to the 8-mode ISO 8178 C1 cycle, known as the non-road steady cycle (NRSC). The loading points or modes and the corresponding engine torques are listed in Table 4. The rated engine speed was 2200 1/min and the intermediate speed 1500 1/min.

Each measurement day, after engine start, warm-up, and uploading phases, the intake air temperature was adjusted at 50 °C downstream the charge air cooler when the load had been set at maximum torque at rated speed. The temperature was controlled manually by regulating cooling water flow to the heat exchanger. The valve setting was kept constant. So, the charge temperature changed with load. The procedure was consistent with what is used in field engines. Before initiating the measurements, it was waited that the engine run had stabilized, the criteria being that the temperatures of coolant water, intake air, and exhaust were stable.

3. Results

3.1. Measurement conditions

During the measurements, the range of the ambient temperature variation was 1–3 °C between the test runs with different fuels. The relative humidity varied from 9 to 13% except for the case of HB100 when the humidity was 8–10%. The ambient pressure ranged from 991 mbar for HB20 to 1019 mbar for HB100 during the experiments. Presumably, the ambient conditions did not affect the results significantly since the temperature and humidity were very similar and the pressure does not have any considerable effect on the performance of a heavily turbocharged engine.

3.2. Combustion analysis

Fig. 2 shows one example of the course of combustion, recorded at full load at intermediate speed for three fuels, DF, HB50 and HB100. As shown, the heat release rates were very similar although there were some differences in the cetane number of the fuels.

For all fuels, the exhaust temperatures upstream the turbocharger turbine were also very similar (Fig. 3). At full load at rated speed, the difference in the temperature was below 10 °C whereas the biggest difference at full load at intermediate speed was approx. 11 °C. If any trend could be observed, the temperatures seemed to be the lowest with HB100.

At each load, the charge pressures were almost equal for each fuel. The charge air temperature varied 1–2 °C depending on the load and fuel.

3.3. Gaseous emissions

Fig. 4 depicts the cycle-weighed NO_x emissions for the studied fuels. The emissions remained almost constant for all fuels. The

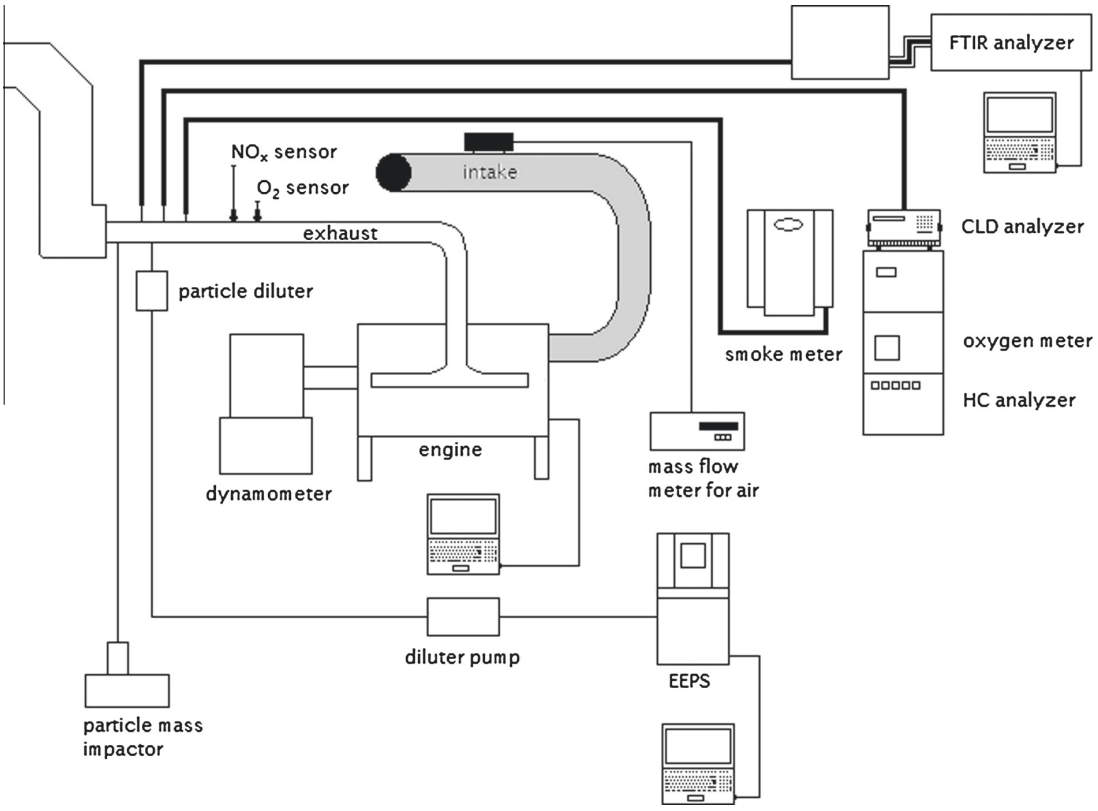

Fig. 1. Experimental set-up.

Table 4
Experimental matrix.

Point	1	2	3	4	5	6	7	8
Speed	Rated				Intermediate			Idle
Load (%)	100	75	50	10	100	75	50	0
Torque (Nm)	410	308	205	41	525	394	263	0

results ranged from 7.0 to 7.2 g/kWh, also showing that the engine was tuned for high NO_x and the use of an SCR catalyst.

At several loads, the NO_x differences between the fuels were within the measuring accuracy but at part and especially minor loads a slight beneficial trend could be detected with HB100 probably due to its higher cetane number.

In contrast to almost constant NO_x, the advanced high-quality CTO renewable fuel (HB) proved to be favorable in terms of CO and HC emissions. Fig. 5 illustrates the cycle-averaged CO emissions which steadily decreased with increasing content of HB in the blends, the lowest CO being recorded with neat HB or HB100 fuel.

At several loads, the percentage reductions in brake specific CO emissions (BSCO) were the higher, the higher was the share of HB fuel in the blend. Fig. 6 depicts the percentage reductions of the CO emissions for the studied fuels. With HB10, the reduction was approx. 3% while 15% was obtained with HB100.

Fig. 7 shows the brake specific HC emissions (BSHC) for all fuels. With HB10, no detectable change was achieved in the BSHC but with higher proportions of HB considerable HC reductions were recorded, illustrated as percentages in Fig. 8. The lowest BSHC was again detected with HB100 or neat renewable fuel, the reduction being approx. 21% relative to the baseline fossil fuel.

From the recorded unregulated gaseous emissions, the methane content seemed to decrease steadily the more, the higher the share of renewable fuel was. The contents were, however, always below 2.2 ppm. N_2O was the lowest with HB100, but the recordings were always lower than 0.6 ppm. At major loads, the formaldehyde content was almost constant at all fuels, but at low load the high renewable share was beneficial. Still, the recordings were always below 3.6 ppm. These compounds were not measured at idle.

3.4. Particulate emissions and smoke

For half of the loads, a bimodal shape was recorded for the particle size distributions. One peak was detected at a particle diameter of app. 10 nm and the other at app. 35–40 nm. In those cases, HB100 very often produced the lowest particle number (PN) emissions at the higher particle size category and the PN increased with decreasing share of renewable fuel, Fig. 9. However, the smaller particles of a size of app. 10 nm might increase with HB100 and some other blends, as also shown in Fig. 9.

At some loads, the shape of the particle size distribution was not bimodal, as depicted for 75% load at rated speed in Fig. 10. Again, the trend was that the higher the renewable fuel share, the lower the maximum PN emissions. It should also be noted that with renewable fuel the PN peak usually occurred at a slightly lower particle size category independent of the particle size distribution shape, Figs. 9 and 10.

At idle, the renewable fuel proved to be clearly more beneficial than the fossil one regarding the PN emissions, Fig. 11. With HB50, the highest PN decreased by almost 50% relative to DF and a reduction of approx. 25% was already achieved with HB10.

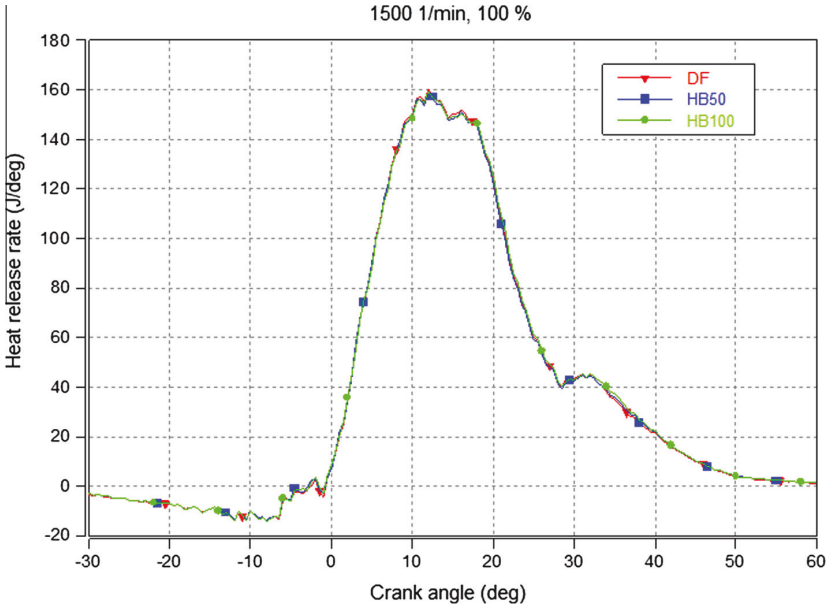

Fig. 2. Heat release rate for three fuels versus crank angle at full load at intermediate speed.

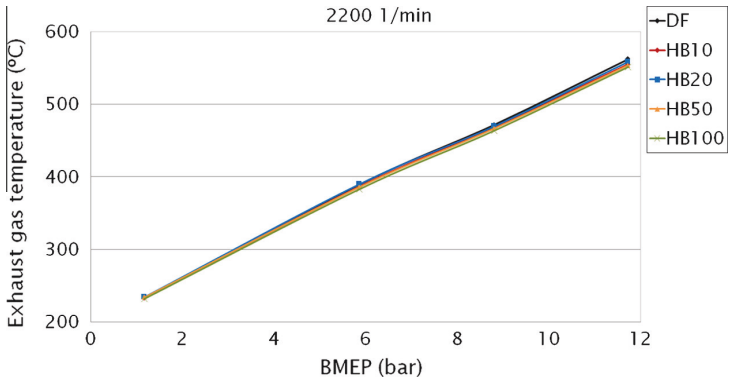

Fig. 3. Exhaust temperature upstream the turbocharger turbine versus engine load at rated speed.

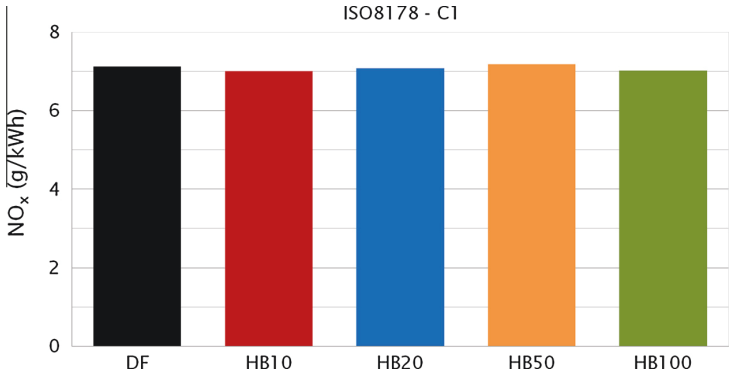

Fig. 4. Cycle-weighed NO_x emissions for various fuels.

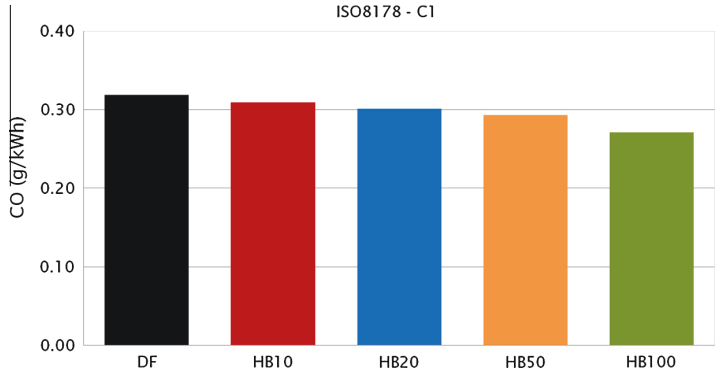

Fig. 5. Cycle-averaged CO emissions for the studied fuels.

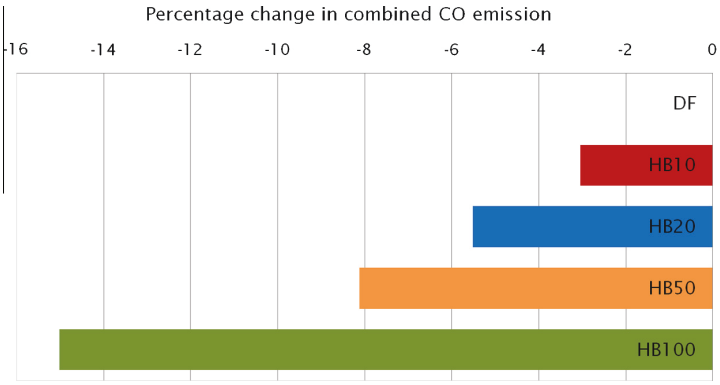

Fig. 6. Relative changes in the cycle-weighed CO emissions for different fuels.

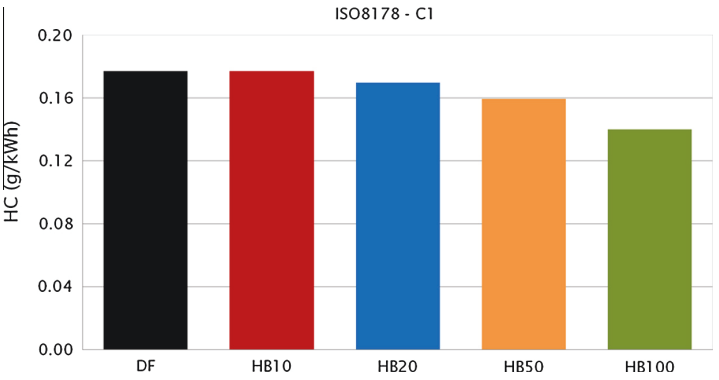

Fig. 7. Cycle-weighed BSHC emissions with various fuels.

Throughout the entire test cycle, the total PN emissions decreased with increasing share of renewable fuel, as illustrated in Fig. 12, where all particles recorded within a size range of 6–520 nm at all load modes were added up, also using the weighing factors of the ISO8178 C1 cycle. With HB100, a reduction of 27% was obtained in PN compared with fossil DF. With HB20, the PN decreased by approx. 7%.

With all fuels, the smoke readings were so low at all loads that no conclusions could be drawn. At intermediate speed, the FSN values varied from 0.003 to 0.024 and at rated speed from 0.014 to 0.090. The readings varied randomly between the fuels.

4. Discussion

As in the current study, the rate of heat release could not be differentiated when HB30 CTO renewable diesel was compared with DF in a single-cylinder passenger car engine in [13].

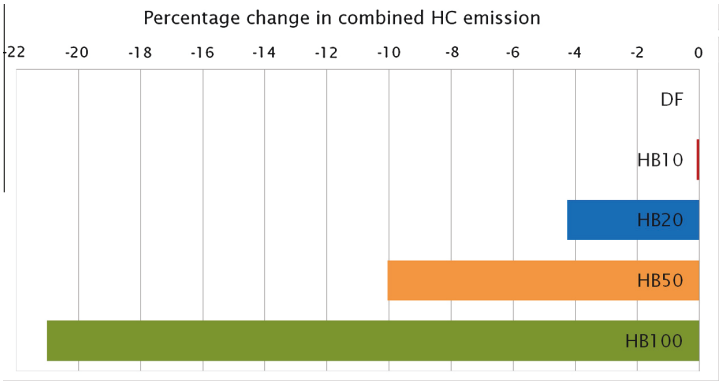

Fig. 8. Percentage reductions of cycle-weighed HC emissions for different fuels.

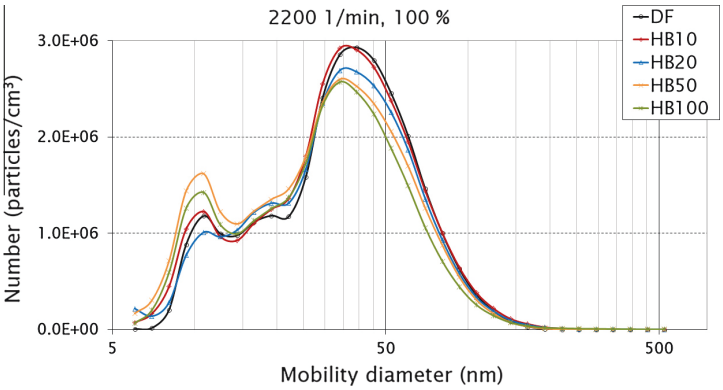

Fig. 9. Exhaust particle size distributions at full load at rated speed for various fuels.

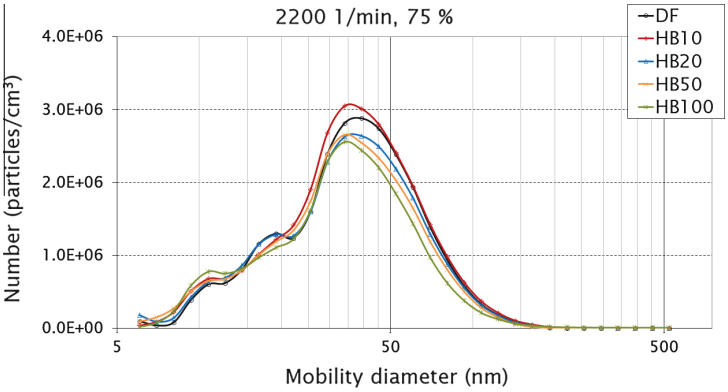

Fig. 10. Particle number emissions versus particle size with different fuels at 75% load at rated speed.

In [13], the efficiency and emissions results were given as a function of indicated specific NO_x ($ISNO_x$) emissions for each studied engine load points – not for a measurement cycle – so comprehensive comparisons with the present study are difficult to make. The NO_x levels were also very low, below 1.5 g/kWh. Nevertheless, HC and CO emissions proved to decrease with HB30 at higher part load at low speed and the efficiency was almost equal with both fuels. At a higher part load at an elevated speed, the CO seemed to increase at very low $ISNO_x$ values, most probably due the increased EGR rate. HC and PM were, however, very similar and the efficiency tended to slightly improve with the HB30 fuel. At full loads at various speeds, there were no substantial differences, nor clear trends between the fuels.

In [12], HB30 and neat BioVerno (HB100) were compared with reference fuel at a constant NO_x level of 0.2 g/kWh at a low part load at a low speed of the single-cylinder engine and at a NO_x of 0.6 g/kWh at a higher part load at a higher engine speed. In both cases, the ISHC decreased considerably with HB100. At the higher

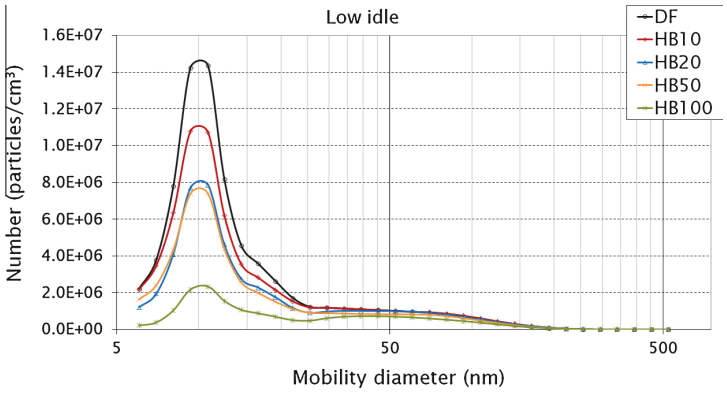

Fig. 11. Exhaust particle size distributions at idle for the studied fuels.

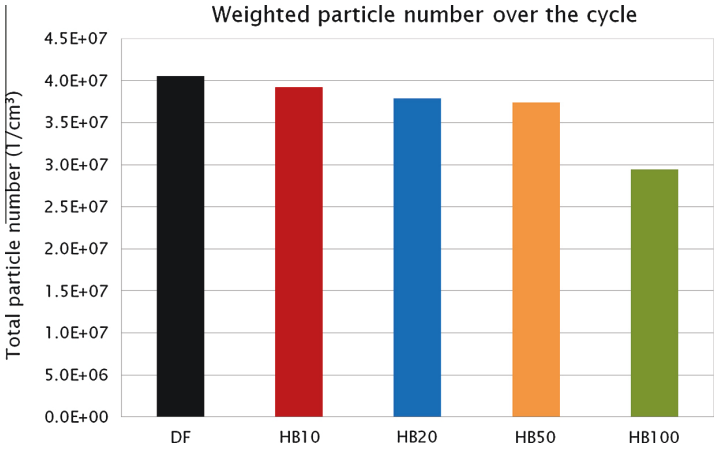

Fig. 12. Total exhaust particles within a size range of 6–520 nm over ISO8178 C1 cycle.

speed, ISPM also decreased with increasing share of CTO renewable diesel, as did the ISCO. The HC and CO results, thus, resemble those achieved in the current study.

In [14], CTO renewable diesel was investigated as a blending component in regular fossil diesel fuel in field tests. The blend contained 20% renewable diesel and 80% fossil diesel (V/V). Approximately 20 000 kilometres were driven with four passenger vehicles, two of them running on DF and two on the blend. During the rather long field test, the measured differences in the volumetric fuel consumption were very small, particularly when comparing with the car-to-car and test-to-test variations.

In [14], emissions measurements were performed at normal and low temperatures. At the normal temperature of +23 °C, the CO differences on average were very small for both fuels. A similar response was detected for total hydrocarbons. Moreover, the NO_x emissions were almost equal. During the field test, a lowering NO_x trend was observed but the averages of both fuels were still almost identical even at the end of the test-run. The cars were equipped with diesel particulate filters (DPFs), so the post-test PM results were very low, only 1–3% of the Euro 5b limit.

In [14], the effects of fuels on emissions were also compared in vehicles of different generations, from Euro 2 until to Euro 6a. The measurements were conducted at two temperatures, +23 °C and at −7 °C. According to the authors, there was no strong evidence that the emissions were notably different when using the HB20 CTO renewable diesel or the baseline DF fuel as all observations are taken into account.

Fischer–Tropsch (FT) diesel is another option to replace fossil diesel fuels [18,19]. When produced from biomass, the fuel is called as biomass-to-liquid or BTL fuel. When the feedstock is natural gas, the product is GTL (Gas-to-Liquid) [19]. The properties of BTL fuels are similar to those of GTL. FT fuels have been widely studied in both light- and heavy-duty engines, e.g. in [19–24]. The large review article of [25] summarizes the results obtained with FT fuels as follows:

- GTL fuels provide good combustion which results in higher CO and HC emission reduction than fossil DF. GTL-DF blends showed higher reductions with increasing GTL content in blends.
- Most findings revealed lower NO_x emissions of GTL fuel than DF. GTL-DF blends showed higher NO_x decrease with the higher fraction of GTL in blends.
- Most of the authors reported lower smoke and PM emissions for GTL relative to DF. Blends of GTL-DF showed lower PM emissions than DF. Blends of GTL with DF also demonstrated reduced smoke emissions in most of the studies.

Hydrotreated vegetable oils and animal fats, HVOs, are the third second-generation renewable fuel alternative suitable to replace

conventional diesel fuels. The use of various HVOs in light- and heavy-duty diesel engines has been published e.g. in [19,24,26–30].

A summary report [31] gives the following ranges for emissions reductions of heavy-duty vehicles of different ages for neat HVO compared with pure DF: NO_x, 8–9%; PM, 27–37%; CO, 16–37%; HC, 26–55%. Particle number emissions have also decreased in two referred studies [31]. Furthermore, the results of [24] with HVO were similar to those of the studies performed with heavy-duty engines operating on GTL and FT-BTL.

Based on the current study, CTO renewable diesel showed performance and emissions results rather similar to those observed with GTL or BTL and oil- or fat-derived HVO fuels. The approximately constant NO_x emissions of the current study perhaps forms a slight discrepancy between the FT and HVO fuels that seemed to also show slight reductions in NO_x. It should, however, be noted that the fuel injection system of the present experimental engine was not at all optimized for the CTO fuel and its blends. Through optimization actions, reductions in NO_x might also be achieved. In the future, more emphasis should therefore be put on the control system and settings optimization in order to also improve the NO_x performance with this renewable diesel. All in all, the studied CTO renewable diesel, UPM BioVerno proved to be a high quality drop-in fuel also for heavy-duty non-road diesel engines.

5. Conclusions

In the present study, a common-rail non-road diesel engine was driven with four different fuel blends of low-sulfur fossil diesel fuel oil and CTO renewable fuel, UPM BioVerno (HB). The fuel blends were HB10, HB20, HB50, and HB100. The HB10 fuel contained 10 vol.%, the HB20 fuel 20 vol.%, and the HB50 fuel 50 vol.% of HB or UPM BioVerno. The HB100 was neat HB. Neat DF was used as a baseline fuel. The engine was tuned at high NO_x emissions for the adoption of an SCR system. However, during the study no exhaust after-treatment equipment was utilized.

The main target was to study how the blends of fossil and renewable diesel affect the performance and exhaust emissions of the modern common-rail diesel engine. The performance and emission measurements were conducted according to the NRSC cycle of the ISO8178 standard. No engine or parameter modifications were made.

Based on the performed measurements, the following conclusions could be drawn:

- The cycle-averaged CO and HC emissions decreased when CTO renewable fuel content of the fuel blend increased. The main reasons were assumed to be the considerably lower content of aromatic compounds and the higher cetane number of the CTO renewable fuel.
- The cycle-weighed NO_x emissions remained almost constant independent of fuel.
- Due to the high-NO_x tuning, the exhaust smoke was very low, almost negligible for all fuels.
- Regarding the studied fuels, no coherent trend was observed in exhaust particle size distributions except at idle, where the increase in the HB content resulted in a clear reduction of ultrafine particle number emissions. The peak number of particulates, however, tended to occur at slightly lower particle size category when the share of renewable fuel increased.

References

[1] Cheng WK, Onorati A. Editorial: biofuels in internal combustion engines. Int J Engine Res 2015;16(5):609. http://dx.doi.org/10.1177/1468087415597824.

[2] Heuser B, Mauermann P, Wankhade R. Combustion and emission behavior of linear c8-oxygenates. Int J Engine Res 2015;16(5):627–38. http://dx.doi.org/10.1177/1468087415594951.

[3] Kalghatgi GT. The outlook for fuels for internal combustion engines. Int J Engine Res 2014;15(4):383–98. http://dx.doi.org/10.1177/1468087415594951.

[4] Wang W-C, Bai C-J, Lin C-T, Prakash S. Alternative fuel produced from thermal pyrolysis of waste tires and its use in a di diesel engine. Appl Therm Eng 2016;93:330–8. http://dx.doi.org/10.1016/j.applthermaleng.2015.09.056.

[5] EUROPEAN Energy COMMISSION, RTD – Energy, ENER – Renewables, R&I, Efficiency, JRC - Institute for Energy and Transport, SET Plan 511 Secretariat, Energy Systems (Increase the resilience, security, smartness of the energy system), issues Paper No. 4 – DRAFT (version 17/12/2015); 2015.

[6] Leipertz A. 12th international congress of engine combustion processes: current problems and modern techniques (ENCOM2015). Int J Engine Res 2016;17(1):3–5. http://dx.doi.org/10.1177/1468087415615500.

[7] Hoppe F, Heuser B, Thewes M, Kremer F, Pischinger S, Dahmen M, Hechinger M, Marquardt W. Tailor-made fuels for future engine concepts. Int J Engine Res 2016;17(1):16–27. http://dx.doi.org/10.1177/1468087415603005.

[8] Di Iorio S, Mancaruso E, Sementa P, Vaglieco BM. A comprehensive analysis of the impact of biofuels on the performance and emissions from compression and spark-ignition engines. Int J Engine Res 2015;16(5):680–90. http://dx.doi.org/10.1177/1468087415591924.

[9] Pabst C, Munack A, Bünger J, Krahl J. Emissions of biofuel blends used in engines with SCR catalyst. MTZ 2014;75(2):44–9. http://dx.doi.org/10.1007/s38313-014-0022-2.

[10] Knothe G. Biodiesel and renewable diesel: a comparison. Prog Energy Combust Sci 2009;36:364–73.

[11] Pongráz E, Niemistö J, García V, Hänninen N, Saavalainen P, Keiski R. Waste-based biofuel technologies in finland – current research and industrial activities, Pollack Periodica. Int J Eng Informat Sci 2015;10(2):157–373. http://dx.doi.org/10.1556/606.2015.10.2.14. Available from: www.akademiai.com.

[12] Vauhkonen V, Heuser B, Holderbaum B, editors. Utilization of renewable diesel from crude tall oil in light duty vehicles, utilization of renewable diesel from crude tall oil in light duty vehicles. In: 3rd TMFB conference 23–25th June, Aachen, Germany; 2015.

[13] Heuser B, Vauhkonen V, Mannonen S, Rohs H, Kolbeck A. Crude tall oil-based renewable diesel as a blending component in passenger car diesel engines. SAE Int J Fuels Lubr 2013;6(3):9. http://dx.doi.org/10.4271/2013-01-2685.

[14] Laurikko JK, Nylund NO, Aakko-Saksa P, Mannonen S, Vauhkonen V, Roslund P. Crude tall oil-based renewable diesel in passenger car field test. SAE technical paper 2014-01-2774, 2014. http://dx.doi.org/10.4271/2014-01-2774.

[15] Schlott S. Synthetic fuels in wait state. MTZ 2015;76(6):8–13. http://dx.doi.org/10.1007/s35146-015-0054-4.

[16] State of Forests and Sustainable Forest Management in Europe. Forest Europe, 2011. <http://www.foresteurope.org/reporting_SFM>

[17] Wright AA. Exhaust emissions from combustion machinery. London: The Institute of Marine Engineering, Science and Technology; 2005.

[18] Lapuerta M, Villajos M, Agudelo JR, Boehman AL. Key properties and blending strategies of hydrotreated vegetable oil as biofuel for diesel engines. Fuel Process Technol 2011;92:2406–11. http://dx.doi.org/10.1016/j.fuproc.2011.09.003.

[19] Murtonen T, Aakko-Saksa P, Kuronen M, Mikkonen S, Lehtoranta K. Emissions with heavy-duty diesel engines and vehicles using FAME, HVO and GTL fuels with and without DOC+POC aftertreatment. SAE Int J Fuels Lubr 2010;2(2):147–66. http://dx.doi.org/10.4271/2009-01-2693.

[20] Kitano K, Misawa S, Mori M, Sakata I, Clark RH. GTL fuel impact on di diesel emissions. SAE technical paper 2007-01-2004, 2007. http://dx.doi.org/10.4271/2007-01-2004.

[21] May M, Vertin K, Ren S, Gui X, Myburgh I, Schaberg P. Development of truck engine technologies for use with Fischer-Tropsch fuels. SAE technical paper 2001-01-3520, 2001. http://dx.doi.org/10.4271/2001-01-3520.

[22] Schaberg PW, Zarling DD, Waytulonis RW, Kittelson DB. Exhaust particle number and size distributions with conventional and Fischer-Tropsch diesel fuels. SAE paper 2002-01-2727, 2002.

[23] Kuen Y, Boehman AL, Armas O. Emissions from different alternative diesel fuels operating with single and split fuel injection. Fuel 2010;89(2010):423–37. http://dx.doi.org/10.1016/j.fuel.2009.08.025.

[24] Aatola H, Larmi M, Sarjovaara T, Mikkonen S. Hydrotreated vegetable oil (HVO) as a renewable diesel fuel: trade-off between NO_x, particulate emission, and fuel consumption of a heavy duty engine. SAE Int J Engines 2009;1(1):1251–62. http://dx.doi.org/10.4271/2008-01-2500.

[25] Sajjad H, Masjuki HH, Varman M, Kalam MA, Arbab MI, Imtenan S, Ashrafur Rahman SM. Engine combustion, performance and emission characteristics of gas to liquid (GTL) fuels and its blends with diesel and bio-diesel. Renew Sustain Energy Rev 2014;30:961–86. http://dx.doi.org/10.1016/j.rser.2013.11.039.

[26] Rantanen L, Linnaila R, Aakko P, Harju T. NExBTL – biodiesel fuel of the second generation. SAE technical paper 2005-01-3771, 2005. http://dx.doi.org/10.4271/2005-01-3771.

[27] Kuronen M, Mikkonen S, Aakko P, Murtonen T. Hydrotreated vegetable oil as fuel for heavy duty diesel engines. SAE technical paper 2007-01-4031, 2007. http://dx.doi.org/10.4271/2007-01-4031.

[28] Erkkilä K, Nylund N, Hulkkonen T, Tilli A, Mikkonen S, Saikkonen P, et al. Emission performance of paraffinic HVO diesel fuel in heavy duty vehicles. SAE technical paper 2011-01-1966, 2011. http://dx.doi.org/10.4271/2011-01-1966.
[29] Pflaum H, Hofmann P, Geringer B, Weissel W. Potential of hydrogenated vegetable oil (HVO) in a modern diesel engine. SAE technical paper 2010-32-0081, 2010. http://dx.doi.org/10.4271/2010-32-0081.
[30] Sugiyama K, Goto I, Kitano K, Mogi K, Honkanen M. Effects of hydrotreated vegetable oil (HVO) as renewable diesel fuel on combustion and exhaust emissions in diesel engine. SAE Int J Fuels Lubr 2012:205–17.
[31] Hartikka T, Kuronen M, Kiiski U. Technical performance of HVO (hydrotreated vegetable oil) in diesel engines. SAE paper 2012-01-1585, 2012. http://dx.doi.org/10.4271/2012-01-1585.

Paper IV

Applied Thermal Engineering 150 (2019) 1168–1176

Contents lists available at ScienceDirect

Applied Thermal Engineering

journal homepage: www.elsevier.com/locate/apthermeng

Research Paper

Effects of alternative marine diesel fuels on the exhaust particle size distributions of an off-road diesel engine

Teemu Ovaska[a,*], Seppo Niemi[a], Katriina Sirviö[a], Olav Nilsson[a], Kaj Portin[b], Tomas Asplund[b]

[a] School of Technology and Innovations, University of Vaasa, P.O. Box 700, FI-65101 Vaasa, Finland
[b] Wärtsilä Corporation, FI-65101 Vaasa, Finland

HIGHLIGHTS

- Renewable naphtha-light fuel oil blend decreased the accumulation mode particles.
- The blend emitted either less or more particles than light fuel oil depending on load.
- Circulation-origin marine gas oil and kerosene generated a high total particle number.

ARTICLE INFO

Keywords:
Diesel engine
Exhaust particle number
Alternative fuel
Light fuel oil

ABSTRACT

The main objective of this study was to find out how alternative fuels affect the exhaust gas particle size distribution. The fuels are later intended for marine applications. Along with low-sulfur marine light fuel oil (LFO), a high-speed off-road diesel engine was fueled by circulation-origin marine gas oil (MGO), rapeseed methyl ester (RME), crude tall oil derived renewable diesel (HVO), the 20/80 vol.-% blend of renewable naphtha and marine LFO, and kerosene. Particle size distributions were measured by means of an engine exhaust particle sizer (EEPS), but soot, gaseous emissions and the basic engine performance were also determined. During the measurements, the 4-cylinder, turbocharged, intercooled engine was run according to the non-road steady cycle complemented by an additional load point. The engine control parameters were kept constant, and any parameter optimization was not made with the studied fuels. Relative to baseline LFO, both naphtha-LFO blend and RME reduced particle numbers above the size range of 50 nm. Circulation-origin MGO and kerosene generated a high total particle number (TPN), most likely due to their higher sulfur contents. MGO and RME were beneficial in terms of carbon monoxide (CO) and hydrocarbon (HC) emissions while nitrogen oxide (NO_x) emissions were the highest with RME. The differences in smoke emission were negligible.

1. Introduction

International shipping produces 5–10% of the total global sulfur emissions [1]. Along with the oxides of sulfur (SO_x) and particles, the carbon dioxide (CO_2) and NO_x emissions, have also to be reduced significantly in order to inhibit the pollution of the earth atmosphere. As an act for the pollution inhibition, the emissions of shipping are considerably regulated worldwide via the MARPOL Annex VI convention of the International Maritime Organization (IMO). These regulations aim to progressively reduce the emissions of SO_x and NO_x. Even outside the Sulfur Emission Control Areas (SECAs), fuel sulfur content has to be under 0.5% in 2020 [2].

Marine sulfur emissions originate mainly from large marine diesel engines, where heavy fuel oil (HFO) is widely combusted. As a residual fuel, HFO has high sulfur and ash contents. The high sulfur content and other fuel characteristics have also been reported to affect the marine exhaust particle emissions [3,4].

Diesel engine exhaust particles form the size distribution with two distinctive particle modes; accumulation mode and nucleation mode [5–8]. The particle mean diameters in nucleation mode are under 50 nm [9], whereas the mean diameter range in soot mode is 50–500 nm [5,10]. Particle number (PN) and mass emissions can be decreased through developing the engine design, exhaust gas after treatment systems, and fuels. Compared to new engine designs or after treatment solutions, alternative liquid fuels can be taken in use relatively rapidly by the operators. Alternative fuels can also offer immediately realizable air quality improvements, and in addition to a SO_x emission decline, the low sulfur content of these new fuels is beneficial

* Corresponding author.
E-mail address: teemu.ovaska@univaasa.fi (T. Ovaska).

https://doi.org/10.1016/j.applthermaleng.2019.01.090
Received 24 September 2018; Received in revised form 10 January 2019; Accepted 26 January 2019
Available online 28 January 2019

for the performance of diesel particulate filters (DPF) [11,12]. Filters, and even more efficient emissions reduction technologies are needed soon. For the first time, the new emission stage (Stage V) also has the limits for the exhaust particle number emissions of the off-road engines, including inland waterway vessels. This regulation of the European Commission and the Council comes gradually into effect within 2019–2020 [13].

Ship owners can meet the emission regulations, especially the IMO's SO_x limitation, by using low-sulfur fuel oils, liquefied natural gas (LNG), or exhaust gas scrubbers. Likely therefore, the low-sulfur fuel oils and other alternative fuel options are going to be used increasingly instead of HFO. Light fuel oils, such as marine diesel oil (MDO) or MGO, are already used in small vessels and the marine auxiliary diesel engines of large ocean-going ships. In Finland, for example, low sulfur marine fuels and LNG have been substitutes for bunkered HFO already for a certain time [1,14,15].

Sustainable and affordable alternative liquid fuels are, however, also needed for the compression ignited (CI) engines. Florentinus et al. [16] assessed qualitatively the technical compatibility of various biofuels in marine engines. Mono-alkyl-esters of long-chain fatty acids, i.e. fatty-acid methyl esters (FAME), di-methyl ether (DME), straight-, and hydrotreated vegetable oils (SVO, HVO) are suitable liquid fuels for both high-speed and medium speed engines [16]. Moreover, Finnish HVO, as studied e.g. by [17], could also be a potential option for medium speed engines.

Moreover, the US Army Single Fuel Forward Policy raised interest to study jet fuels in CI engines which are used in different kind of military vehicles. The aircraft gas turbine engines have been previously run with Jet Propellant 4 (JP-4) fuel which has been replaced by the low sulfur JP-8 fuel, similar to kerosene-based Jet A-1 fuel of the commercial aviation. Jet A-1 fuel has been identified to have same kind of properties than diesel fuel oils (DFO) or low-sulfur LFO [18].

However, the alternative fuel option has to also be compatible with the other systems in ship. With e.g. FAME, several issues have to be considered, like a tendency to oxidation during long term storage, affinity to water and risk of microbial growth, degraded low temperature flow properties, and material deposition on exposed surfaces, including filter elements. The problems may arise especially with over 20 vol.-% blends of FAME [16]. Kerosene-based jet fuel has typically lower cetane number and viscosity compared to LFO, MGO or MDO used in the CI engines in marine and land-use applications. Low cetane number extends the length of the ignition delay, which affects the combustion timing. Extended delay leads to the changes of cold-starting performance, combustion noise level, and exhaust emissions. Due to low fuel viscosity, the fuel injection system performance can deteriorate and the fuel pump wear and leakage may occur [18].

This paper presents how the selected alternative marine fuels affected exhaust gas particle size distributions in the study which was the first stage of a large marine fuel research project. Circulation-origin marine gas oil (MGO) and a blend of renewable naphtha and marine light fuel oil (LFO) were selected to this study because both fuels are novel marine fuel options. Both could meet the sustainability and affordability goals set by the ship owners. Along with these fuels, the other studied low-sulfur fuels were LFO, rapeseed methyl ester (RME), crude tall oil derived renewable diesel (HVO), and kerosene. High-speed engine experiments were conducted before going to medium-speed engine tests. Alongside the exhaust gas particle number and size distributions, the exhaust smoke, gaseous emissions and basic engine performance were determined. The blend fuel contained 20 vol.-% of naphtha and 80 vol.-% of LFO whereas neat LFO was used as the reference fuel. The high-speed off-road diesel engine was driven according to the non-road steady cycle (NRSC) plus at one additional load point. During the experiments, the default engine control parameters were kept constant, and no parameter optimization was applied with the studied fuels.

2. Experimental setup

2.1. Engine and fuels

The experiments were performed with a diesel engine installed in a test bed and loaded by an eddy-current dynamometer. The running cycle was the ISO 8178 C1, added by the 25% load point at intermediate speed.

The 4-cylinder test engine was a turbocharged, intercooled (air-to-water) off-road diesel engine, equipped with a common-rail fuel injection system. The displacement of the engine was 4.4 dm^3 (bore 108 mm, stroke 120 mm) and the rated power 101 kW. The engine was not equipped with any exhaust gas after-treatment devices. The engine lubricating oil was Valtra Engine CR-4 10 W-40.

In addition to baseline LFO, the effects of naphtha-LFO blend, MGO, HVO, RME, and kerosene on the exhaust gas particle size distribution were investigated. Naphtha-LFO blend contained 20 vol.-% of naphtha. Naphtha was a side-product of wood-based renewable diesel production. MGO was a Finnish marine fuel produced from recycled lubricating oils. Kerosene was Jet A-1 type aviation fuel. For the fuels, cetane number, density, sulfur content and kinematic viscosity at 40 °C were analyzed by the fuel laboratory of the University of Vaasa. Table 1 shows the all analyzed fuel properties. The values for the fuel polyaromatic content are based on the available literature in Table 1. Based on the information received from the fuel supplier, naphtha may contain negligible traces of polyaromatic compounds. Nevertheless, the polyaromatic content of naphtha-LFO blend can still be assumed to meet the SFS-EN 590:2013 standard.

2.2. Analytical procedures

The particle number and size distribution, soot, gaseous emissions and residual oxygen content were measured in the laboratory conditions and sampled from the raw engine exhaust. The air mass flow rate was measured from the intake air duct of the engine. Each day before the measurements, the analyzers were calibrated manually once a day

Table 1
Fuel specifications.

Parameter	Method	LFO	MGO	RME	HVO	Naphtha-LFO	Kerosene	Unit
Cetane number	EN 15195	52	68	53	65	51	41	–
Density (15 °C)	EN ISO 12185/ASTM D7042	827	843	883	813	805	787	kg/m^3
Sulfur content	EN ISO 20884/EN ISO 20846	8.3	< 100	< 5	< 5	6.8	1000	mg/kg
Kin. viscosity (40 °C)	EN ISO 3104/ASTM D7042	1.84	7.69	4.49	3.5	1.37	0.94	mm^2/s
Polyaromatics		< 8[a]	0.9[b]	0[c]	0.2[d]	< 8[a]	< 26.5[e]	wt.-%

[a] The maximum allowable polyaromatic content of the fuel standard EN590 [19].
[b] Analyzed by the fuel supplier.
[c] [20].
[d] [17].
[e] The maximum allowable polyaromatic content of the fuel manufacturer [21].

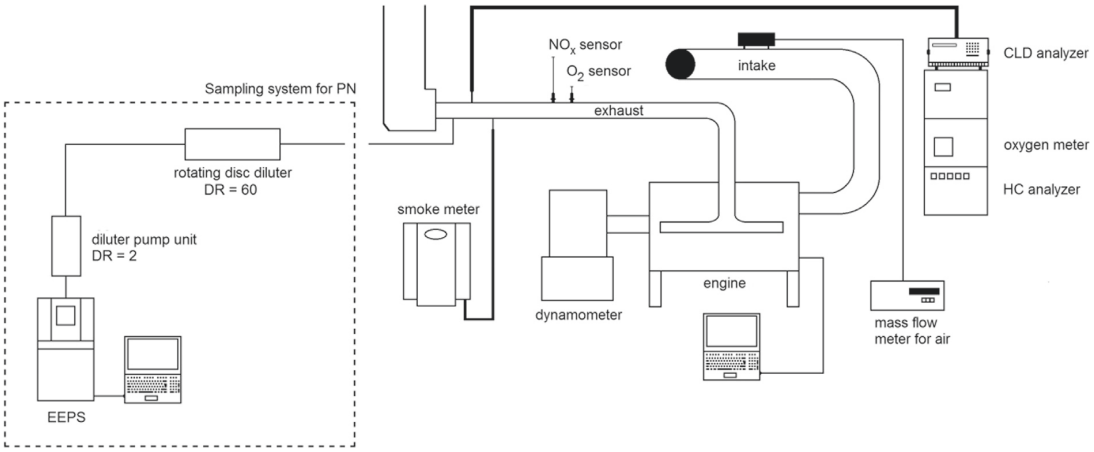

Fig. 1. Experimental setup.

according to the instructions of the instrument manufacturers. The experimental setup is in Fig. 1.

The particles from a size range of 5.6–560 nm were measured by an engine exhaust particle sizer (EEPS, model 3090, TSI Inc.), for which the sample flow rate was adjusted at 5.0 l/min. The "SOOT" inversion was applied in the EEPS data processing [22]. The exhaust sample was first diluted with ambient air by a rotating disc diluter (RDD) (model MD19-E3, Matter Engineering AG). The dilution ratio used in the RDD was constant 60. The exhaust aerosol sample was conducted to the RDD and a dilution air was kept at 150 °C. The diluted sample (5 lpm) was further diluted by purified air with a dilution ratio of 2. Thus, the total dilution ratio was 120.

The particle number (PN) was recorded consecutively three times. Each recording was one-minute long. One-minute stable time periods were chosen for the results recordings of the PN and particle size distributions. The averaging interval of 2 s was used for every period. The average PN values, calculated from the recordings, were multiplied by the dilution ratio of the exhaust sample. The uncertainty of the PN measurement was approximated by calculating the standard deviation of the PN averages, taken from each one-minute recording. The recorded smoke value was the average of three consecutively measured smoke numbers (model 415S, AVL). Nitrogen oxides (NO_x), hydrocarbons (HC) and carbon monoxide (CO) were measured by an Eco Physics CLD 822Mh, J.U.M. VE7, and Siemens Ultramat 6, respectively.

The sensor data were collected by means of software, made in the LabVIEW system-design platform. In addition to the gaseous emissions, the systems recorded the temperatures of cooling water, intake air and exhaust gas plus the pressures of the intake air and exhaust gas. The engine control parameters were followed via WinEEM4 engine management software.

2.3. Experimental matrix and running procedure

The measurements were conducted according to the eight-point test cycle C1 of the ISO 8178-4 standard, known as NRSC, Table 2. The rated speed of the engine was 2200 rpm and the intermediate speed was chosen to be 1500 rpm. Additionally, the measurements were taken at 25% load (3.2 bar) at intermediate speed. With the low-viscosity kerosene, the default engine control parameters made the engine running possible only at intermediate speed. Because no engine parameter optimization was applied during the experiments, the additional load point was chosen to gather more information about the effects of kerosene on the exhaust particle size distribution. An eddy-current dynamometer of model Horiba WT300 was employed to load the engine.

Table 2
Experimental matrix [23].

Point	1	2	3	4	5	6	7	8
Speed	Rated				Intermediate			Idle
Load (%)	100	75	50	10	100	75	50	0
Torque (Nm)	351	263	176	35	450	338	225	0
BMEP (bar)	10.0	7.5	5.0	1.0	12.9	9.7	6.4	0

A canister of 30 L was used as a fuel tank. After the tests with each fuel were completed, the fuel filter was emptied, and the engine was run with new fuel for 10 min. At each load point, the intake air temperature was adjusted at 100 °C downstream the charge air cooler to also ensure proper ignition for low cetane fuels. The temperature was controlled manually by regulating cooling water flow to the heat exchanger. Before the recordings, it was waited that the engine had stabilized, the criteria being that the temperatures of coolant water, intake air and exhaust were stable. The length of the measurement period was not tied to a certain time.

The particle number and size distribution were recorded continuously at each load point. For each fuel, engine warm up and measurements were performed in an exactly similar way.

3. Results

3.1. Particle size distributions

Generally at rated and at intermediate speed, naphtha-LFO blend and RME reduced particle numbers within the size range of 37–200 nm compared to LFO while kerosene and methyl ester showed higher particle numbers within the size range of 8–13 nm than the other fuels. At this range, HVO was favorable at intermediate speed and at low idle. Below, the distributions are examined more thoroughly at certain loads.

Fig. 2 shows the particle size distributions at full load at rated speed. The distribution was bimodal, like at many other loads, one peak being detected at a particle size of 10 nm and the other within a size range of 30–60 nm. At the size of approx. 10 nm, the least particles were observed with HVO and LFO. Between 14 and 340 nm, the smallest particle numbers were recorded with RME, while MGO produced the highest PN.

At 75% load at rated speed, a bimodal distribution was also detected with all fuels, Fig. 3. While the particle number was clearly the lowest for LFO at 10 nm, RME emitted the least particles within the size range of 37–260 nm, as at full load. MGO emitted a high PN within the entire size range. The nucleation mode particles were also high with RME.

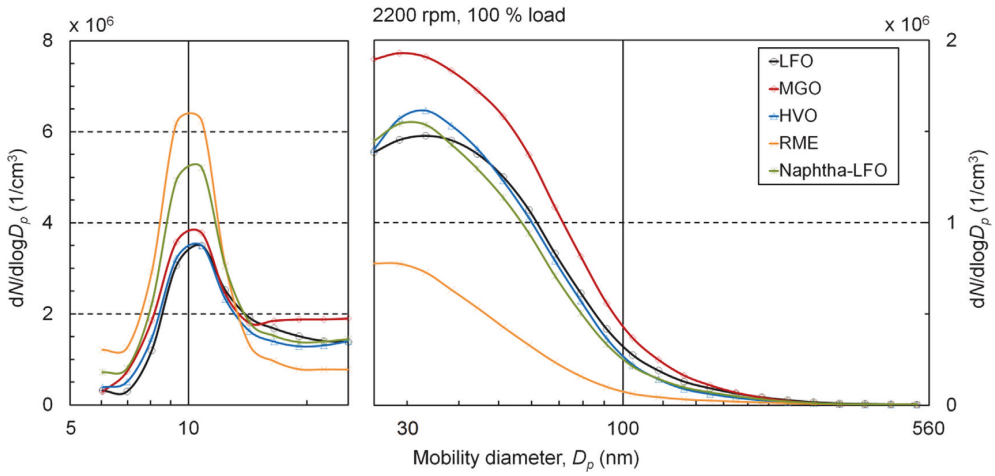

Fig. 2. Exhaust particle size distributions at full load at rated speed for different fuels. It should be noted that the left and right scales of the y axes are different.

For full and half loads at intermediate speed, the particle size distributions are illustrated in Figs. 4 and 5. Again, there was one peak at a particle size of approx. 10 nm and the other within the size range of 30–60 nm. The least particles between 37 and 260 nm were detected with RME.

As at rated speed, the use of naphtha-LFO blend reduced again particle numbers within the size range of 37–200 nm compared to neat LFO. At full load, RME and kerosene produced the most particles at the size category of 10 nm while HVO showed the lowest PN. At this category at half load, the PN was far the highest with kerosene and again the lowest with HVO. At intermediate speed, relative to other fuels, the MGO results were slightly more favorable than at rated speed.

Both at rated and intermediate speeds, the biggest differences in the PN emissions were detected at the particle size of approx. 10 nm, either HVO or LFO generating mostly the lowest particle numbers. Kerosene, only used at intermediate speed, produced often the highest amount of particles at 10 nm. At intermediate speed, the distribution shapes differed from those at rated speed since the peaks between 30 and 60 nm were now much lower compared to those at approx. 10 nm.

The measured total particle number (TPN, from 5.6 to 560 nm) is shown at rated speed in Fig. 6 and at intermediate in Fig. 7. For all fuels at rated speed, the TPN decreased when the load decreased from full to 75% load and remained then almost constant at half load. It increased, however, when the load decreased further, being clearly the highest at 10% load.

At full and 10% loads, the TPN were the lowest when HVO was used. At other loads at rated speed, RME had the lowest TPN. As a whole, naphtha-LFO blend was very competitive with neat LFO. MGO generated the highest TPN at all loads at rated speed.

At intermediate speed, the TPN was at the lowest at full and the highest at 75% load. The TPN decreased when the load decreased from 75 to 25%. Regardless of load, HVO generated the lowest TPN whereas kerosene showed the highest. At some loads, naphtha-LFO generated a higher TPN than LFO, at other loads a lower one. MGO resulted again in a somewhat higher TPN than LFO.

The measured TPN was divided into two categories depending on how many of the particles out of TPN were detected below or above the size category of 23 nm. The shares of the particles above the size of 23 nm were calculated for the fuels, Table 3. At full load at rated speed, 40% of the particles were detected above the size of 23 nm, and thus, 60% below. The lowest average share of the particles above 23 nm was detected with RME, and the highest share with HVO. At 75% load at intermediate speed, the shares of the particles above 23 nm were only 4.3–5.8%.

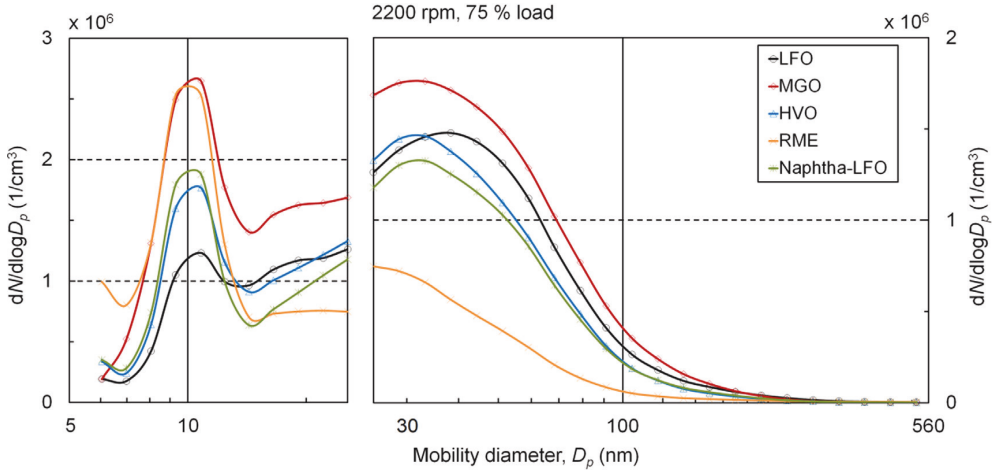

Fig. 3. Exhaust particle size distributions at 75% load at rated speed for studied fuels. Please note the different scales of the y axes.

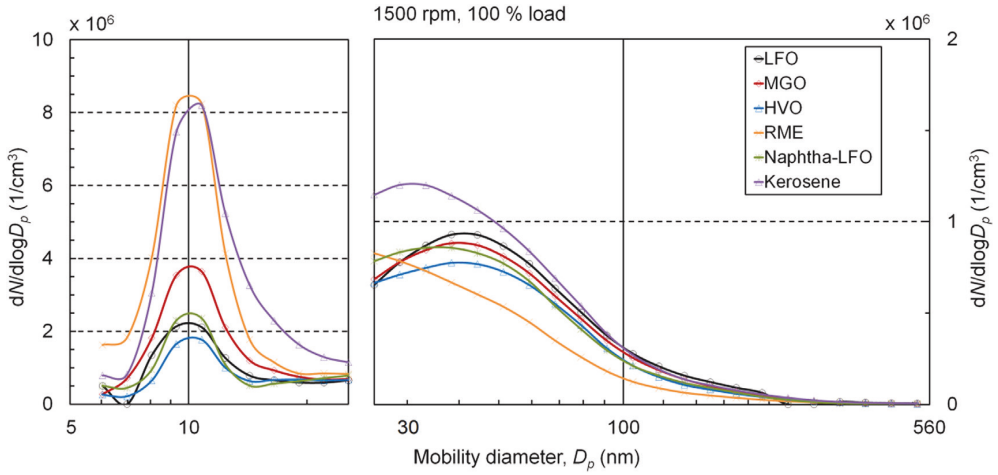

Fig. 4. Exhaust particle size distributions at full load at intermediate speed for different fuels. Please note the different scales of the y axes.

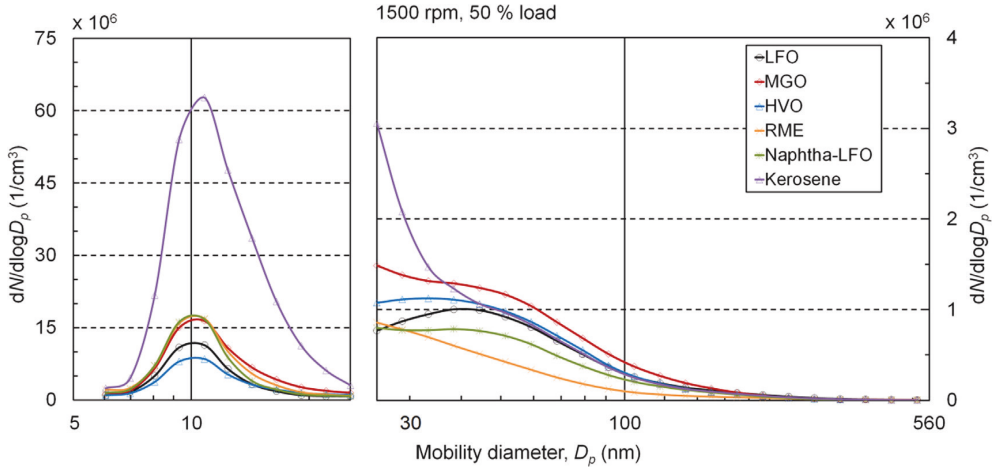

Fig. 5. Exhaust particle size distributions at half load at intermediate speed for studied fuels. Please note the different scales of the y axes.

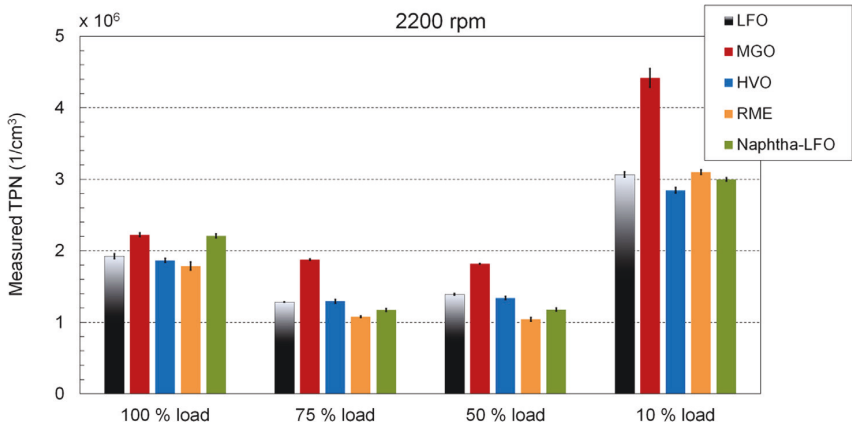

Fig. 6. Measured TPN at rated speed.

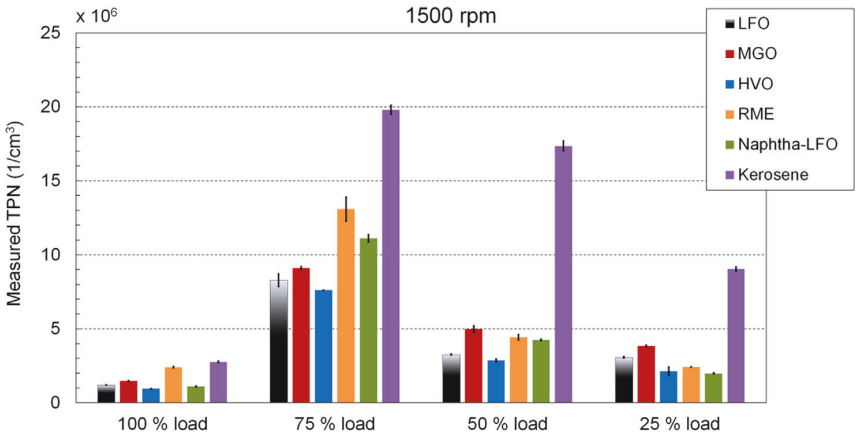

Fig. 7. Measured TPN at intermediate speed.

Table 3
The share of particles larger than 23 nm out of the TPN for all fuels at different loads.

Speed	Rated				Intermediate			Idle
Load (%)	100 %	75 %	50 %	10 %	100 %	75 %	50 %	0 %
LFO	40	59	58	57	44	5.6	17	7.2
MGO	44	48	51	36	34	5.5	15	8.0
HVO	41	50	55	53	46	5.8	21	22
RME	18	27	34	30	15	4.5	7.2	20
Naphtha-LFO	33	53	57	55	43	4.3	10	7.9

Table 4
Cycle-weighted brake specific emissions of, HC, NO_x and CO and smoke number ranges from lowest to highest within the NRSC cycle with different fuels. The specific PN emission was determined over the size range of 5.6–560 nm.

	HC (g/kWh)	NO_x (g/kWh)	CO (g/kWh)	Smoke (FSN)
LFO	0.24	9.3	0.33	0.014–0.038
MGO	0.16	9.3	0.28	0.014–0.033
HVO	0.20	8.9	0.32	0.013–0.031
RME	0.12	10.8	0.30	0.005–0.015
Naphtha-LFO	0.29	–	0.36	0.011–0.031

3.2. Gaseous emissions and smoke

Table 4 shows the brake specific emissions of HC, NO_x, and CO and smoke number ranges. In general, MGO and RME were favorable in terms of CO and HC emissions while NO_x emissions were the lowest with HVO. The smoke numbers were altogether minor with all fuels. Due to the intended use of an SCR catalyst, high NO_x tuning of the test engine had most likely a decreasing effect on smoke.

4. Discussion

In the present study, all particle size distributions measured from the exhaust gas of the high-speed off-road diesel engine had a bimodal shape. This common shape of engine-out size distributions has also been observed both in on-road and laboratory conditions in case of heavy-duty diesel truck [24], light-duty diesel [7], natural gas buses [25], direct-injected gasoline vehicle [26,27] and off-road diesels [17,28–30]. Moreover, Ntziachristos et al. [31] detected bimodal particle size distributions in the exhaust gas of a medium-speed marine diesel engine when LFO was used at low load.

The nucleation mode particles have a non-volatile core which is considered to initiate in the cylinder or in the tailpipe [9,32]. The most of the nucleation mode particles are believed to form during dilution of the exhaust gas. Their formation has been reported to be sensitive to the engine parameters [33], fuel and lubricant oil characteristics [34], exhaust after-treatment [35], and dilution conditions such as dilution ratio, temperature and relative humidity of the dilution air [36]. However, Rönkkö et al. [9] reported that their formation was insensitive to the fuel sulfur content, dilution air temperature, and relative humidity of ambient air.

Nucleation, condensation and coagulation may change the particle size distribution during the exhaust gas sampling [37]. In this study, the exhaust gas sample was diluted at two stages in order to decrease the particle concentration of the sample for the EEPS. The first dilution was made with heated air (150 °C) in order to prevent the condensation of ambient moisture to sampling lines. However, the first dilution was not sufficiently hot to the prevention of nucleation mode formation. According to Vaaraslahti et al. [38], the nucleation mode evaporates completely when an exhaust sample is heated enough. Thus, the authors of this paper believe the nucleation mode formation could have been avoided if a thermodenuder [39] was adopted during the PN measurement.

Unlike the nucleation mode, the accumulation mode is not sensitive to dilution conditions [35,40]. Accumulation mode particles are formed in the cylinder, when either the fuel or the remnants of lubricating oil do not burn completely during combustion.

Despite the complex nature of nucleation mode, the PN averages calculated from the EEPS scans were found to remain fairly constant, mostly, and be repetitious in this study. The variation of the particle numbers between the three consecutive one-minute EEPS scans can be seen in Fig. 8. The average values were calculated from the recordings of those three EEPS measurement channel, where the PN peaked with different fuels at full load at rated speed.

The physical properties of the liquid fuel tend to control fuel spray characteristics while the fuel composition determines the pathways of chemical reactions during combustion [11]. Besides the fuel sulfur content, particle formation is also influenced by other fuel characteristics such as the fuel density [41,42], viscosity [43,44], and cetane number [45,46]. The start of injection is determined by the fuel density, viscosity, and compressibility. After the injection has started, fuel cetane number determines the moment when combustion starts. Higher fuel density and viscosity lead to an advanced start of injection. A higher cetane number leads to a shortened ignition delay plus advanced combustion [47]. Too viscous fuel increases pumping losses in the injection system and the injection pressure at the pump end may increase when conventional in-line pumps are adopted. All this may cause

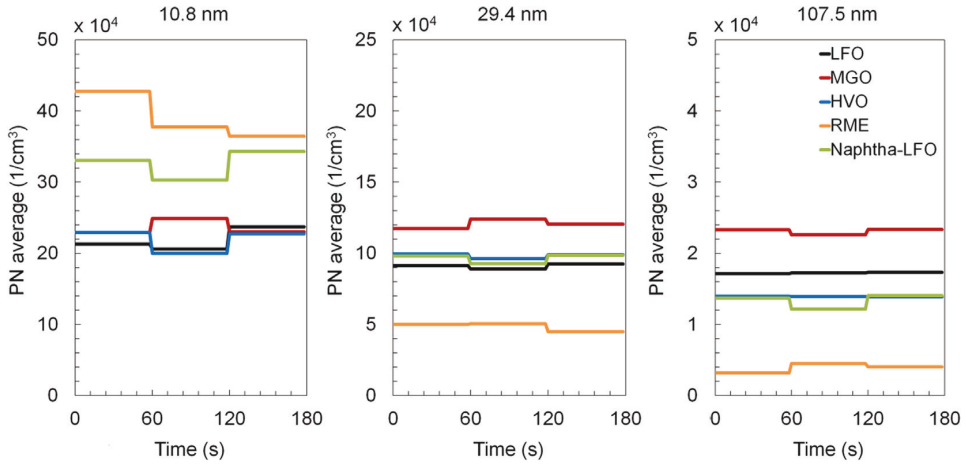

Fig. 8. The variation of the average particle number between the three consecutive one-minute EEPS scans at the three EEPS channels (10.8 nm, 29.4 nm and 107.5 nm).

disruptions in the combustion process [48,49]. Higher fuel density and viscosity may lead to incomplete combustion due to poor fuel atomization. Therefore, the soot emission will increase [50].

In this study, MGO had the second highest density and highest viscosity, which may partly explain why MGO generated the highest TPN at all loads at rated speed even though the cetane number was quite high. At intermediate speed with kerosene, on the other hand, the lowest density and viscosity did not compensate for the effect of the lowest cetane number on clearly the highest TPN. RME had the highest density and second highest viscosity, but the particle numbers within the size range of 37–200 nm were still the lowest. However, RME contained approx. 10% oxygen which usually results in lower soot and thus lower accumulation mode particles. Naphtha-LFO blend had a slightly lower cetane number and kinematic viscosity than LFO but a clear difference at density that might explain the reduced particle numbers within the size range of 37–200 nm relative to LFO.

During the combustion, the aromatic content of fuel has a role as precursors of particulates [51–53] although researchers have received divergent results about the effect of the fuel aromatic content on PM emission [42]. Zetterdahl et al. [53] reported that an increase in the aromatic concentration in low-sulfur diesel fuel led to decreased or unchanged number of particles emitted. However, Talibi et al. [54] concluded that the increasing number of methyl branches on the aromatic ring results in an increased PN, and Peña et al. [55] found that the sizes of primary particles decreased with the addition of methyl group(s) on the aromatic ring. The concentrations of aliphatics and oxygenated groups in soot particles were also decreased. They suggested that the combustion of aromatic fuel, if aliphatic chains are present, tends to produce soot with a compact nanostructure. Due to the same propensity, the content of amorphous, oxygenated, and aliphatic carbonaceous materials in the soot may decrease. Therefore, the reactivity with oxygen decreases too [55]. Nabi et al. [50] concluded that exhaust particle number and mass emission was higher with MGO compared to diesel fuel due to the higher C/H ratio in MGO. Therefore, they assumed that the aromatic content of MGO would also be higher. This expectation was based on the study of Kalligeros et al. [56], who stated that aromatics increase the fuel C/H ratio.

In this study, despite the complex nature of nucleation mode PN formation, the favorable PN results of HVO at the size category of 10 nm are assumed to be caused by the almost zero content of polycyclic aromatic hydrocarbons. On the other hand, the difference in PN at the size 10 nm between MGO and reference fuel LFO cannot be explained by the polyaromatics. The kinematic viscosity of MGO was not much higher than it was for the other fuels, and the content of the polycyclic aromatic compound of MGO was 0.9 wt.-%. This is lower than for LFO for which the maximum allowable content of the polyaromatics is 8 wt.-% [19]. MGO (< 100 mg/kg) and kerosene (1000 mg/kg) contained, however, more sulfur than other fuels, kerosene considerably more. Because a higher content of sulfur was available before combustion, more sulfur oxides, mainly SO_2 and a small fraction of SO_3, were present after fuel burning especially in the case of kerosene. The nucleation mode of particles may be caused by sulfuric acid originating from reaction between SO_3 and water vapor [9,38,57,58]. Therefore, the high PN of MGO and especially of kerosene at the size 10 nm was assumed to be caused by the same reaction and thus due to the higher sulfur contents of these fuels.

Unlike HVO, RME produced often the most nucleation mode particles. This result is in line with the several studies of other researchers [44,59–61]. Heikkilä et al. [59] suggested that the relatively high share of nucleation mode particles with RME may be due to its content of viscous, high boiling point molecules, triglycerides and glycerol. Moreover, RME also contains ash forming elements, such as alkali metals and metalloids that may contribute significantly to the formation of the nucleation mode particles.

The accumulation mode particles, however, were reduced with RME most likely due to oxygen bounded in mono-alkyl-ester molecules. Thus, the more complete combustion was enabled and the more effective soot oxidation was promoted during RME usage compared the usage of other fuels in this study [62,63]. Nyström et al. [64] detected a lower PN around the peak values of 75–116 nm when a high-speed off-road diesel engine was fueled with RME compared to low-sulfur diesel fuel. Earlier studies have also been reported how RME and other FAMEs, either as neat or the blending component, have the similar decreasing effect on accumulation mode particle numbers [59,65,66].

The present study was intended for being able to prepare experiments with a medium-speed engine carefully. In a later study, some of the current fuels were used in a medium-speed engine. Significant combustion differences exist as large marine engines has higher stroke-to-bore ratio compared to smaller high-speed engines. Furthermore, large marine engines are operated with lower engine speeds and higher air-to-fuel ratios than the small engines in land use. High stroke-to-bore ratio, and low engine speed gives more time for fuel to combust which promotes soot oxidation [31]. As presented by Ntziachristos et al. [31], use of the LFO fuel in a marine engine may result to much lower specific mass emissions of particles compared to the emission limitation intended for road vehicles at some loads. Therefore, the presented PN reductions may be presupposed when the fuels of this study are later intended for marine applications. No parameter optimization was

applied with the studied fuels at this first stage to be able to compare the fuels first without any modifications. At the next stages, parameters have to be optimized.

5. Conclusions

This study concentrated on working out how different alternative off-road engine fuels affect the exhaust particle size distributions of a high-speed diesel engine. The examined fuels were a blend of renewable wood-based naphtha and marine low-sulfur LFO, circulation-origin MGO, RME, HVO, and kerosene. LFO worked as baseline fuel. The measurements were performed according to the NRSC test cycle. Based on the obtained results, the following conclusions could be drawn:

- A bimodal shape was detected in all particle size distributions.
- Considering the complex nature of nucleation mode PN formation, no consistent conclusions could be drawn concerning the particle numbers under the size category of 50 nm.
- Except at idle, the particle numbers above 50 nm were the lowest with RME most likely due to oxygen bounded in mono-alkyl-ester molecules.
- Relative to LFO, both naphtha-LFO blend and RME reduced particle numbers above 50 nm at rated and intermediate speeds.
- Circulation economy based MGO generated the highest total particle number (TPN) at all loads at rated speed, most likely due to the higher fuel sulfur content. At intermediate speed, still higher TPN values were recorded for kerosene, the sulfur content of which was higher by one order of magnitude relative to MGO.
- In terms of TPN at intermediate speed, renewable HVO was more beneficial than LFO. At rated speed, the HVO results were quite similar to those of LFO.
- Concerning the TPN as a whole, the blend of renewable naphtha and LFO was competitive with LFO. At some loads, the blend emitted more particles, at other loads less than LFO.
- MGO and RME were favorable in terms of CO and HC emissions while the lowest NOx emissions were recorded with HVO.
- Smoke emission was negligible for all fuels.

Declarations of interest

None.

Acknowledgements

This study was funded from the European Union's Horizon 2020 research and innovation programme under the grant agreement No 634135 (Hercules-2). The Novia University of Applied Sciences allowed us to use the engine laboratory for this study. The authors wish to thank Dr. Tony Pellfolk and Mr. Holger Sved for this possibility. In addition, the authors wish to thank Mrs. Michaela Hissa, Mrs. Sonja Heikkilä and Ms. Nelli Vanhala for their assistance during the measurement campaigns.

Appendix A. Supplementary material

Supplementary data to this article can be found online at https://doi.org/10.1016/j.applthermaleng.2019.01.090.

References

[1] Reducing Sulphur Emissions from Ships - The Impact of International Regulation, OECD International Transport Forum, 2016 [accessed 21 Aug 2018]. Available from: https://www.itf-oecd.org/sites/default/files/docs/sulphur-emissions-shipping.pdf.
[2] Internal Maritime Organization, Prevention of Air Pollution from Ships, http://www.imo.org/en/OurWork/Environment/PollutionPrevention/AirPollution/Pages/Air-Pollution.aspx, 2018 [cited 17 August 2018].
[3] A. Sarvi, J. Lyyränen, J. Jokiniemi, R. Zevenhoven, Particulate emissions from large-scale medium-speed diesel engines: 1. Particle size distribution, Fuel Process Technol. 92 (10) (2011) 1855–1861, https://doi.org/10.1016/j.fuproc.2011.04.031.
[4] M. Zetterdahl, J. Moldanová, X. Pei, R.K. Pathak, B. Demirdjian, Impact of the 0.1% fuel sulfur content limit in SECA on particle and gaseous emissions from marine vessels, Atmos. Environ. 145 (2016) 338–345, https://doi.org/10.1016/j.atmosenv.2016.09.022.
[5] D.B. Kittelson, Engines and nanoparticles: a review, J. Aerosol Sci. 5–6 (1998) 575–588, https://doi.org/10.1016/S0021-8502(97)10037-4.
[6] T. Rönkkö, A. Virtanen, K. Vaaraslahti, J. Keskinen, L. Pirjola, M. Lappi, Effect of dilution conditions and driving parameters on nucleation mode particles in diesel exhaust: Laboratory and on-road study, Atmos. Environ. 40 (16) (2006) 2893–2901, https://doi.org/10.1016/j.atmosenv.2006.01.002.
[7] A.D. Filippo, M.M. Maricq, Diesel nucleation mode particles: Semivolatile or solid? Environ. Sci. Technol. 42 (21) (2008) 7957–7962, https://doi.org/10.1021/es8010332.
[8] T. Lähde, T. Rönkkö, A. Virtanen, A. Solla, M. Kytö, C. Söderström, et al., Dependence between nonvolatile nucleation mode particle and soot number concentrations in an EGR equipped heavy-duty diesel engine exhaust. Environ. Sci. Technol. 44 (8) (2010) 3175–3180.
[9] T. Rönkkö, A. Virtanen, J. Kannosto, J. Keskinen, M. Lappi, L. Pirjola, Nucleation mode particles with a nonvolatile core in the exhaust of a heavy duty diesel vehicle, Environ. Sci. Technol. 41 (18) (2007) 6384–6389, https://doi.org/10.1021/es0705339.
[10] Y. Zhang, J. Ghandhi, D. Rothamer, Comparisons of particle size distribution from conventional and advanced compression ignition combustion strategies, Int. J. Engine Res. 19 (7) (2018) 699–717, https://doi.org/10.1177/1468087417721089.
[11] P. Eastwood, Particulate Emissions from Vehicles, John Wiley & Sons Ltd, Chichester, 2008.
[12] F. Millo, M. Rafigh, M. Andreata, T. Vlachos, P. Arya, P. Miceli, Impact of high sulfur fuel and de-sulfation process on a close-coupled diesel oxidation catalyst and diesel particulate filter, Fuel 198 (2017) 58–67, https://doi.org/10.1016/j.fuel.2017.01.006.
[13] EU Regulation 2016/1628, Regulation of the European Parliament and of the Council on requirements relating to gaseous and particulate pollutant emission limits and type-approval for internal combustion engines for non-road mobile machinery, 2016 [accessed 17 Aug 2018]. Available from: https://eur-lex.europa.eu/legal-content/EN/TXT/PDF/?uri=CELEX:32016R1628&from=EN.
[14] J. Kalli, T. Karvonen, T. Makkonen, Sulphur Content in Ships Bunker Fuel in 2015 - A study on the impacts of the new IMO regulations and transportation costs, Publications of the Ministry of Transport and Communications, Helsinki, 2009 [accessed 17 Aug 2018]. Available from: https://www.lvm.fi/documents/20181/817543/Julkaisuja+31-2009/cfb920d0-d1c5-4c4f-94e2-7a92e58adc9d?version=1.0.
[15] S. Jääskeläinen, Alternative transport fuels infrastructure - Finland´s national plan, Publications of the Ministry of Transport and Communications, Helsinki, Finland, 2017 [accessed 17 Aug 2018]. Available from: https://julkaisut.valtioneuvosto.fi/bitstream/handle/10024/80230/Report%205-2017.pdf?sequence=1.
[16] A. Florentinus, C. Hamelinck, A. van den Bos, R. Winkel, M. Cuijpers, Potential of biofuels for shipping - Final Report, Prepared by Ecofys for European Maritime Safety Agency (EMSA), 2012 [accessed 17 Aug 2018]. Available from: https://www.ecofys.com/files/files/ecofys_2012_potential_of_biofuels_in_shipping_02.pdf.
[17] S. Niemi, V. Vauhkonen, S. Mannonen, T. Ovaska, O. Nilsson, K. Sirviö, et al., Effects of wood-based renewable diesel fuel blends on the performance and emissions of a non-road diesel engine, Fuel 186 (2016) 1–10, https://doi.org/10.1016/j.fuel.2016.08.048.
[18] G. Fernandes, J. Fuschetto, Z. Filipi, D. Assanis, H. McKee, Impact of military JP-8 fuel on heavy-duty diesel engine performance and emissions, Proc. Inst. Mech. Eng. Part D: J. Automobile Eng. 221 (8) (2007) 957–970, https://doi.org/10.1243/09544070JAUTO211.
[19] SFS-EN 590:2013, Automotive fuels, Diesel. Requirements and test methods. Finnish Petroleum Federation, 2013.
[20] H. Aatola, M. Larmi, T. Sarjovaara, S. Mikkonen, Hydrotreated vegetable oil (HVO) as a renewable diesel fuel: trade-off between NO_x, particulate emission, and fuel consumption of a heavy duty engine, SAE Int. J. Engines 1 (1) (2009) 1251–1262, https://doi.org/10.4271/2008-01-2500.
[21] Product data sheet, Aviation Jet Fuel Jet A-1, Neste Oyj, Espoo, 2015.
[22] X. Wang, M.A. Grose, R. Caldow, B.L. Osmondson, J.J. Swanson, J.C. Chow, et al., Improvement of engine exhaust particle sizer (EEPS) size distribution measurement – II. Engine exhaust aerosols, J. Aerosol. Sci. 92 (2016) 83–94, https://doi.org/10.1016/j.jaerosci.2015.11.003.
[23] Dieselnet, http://www.dieselnet.com, 2018 [accessed 17 August 2018].
[24] D.B. Kittelson, W.F. Watts, J.P. Johnson, On-road and laboratory evaluation of combustion aerosols, Part1: Summary of diesel engine results, J. Aerosol Sci. 37 (8) (2006) 913–930, https://doi.org/10.1016/j.jaerosci.2005.08.005.
[25] A. Thiruvengadam, M.C. Besch, S. Yoon, J. Collins, H. Kappanna, D.K. Carder, et al., Characterization of particulate matter emissions from a current technology natural gas engine, Environ. Sci. Technol. 48 (14) (2014) 8235–8242, https://doi.org/10.1021/es5005973.
[26] L. Pirjola, P. Karjalainen, J. Heikkilä, S. Saari, T. Tzamkiozis, L. Ntziachristos, et al., Effects of fresh lubricant oils on particle emissions emitted by a modern gasoline direct injection passenger car, Environ. Sci. Technol. 49 (6) (2015) 3644–3652, https://doi.org/10.1021/es505109u.
[27] P. Karjalainen, L. Pirjola, J. Heikkilä, T. Lähde, T. Tzamkiozis, L. Ntziachristos, et al., Exhaust particles of modern gasoline vehicles: A laboratory and an on-road

study, Atmos. Environ. 97 (2014) 262–270, https://doi.org/10.1016/j.atmosenv.2014.08.025.
[28] M. Anderson, K. Salo, Å.M. Hallquist, E. Fridell, Characterization of particles from a marine engine operating at low loads, Atmos. Environ. 101 (2015) 65–71, https://doi.org/10.1016/j.atmosenv.2014.11.009.
[29] L. Pirjola, T. Rönkkö, E. Saukko, H. Parviainen, A. Malinen, J. Alanen, et al., Exhaust emissions of non-road mobile machine: Real-world and laboratory studies with diesel and HVO fuels, Fuel 202 (2017) 154–164, https://doi.org/10.1016/j.fuel.2017.04.029.
[30] T. Ovaska, S. Niemi, T. Katila, O. Nilsson, Exhaust particle size distributions of a non-road diesel engine in an endurance test, Agronomy Res. 16 (S1) (2018) 1159–1168, https://doi.org/10.15159/AR.18.087.
[31] L. Ntziachristos, E. Saukko, K. Lehtoranta, T. Rönkkö, H. Timonen, P. Simonen, et al., Particle emissions characterization from a medium-speed marine diesel engine with two fuels at different sampling conditions, Fuel 186 (2016) 456–465, https://doi.org/10.1016/j.fuel.2016.08.091.
[32] P. Nousiainen, S. Niemi, T. Rönkkö, P. Karjalainen, J. Keskinen, H. Kuuluvainen, et al., Effect of injection parameters on exhaust gaseous and nucleation mode particle emissions of a Tier 4i nonroad diesel engine, SAE Technical Paper 2013; 2013-01-2575. https://doi.org/10.4271/2013-01-2575.
[33] T. Lähde, T. Rönkkö, M. Happonen, C. Söderström, A. Virtanen, A. Solla, et al., Effect of fuel injection pressure on a heavy-duty diesel engine nonvolatile particle emission, Environ. Sci. Technol. 45 (6) (2011) 2504–2509, https://doi.org/10.1021/es103431p.
[34] K. Vaaraslahti, J. Keskinen, B. Giechaskiel, A. Solla, T. Murtonen, H. Vesala, Effect of lubricant on the formation of heavy-duty diesel exhaust nanoparticles, Environ. Sci. Technol. 39 (21) (2005) 8497–8504.
[35] M.M. Maricq, R.E. Chase, N. Xu, P.M. Laing, The effects of the catalytic converter and fuel sulfur level on motor vehicle particulate matter emissions: light duty diesel vehicles, Environ. Sci. Technol. 36 (2) (2002) 283–289.
[36] U. Mathis, J. Ristimaki, M. Mohr, J. Keskinen, L. Ntziachristos, Z. Samaras, P. Mikkanen, Sampling conditions for the measurement of nucleation mode particles in the exhaust of a diesel vehicle, Aerosol Sci. Technol. 38 (12) (2004) 1149–1160.
[37] C.C. Barrios, A. Domínguez-Sáez, J.R. Rubio, M. Pujadas, Development and evaluation of on-board measurement system for nanoparticle emissions from diesel engine, Aerosol Sci. Technol. 45 (5) (2011) 570–580, https://doi.org/10.1080/02786826.2010.550963.
[38] K. Vaaraslahti, A. Virtanen, J. Ristimäki, J. Keskinen, Nucleation mode formation in heavy-duty diesel exhaust with and without a particulate filter, Environ. Sci. Technol. 38 (18) (2004) 4884–4890, https://doi.org/10.1021/es0353255.
[39] W.J. An, R.K. Pathak, B.H. Lee, S.N. Pandis, Aerosol volatility measurement using an improved thermodenuder: Application to secondary organic aerosol, J. Aerosol Sci. 38 (3) (2007) 305–314, https://doi.org/10.1016/j.jaerosci.2006.12.002.
[40] D.B. Kittelson, W. Watts, J. Johnson, Diesel aerosol sampling methodology; CRC E-43 Final Report; University of Minnesota, Minneapolis, 2002.
[41] J.P. Szybist, J. Song, M. Alam, A.L. Boehman, Biodiesel combustion, emissions and emission control, Fuel Process. Technol. 88 (7) (2007) 679–691, https://doi.org/10.1016/j.fuproc.2006.12.008.
[42] F. Bach, H. Tschöke, H. Simon, Influence of alternative fuels on diesel engine aftertreatment, 7th International Colloquium Fuels - Mineral Oil Based and Alternative Fuels 14–15th January, Ostfildern, Germany, (2009).
[43] U. Mathis, M. Mohr, R. Kaegi, A. Bertola, K. Boulouchos, Influence of diesel engine combustion parameters on primary soot particle diameter, Environ. Sci. Technol. 39 (6) (2005) 1887–1892, https://doi.org/10.1021/es049578p.
[44] A. Tsolakis, Effects on particle size distribution from the diesel engine operating on RME-biodiesel with EGR, Energy Fuels 20 (4) (2006) 1418–1424, https://doi.org/10.1021/ef050385c.
[45] R. Li, Z. Wang, P. Ni, Y. Zhao, M. Li, L. Li, Effects of cetane number improvers on the performance of diesel engine fuelled with methanol/biodiesel blend, Fuel 128 (2014) 180–187, https://doi.org/10.1016/j.fuel.2014.03.011.
[46] M.M. Alrefaai, G.D.G. Peña, A. Raj, S. Stephen, T. Anjana, A. Dindi, Impact of dicyclopentadiene addition to diesel on cetane number, sooting propensity, and soot characteristics, Fuel 216 (2018) 110–120, https://doi.org/10.1016/j.fuel.2017.11.145.
[47] B. Kegl, M. Kegl, S. Pehan, Green Diesel Engine. Biodiesel Usage in Diesel Engines, Springer-Verlag, London, 2013.
[48] J.C. Guibet, Fuels and Engines: Technology, Energy, Environment, vol. 1, (1999).
[49] G. Kalghatgi, Fuel/Engine Interactions, SAE International, Warrendale, PA, 2014.
[50] Md.N. Nabi, R. Brown, Z. Ristovski, J. Hustad, A comparative study of the number and mass of fine particles emitted with diesel fuel and marine gas oil (MGO), Atmos. Environ. 57 (2012) 22–28, https://doi.org/10.1016/j.atmosenv.2012.04.039.
[51] L. Ntziachristos, Z. Samaras, P. Pistikopoulos, N. Kyriakis, Statistical analysis of diesel fuel effects on particle number and mass emissions, Environ. Sci. Technol. 34 (24) (2000) 5106–5114, https://doi.org/10.1021/es000074a.
[52] D.R. Tree, K.I. Svensson, Soot processes in compression ignition engines, Prog. Energ. Combust. 33 (3) (2007) 272–309, https://doi.org/10.1016/j.pecs.2006.03.002.
[53] M. Zetterdahl, K. Salo, E. Fridell, J. Sjöblom, Impact of aromatic concentration in marine fuels on particle emissions, J. Marine Sci. Appl. 16 (3) (2017) 352–361, https://doi.org/10.1007/s11804-017-1417-7.
[54] M. Talibi, P. Hellier, N. Ladommatos, Impact of increasing methyl branches in aromatic hydrocarbons on diesel engine combustion and emissions, Fuel 216 (2018) 579–588, https://doi.org/10.1016/j.fuel.2017.12.045.
[55] G.D.G. Peña, M.M. Alrefaai, S.Y. Yang, A. Raj, J.L. Brito, S. Stephen, et al., Effects of methyl group on aromatic hydrocarbons on the nanostructures and oxidative reactivity of combustion-generated soot, Combust. Flame 172 (2016) 1–12, https://doi.org/10.1016/j.combustflame.2016.06.026.
[56] S. Kalligeros, F. Zannikos, S. Stournas, E. Lois, G. Anastopoulos, C. Teas, et al., An investigation of using biodiesel/marine diesel blends on the performance of a stationary diesel engine, Biomass Bioenergy 24 (2) (2003) 141–149, https://doi.org/10.1021/es0515452.
[57] F. Arnold, L. Pirjola, H. Aufmhoff, T. Schuck, T. Lähde, K. Hämeri, First gaseous sulphuric acid measurements in automobile exhaust: Implications for volatile nanoparticle formation, Atmos. Environ. 40 (37) (2006) 7079–7105, https://doi.org/10.1016/j.atmosenv.2006.06.038.
[58] S. Biswas, S. Hu, V. Verma, J.D. Herner, W.H. Robertson, A. Ayala, et al., Physical properties of particulate matter (PM) from late model heavy-duty diesel vehicles operating with advanced PM and NO_x emission control technologies, Atmos. Environ. 42 (22) (2008) 5622–5634, https://doi.org/10.1016/j.atmosenv.2008.03.007.
[59] J. Heikkilä, A. Virtanen, T. Rönkkö, J. Keskinen, P. Aakko-Saksa, T. Murtonen, Nanoparticle emissions from a heavy-duty engine running on alternative diesel fuels, Environ. Sci. Technol. 43 (24) (2009) 9501–9506, https://doi.org/10.1021/es9013807.
[60] V. Jayaram, H. Agrawal, W.A. Welch, J.W. Miller, D.R. Cocker III, Real-time gaseous, PM and ultrafine particle emissions from a modern marine engine operating on biodiesel, Environ. Sci. Technol. 45 (6) (2011) 2286–2292, https://doi.org/10.1021/es1026954.
[61] L.G. Lackey, S.E. Paulson, Influence of feedstock: Air pollution and climate-related emissions from a diesel generator operating on soybean, canola, and yellow grease biodiesel, Energy Fuels 26 (1) (2011) 686–700, https://doi.org/10.1021/ef2011904.
[62] H.H. Yang, S.M. Chien, M.Y. Lo, J.C.W. Lan, W.C. Lu, Y.Y. Ku, Effects of biodiesel on emissions of regulated air pollutants and polycyclic aromatic hydrocarbons under engine durability testing, Atmos. Environ. 41 (34) (2007) 7232–7240, https://doi.org/10.1016/j.atmosenv.2007.05.019.
[63] M. Lapuerta, O. Armas, J. Rodriguez-Fernandez, Effect of biodiesel fuels on diesel engine emissions, Progr. Energy Combust. Sci. 34 (2) (2008) 198–223, https://doi.org/10.1016/j.pecs.2007.07.001.
[64] R. Nyström, I. Sadiktsis, T.M. Ahmed, R. Westerholm, J.H. Koegler, A. Blomberg, et al., Physical and chemical properties of RME biodiesel exhaust particles without engine modifications, Fuel 186 (2016) 261–269, https://doi.org/10.1016/j.fuel.2016.08.062.
[65] H. Jung, D.B. Kittelson, M.R. Zachariah, Characteristics of SME biodiesel-fueled diesel particle emissions and the kinetics of oxidation, Environ. Sci. Technol. 40 (16) (2006) 4949–4955, https://doi.org/10.1021/es0515452.
[66] P. Rounce, A. Tsolakis, A.P.E. York, Speciation of particulate matter and hydrocarbon emissions from biodiesel combustion and its reduction by aftertreatment, Fuel 96 (2012) 90–99, https://doi.org/10.1016/j.fuel.2011.12.071.

Paper V

energies

MDPI

Article

Effect of Alternative Liquid Fuels on the Exhaust Particle Size Distributions of a Medium-Speed Diesel Engine

Teemu Ovaska [1,*], Seppo Niemi [1], Katriina Sirviö [1], Sonja Heikkilä [1], Kaj Portin [2] and Tomas Asplund [2]

[1] School of Technology and Innovations, University of Vaasa, P.O. Box 700, FI-65101 Vaasa, Finland; seppo.niemi@univaasa.fi (S.N.); katriina.sirvio@univaasa.fi (K.S.); sonja.heikkila@univaasa.fi (S.H.)
[2] Wärtsilä Corporation, FI-65101 Vaasa, Finland; kaj.portin@wartsila.com (K.P.); tomas.asplund@wartsila.com (T.A.)
* Correspondence: teemu.ovaska@univaasa.fi

Received: 9 April 2019; Accepted: 27 May 2019; Published: 29 May 2019

Abstract: We mainly aimed to determine how alternative liquid fuels affect the exhaust particle size distributions (PSD) emitted by a medium-speed diesel engine. The selected alternative fuels included: circulation-origin marine gas oil (MGO), the 26/74 vol. % blend of renewable naphtha and baseline low-sulfur marine light fuel oil (LFO), and kerosene. PSDs were measured by means of an engine exhaust particle sizer from the raw exhaust of a four-cylinder, turbocharged, intercooled engine. During the measurements, the engine was loaded by an alternator, the maximum power output being set at 600 kW(e) at a speed of 1000 rpm. The partial loads of 450, 300, 150 and 60 kW(e) were also used for measurements. At each load, the PSDs had a distinct peak between 20 and 100 nm regardless of fuel. Relative to the other fuels, circulation-origin MGO emitted the lowest particle numbers at several loads despite having the highest viscosity and highest density. Compared to baseline LFO and kerosene, MGO and the blend of renewable naphtha and LFO were more beneficial in terms of total particle number (TPN). Irrespective of the load or fuel, the TPN consisted mainly of particles detected above the 23 nm size category.

Keywords: diesel engine; medium-speed; exhaust particle number; alternative fuel; renewable naphtha; circulation-origin MGO; kerosene; light fuel oil

1. Introduction

Medium-speed diesel engines are largely used for power generation on land and sea. In addition to base load and peak shaving, combustion engines are used to stabilize the electricity grid in the case of sudden peak power demands if the energy production is widely based on the renewable sources. Small amounts of harmful pollutant emissions may be generated due to the combustion of either liquid or gaseous fuel in the engine cylinder. Gaseous and particulate emissions are regulated worldwide to inhibit the effects of pollutants on the ambient air quality, human health, and climate change.

For stationary engines of generating sets above 560 kW, the emission regulations of non-road mobile machinery (NRMM) must be met. In the newest Stage V, the NRMM set of regulation includes limits for exhaust particle number (PN) emissions [1]. The PN emission limitation will also be applied to inland waterway vessels when the regulation comes gradually into effect within 2019–2020.

The effect of the high sulfur content and other fuel characteristics on the particle emissions of medium-speed diesel engines have been reported [2,3]. Diesel engine exhaust contains particles that usually form a bimodal size distribution: one mode consists of nucleation particles (mean diameter

under 50 nm) and the other of accumulation particles (50–500 nm) [4–8]. When either the fuel or the remnants of lubricating oil do not burn completely during combustion, accumulation mode particles form in the cylinder. The majority of the nucleation mode particles are thought to form when the exhaust gas mixes with the ambient air [6,9].

Clean renewable fuels are one material that can be used to reduce exhaust pollutants below the legislation limits, simultaneously increasing the sustainability of combustion-based power generation. We concentrated on determining the effects of three fuel options on the particulate number (PN) emissions of a medium-speed diesel engine intended for power plants and marine applications. Of the fuels, marine gas oil (MGO) was a product of the circulation economy. Naphtha was a residue of the manufacturing process of renewable diesel. Wood and forest residues formed the feedstock and the process used crude tall oil (CTO) as the raw material. Kerosene-based Jet A-1 fuel, used widely in commercial aviation, has properties similar to diesel fuel oils (DFO) or low-sulfur light fuel oil (LFO). Thus, kerosene was selected for investigation. The interest in studying jet fuels has increased after the U.S. Army Single Fuel Forward Policy was introduced. The aircraft gas turbine engines are now fueled by kerosene-based Jet Propellant 8 (JP-8) fuel, which has been the low-sulfur substitute for JP-4. Regarding fuel properties, JP-8 is similar to Jet A-1 [10].

The PN has earlier been reported to significantly decrease when using low-sulfur marine fuels instead of heavy fuel oil (HFO) [3,11,12]. Anderson et al. [11] determined how distillate fuels affect the exhaust particle size distribution (PSD) of a marine high-speed diesel engine in laboratory conditions. Zetterdahl et al. [3] investigated the number of particles emitted with low sulfur residual marine fuel oil on-board a ship. Sarvi et al. [2] studied the differences in the PSDs when LFO and HFO were used in a medium-speed diesel engine.

Nabi et al. [13] investigated how two low-sulfur fuels, MGO and regular on-road diesel fuel, affect the PN emissions from a marine high-speed diesel engine. As a preparative investigation for the present study, Ovaska et al. [14] studied the effects of circulation-origin MGO, a blend of renewable naphtha and marine LFO, and kerosene on the exhaust PSDs of a high-speed diesel engine. The blend was found to decrease the accumulation mode particles. However, combustion in a marine medium-speed engine differs from that in a smaller high-speed engine. Medium-speed engines are operated at lower engine speeds and higher air-to-fuel ratios. Lower engine speed allows more time for fuel to combust, which promotes soot oxidation. Compared to the emission limitation intended for road vehicles at some loads, the use of the LFO fuel in a marine engine may result in much lower specific mass emissions of particles [12].

Despite the sustainable and affordable alternative liquid fuels are needed for the reduction of exhaust pollutants from compression ignited (CI) engines, the technical compatibility of the alternative fuel has to be assessed [15]. Especially for marine applications where alternative fuel options are used, fuel must be compatible with the other systems. Kerosene-based jet fuel has typically lower viscosity and cetane number compared to LFO or MGO used in the CI engines in marine and land-use applications. Ignition delay is extended by a low cetane number. Thus, the cetane number affects the combustion timing. Due to the extended delay, changes in cold-starting performance, combustion noise level, and exhaust emissions are expected. Low fuel viscosity may worsen the fuel injection system performance, which leads to fuel pump wear and fuel leakage [10].

Poor lubricity is characteristic, for example, for neat naphtha, and thus it may be assumed to cause problems in the entire engine fuel system. The lubricity features of naphtha can be improved by blending. However, use of blended fuels by the marine or power plant operators requires accurate knowledge of the physical and chemical properties of the blends. The blend stability and the compatibility issues with the engine and lubricants have to be carefully assessed to avoid operational problems such as carbon deposition, lubricating oil dilution, piston ring sticking, or injector nozzle choking [16–18].

This paper presents how the selected alternative fuels affected the PSD of the medium-speed experimental engine. The main aim was to determine the effect of two completely novel fuel options:

circulation-origin MGO and a blend of renewable naphtha and marine LFO. Both meet the sustainability and affordability goals set by the ship owners. Along with these fuels, the other studied low-sulfur fuels were LFO (baseline) and kerosene. Alongside the exhaust particle number and size distributions, gaseous emissions and basic engine performance were determined. The engine was loaded by an alternator, with a maximum power output set to 600 kW(e) at a speed of 1000 rpm. Partial loads were also used for the measurements. The default engine control parameters were kept constant during the experiments. No parameter optimization was applied with the studied fuels.

2. Materials and Methods

The experimental measurements were performed at the University of Vaasa (UV) at the Internal Combustion Engine (ICE) laboratory of Vaasa Energy Business Innovation Centre (VEBIC), Finland.

2.1. Engine and Fuels

The experiments were performed with a medium-speed diesel engine connected to an alternator on a common base-frame. The engine was a turbocharged, intercooled (air-to-water), 4-cylinder engine, not equipped with any exhaust gas after-treatment devices. The engine specifications are provided in Table 1. In addition to baseline LFO, the effects of naphtha-LFO blend, MGO, and kerosene on the exhaust PSD were investigated (Table 2).

Table 1. Engine specifications.

Parameter	Value
Cylinder Number	4
Bore (mm)	200
Stroke (mm)	280
Swept volume/cylinder (dm^3)	8.8
Speed (rpm)	1000
Selected Maximum Alternator Power Output at 1000 rpm (kW(e))	600

Table 2. Fuel specifications.

Parameter	Method	Light Fuel Oil (LFO)	Kerosene	Marine Gas Oil (MGO)	Naphtha-LFO	Unit	ISO 8217:2017(E), Distillate Marine Fuel Category ISO-F-DMX	
							Min.	Max.
Kin. viscosity (40 °C)	EN ISO 3104/ASTM D7042	3.1	0.99	3.7	1.8	mm^2/s	1.4	5.5
Density (15 °C)	EN ISO 12185/ASTM D7042	836	787	838	810	kg/m^3	-	-
Cetane number	EN 15195	58	44	54	52	-	-	-
Sulfur content	EN ISO 20884/EN ISO 20846	0.0006	0.09	0.003	0.00045	wt.%	-	1
Carbon	ASTM D5291	84.5	85.1	84.8	85.0	wt.%	-	-
Hydrogen	ASTM D5291	13.4	13.9	13.7	13.8	wt.%	-	-

The naphtha content in the naphtha-LFO blend was 26 vol. %. The naphtha was a side-product of wood-based renewable diesel production. The MGO was a Finnish marine fuel produced from recycled lubricating oils. The kerosene was Jet A-1 type aviation fuel. The baseline LFO was light fuel oil with low sulfur content of below 1 wt.%, fulfilling the ISO 8217:2017(E) standard requirements as did the other fuels regarding sulfur [19]. For the fuels, kinematic viscosity at 40 °C, density, cetane number, sulfur content, and the contents of carbon and hydrogen were analyzed by the fuel laboratory of the University of Vaasa, Vaasa, Finland.

2.2. Analytical Instruments

In this study, particles ranging from 5.6 to 560 nm were recorded using an engine exhaust particle sizer (EEPS). The adopted measurement instruments for gaseous emissions and combustion analysis are listed in Table 3.

Table 3. Measuring equipment for gaseous emissions.

Parameter	Device	Technology
Particle number and size distribution	TSI EEPS 3090, Shoreview, MN, USA	spectrometer
Hydrocarbons	J.U.M. VE7, Karlsfeld, Germany	heated flame ionization detection (HFID)
NO_x	Eco Physics CLD 822 M h, Dürnten, Switzerland	chemiluminescence
CO	Siemens Ultramat, München, Germany	non dispersive infra-red (NDIR)
Oxygen content	Siemens Oxymat 61, München, Germany	paramagnetic
Cylinder pressure, heat release	Kistler KiBox®, Winterthur, Switzerland	-

The analyzers were calibrated manually once a day according to the manufacturers' instructions prior to the measurements. The sample flow rate was adjusted to 5.0 L/min for the EEPS. In the data processing, the "SOOT" inversion was applied [20]. The arrangement of the test bench with auxiliary systems and measurement devices is depicted in Figure 1.

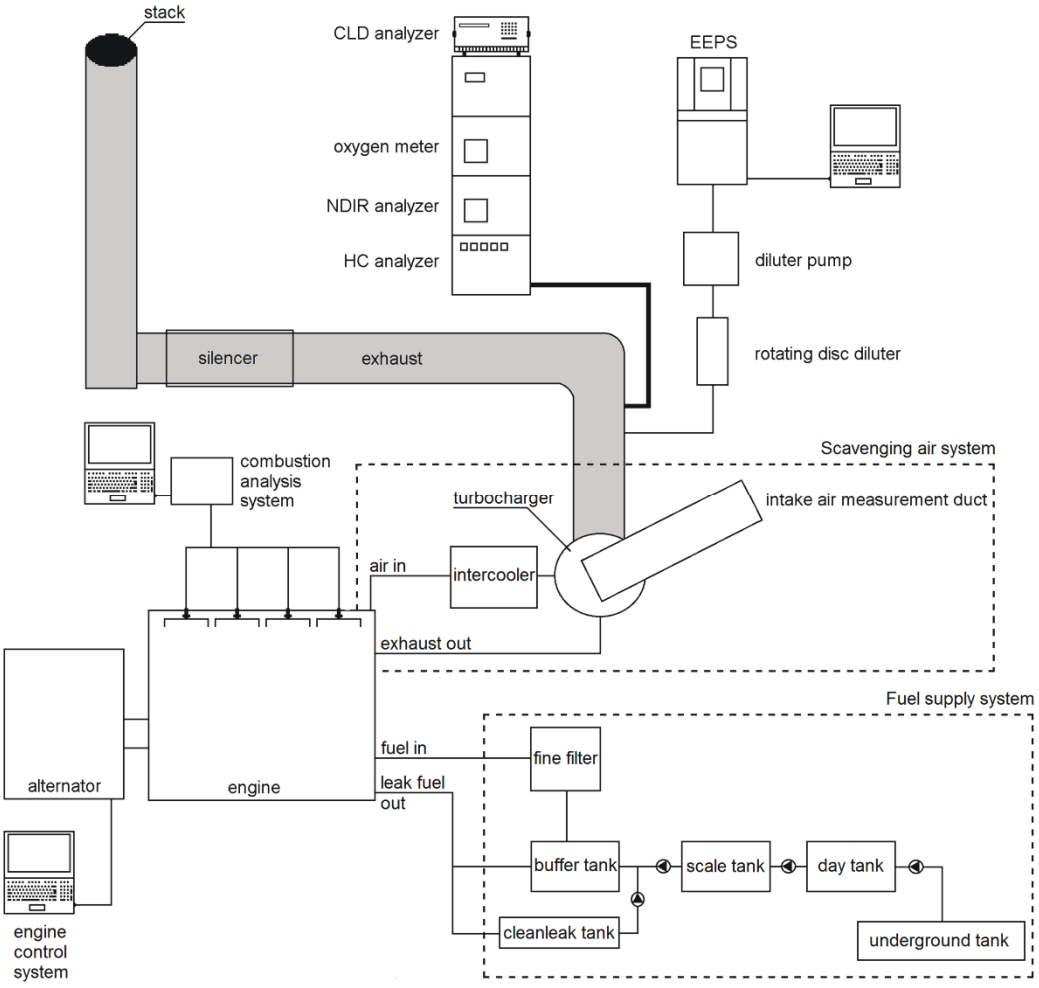

Figure 1. Experimental set-up.

The exhaust sample was first diluted with ambient air in a rotating disc diluter (RDD) (model MD19-E3, Matter Engineering AG, Wohlen, Switzerland). During the measurements, the dilution ratio in the RDD was a constant 60. The exhaust aerosol sample was passed through the RDD, which maintained dilution air at 150 °C. The diluted sample (5 L/min) was further diluted using purified air with a dilution ratio of 2 to fit the sample volume flow to measurable for the EEPS. Thus, the total dilution ratio used in PSD measurements was 120.

The particle number (PN) was recorded consecutively three times. Each recording was one minute long, after which the averaged interval of 2 seconds was used when the data were stored. The uncertainty of the PN measurement was approximated by calculating the standard deviation of the PN averages, taken from each one-minute recording. By means of the extended measurement period of eight minutes, the stability of the PN measurement was monitored.

Total particle number (TPN, from 5.6 to 560 nm) was calculated from the PN recordings by adding the PN concentrations indicated in the size bins of the EEPS spectrometer during the one averaging interval. For the presented TPN results of this paper, the average of PN sums was calculated. The averages of the normalized PN concentrations (dN/dlogD_p, where N is particle concentration and D_p the mobility diameter of a particle) were calculated from each bin in order to illustrate the PSDs. The calculated TPN averages and the averages of the normalized PN concentrations were multiplied by the total dilution ratio of the exhaust sample to present the corresponding concentrations in the raw exhaust.

The sensor data were collected and the engine control parameters were applied via engine management software. By using the software, the temperatures of cooling water, intake air, and exhaust gas, plus the pressures of the intake air and exhaust gas were recorded. Cylinder pressure and heat release were also monitored simultaneously from all four cylinders.

Emissions of total hydrocarbons (HC), nitrogen oxides (NO_x), and carbon monoxide (CO), plus oxygen content were also measured on dry basis. Based on the measured HC, NO_x, and CO concentrations, the brake-specific emissions of HC, NO_x, and CO were calculated according to the ISO 8178 standard [21].

2.3. Experimental Matrix and Running Procedure

The engine was loaded by the alternator, the maximum power output being set to 600 kW(e) at a speed of 1000 rpm. The speed was kept constant. The measurements were also recorded at the partial loads of 450, 300, 150, and 60 kW(e). Mainly, the procedure followed the D2 test cycle of the ISO 8178-4 standard. The only controllable variable regarding the engine loading was the power output of the alternator due to the test installation. The output of the test installation was measured as net electric power downstream the frequency converter used to control the engine-driven generator set. We used the net electric power as the most accurate measure of the produced output.

At each load point, recordings were collected after the engine had stabilized, i.e., the temperatures of coolant water, intake air, and exhaust were stable. The length of the measurement period was not tied to a certain time.

Despite the PN and PSD, all measurement values were recorded once at each load point.

3. Results

3.1. Particle Size Distributions

With all fuels at different loads, a bimodal shape was detected for the distributions. One low peak was detected at a particle size of ca. 10 nm and the maximum within the range of 30 to 100 nm. The accumulation mode peaks were normally higher by two orders of magnitude compared to the nucleation mode peaks.

Figure 2 shows the PSDs at full load. The highest peak was detected with LFO. Below a particle size of 50 nm, the naphtha-LFO blend generated the lowest PN, and LFO or kerosene the highest. In

the range of 85 to 200 nm, kerosene emitted the fewest particles whereas the order of other fuels varied. For all fuels, the peak PN was detected at different particle size bins.

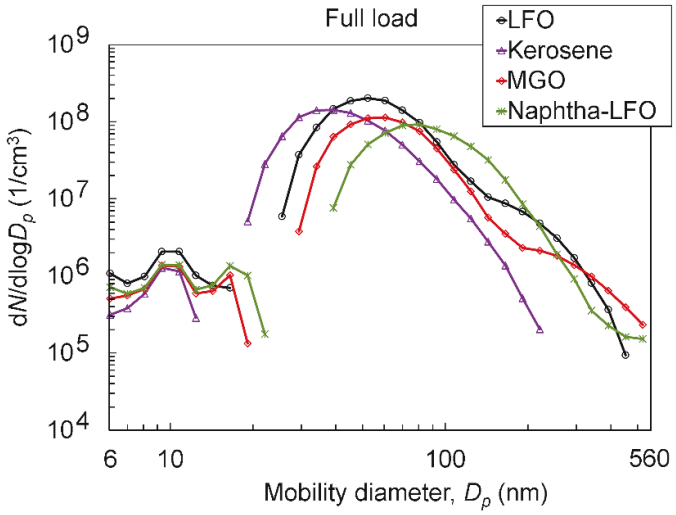

Figure 2. Exhaust particle size distributions (PSD) at full load.

Both at 75% and half loads, one distinct peak was observed between 20 and 50 nm regardless of fuel (Figures 3 and 4). The detected PN was the lowest for naphtha-LFO between 20 and 35 nm. From 35 to 100 nm, the lowest PN was recorded for MGO.

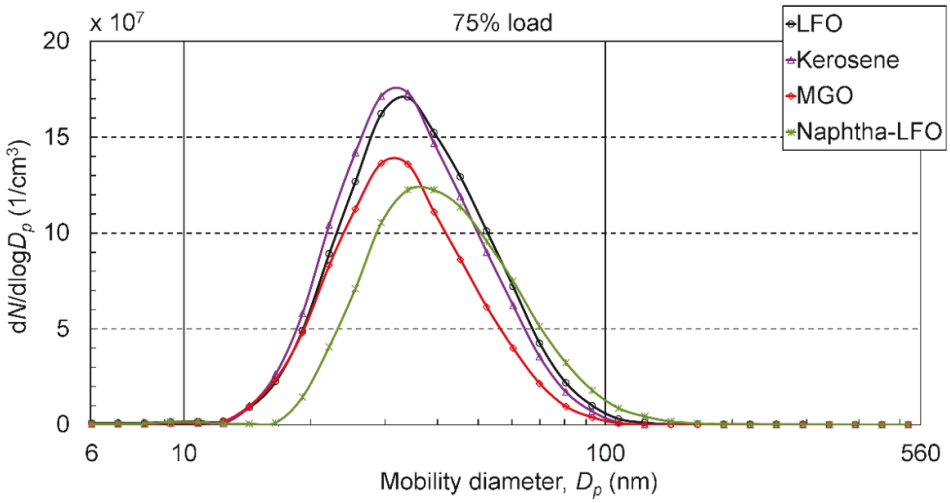

Figure 3. Exhaust PSDs at 75% load.

At 75% load, the lowest peak of the distributions was produced by naphtha-LFO. The blend, kerosene, and baseline LFO peaked at the size bin of 34 nm, whereas MGO peaked at 29.4 nm. The greatest peak was recorded with kerosene at 29.4 nm, but the maximum of LFO was almost as high.

At half load, again, naphtha-LFO showed the lowest peak. With naphtha-LFO (34 nm), MGO (29.4 nm), and LFO (34 nm), the PN peaked at the same size bins as at 75% load.

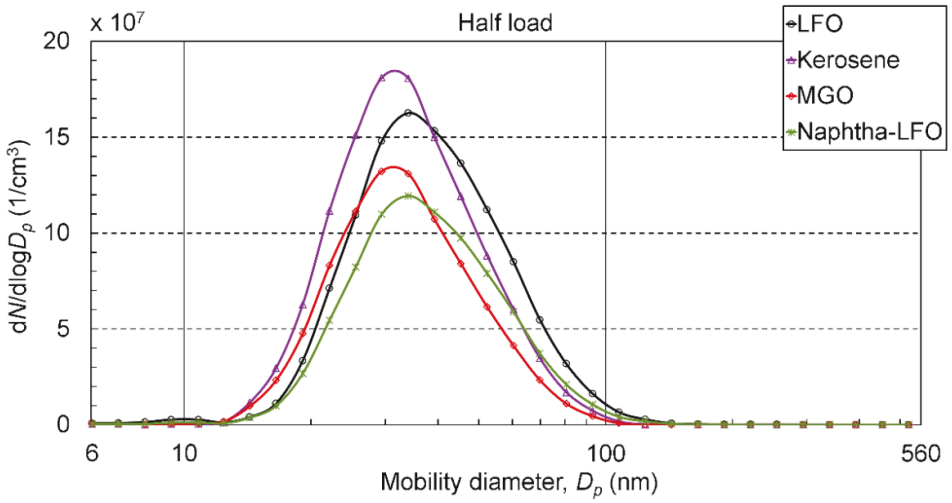

Figure 4. Exhaust PSDs at half load.

Figure 5 illustrates the PSDs for the 25% load. Again, one distinct peak was detected between 20 and 50 nm regardless of fuel. From the size category of 35 nm and larger, the lowest PN was produced by MGO and the greatest by kerosene. The lowest peak out of the distributions was produced by MGO at the size bin of 29.4 nm and the highest peak was produced by kerosene at 39.2 nm. Between MGO and kerosene, LFO peaked at 34 nm, and naphtha-LFO at the same size bin as kerosene.

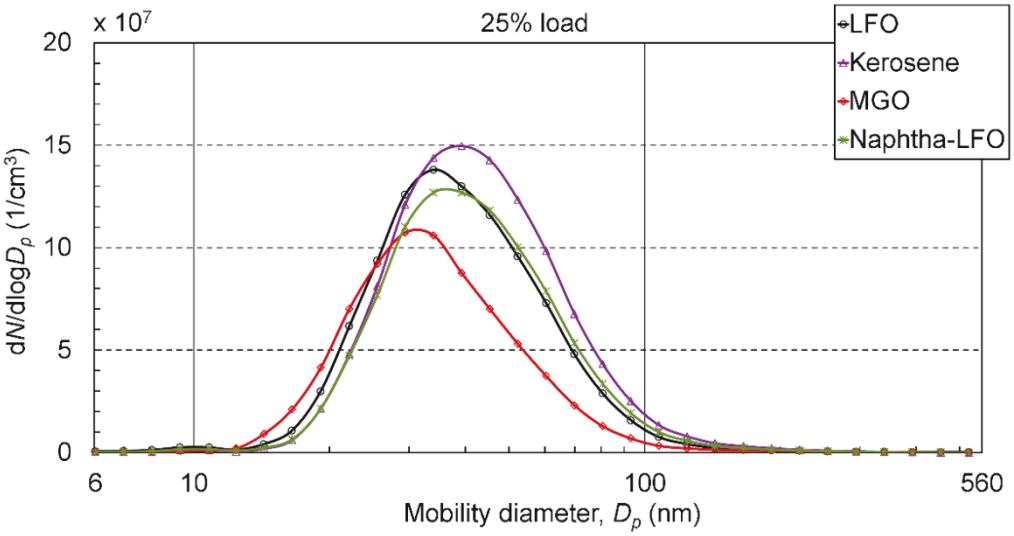

Figure 5. Exhaust PSDs at 25% load.

At 10% load, the detected PN was the lowest for naphtha-LFO between the size categories of 20 and 30 nm (Figure 6). From the size category of 29 nm and larger, the lowest PN was detected for MGO. The recorded distribution for MGO peaked again at the size of 29.4 nm, the peak also being the lowest. The second lowest peak was for naphtha-LFO at 45.3 nm, for LFO at 39.2 nm, and then for kerosene at 34 nm.

For all loads, the lowest peak was usually measured for MGO or naphtha-LFO, and the highest for kerosene. The positions of the peaks varied but MGO often showed a peak at lower particle size than the other fuels.

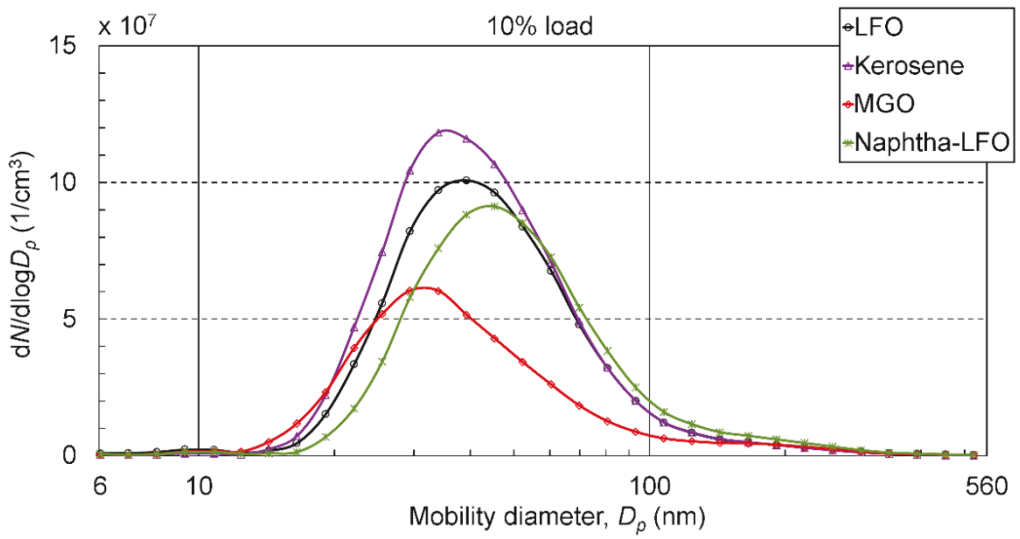

Figure 6. Exhaust PSDs at 10% load.

3.2. Total Particle Number Emissions

Figure 7 depicts the total particle number (TPN, from 6 to 560 nm) for all engine loads. In total, MGO and naphtha-LFO emitted fewer particles than LFO and kerosene. By far the highest TPN for kerosene was observed at half load, for MGO at 75% load, and for the blend at 25% load.

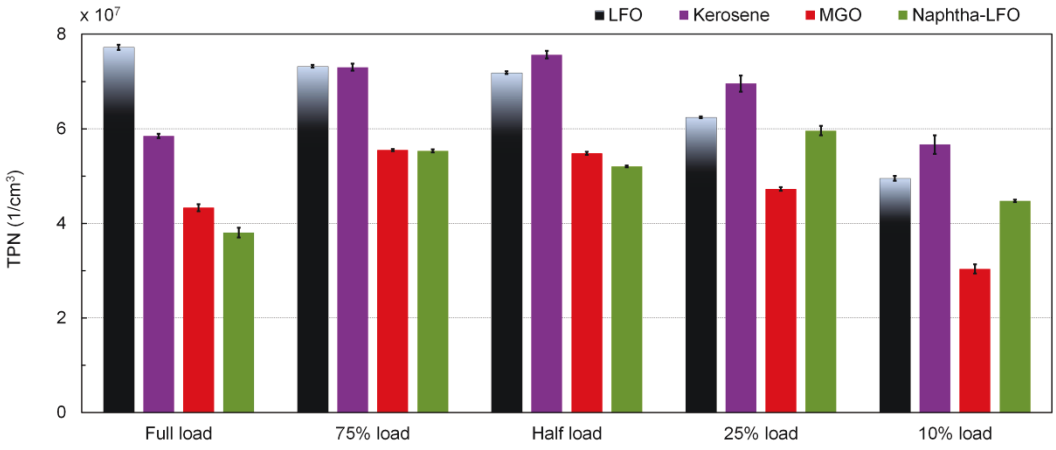

Figure 7. Total particle number (TPN) at different engine loads.

At full load, the blend produced the lowest TPN, whereas baseline LFO produced the highest. At 75% load, the lowest (almost equal) particle numbers were measured for MGO and naphtha-LFO. LFO and kerosene emitted the highest TPNs. As at full load, the blend produced the lowest TPN at half load; the highest TPN was detected with MGO. At 25% and 10% loads, MGO produced the lowest TPN, whereas kerosene the highest.

At full load, kerosene produced the fewest particles at sizes greater than 70 nm. The highest PN was observed with LFO at around 50 nm. The maximum PN was detected with kerosene at the size of 40 nm, whereas with naphtha-LFO, the maximum was detected at 80 nm.

At both 75% and half loads, naphtha-LFO emitted the least particles within 15–35 nm, but between 40 and 100 nm, MGO was the most favorable. At half load, the particle numbers above 40 nm were the highest with LFO. Now, the maximum PN of fuels varied between 25 and 40 nm. MGO produced the lowest and kerosene the highest PN from 30 nm onward. As at 25% load, MGO was clearly the most favorable at 35–100 nm. Irrespective of load, the blend often generated the least PN at approx. 25 nm, but compared to LFO, it produced more particles at the 100 nm size category.

Table 4 lists the shares of the particles detected above the size category of 23 nm. In this study, the TPN consisted mainly of the particles above this size category. For all fuels, the share of particles larger than 23 nm was the highest at full load, being always higher than 95%. Regarding all loads, the lowest average share of the particles above 23 nm was detected with kerosene, and the highest share with naphtha-LFO.

Table 4. Shares of the particles detected above the size category of 23 nm.

Fuel	Full Load	75% Load	Half Load	25% Load	10% Load
LFO	99.2	84.9	88.7	88.5	92.0
Kerosene	99.0	81.0	80.8	80.5	82.5
MGO	95.6	82.7	81.9	92.7	91.0
Naphtha-LFO	98.6	93.0	88.1	91.2	95.7

3.3. Gaseous Emissions

Although the gaseous emissions of HC, NO_x, and CO, and oxygen content were measured, any relationship between the PN emission and gaseous emissions, e.g., NO_x–PM trade-off, were not investigated. Calculated for each fuel at full load, the brake specific emissions of HC, NO_x and CO are presented as supportive background information for the test engine emission levels in Table 5. The HC emission varied from 0.34 to 0.40 g/kWh, NO_x from 15.1 to 16.3 g/kWh, and CO from 0.37 to 0.40 g/kWh. The naphtha-LFO blend produced the lowest HC emissions and kerosene the highest NO_x emission. The high NO_x levels indicated that the engine was tuned to high efficiency and low fuel consumption. Consequently, smoke and PM were inherently low.

Table 5. Brake specific emissions of hydrocarbons (HC), nitrogen oxides (NO_x), and carbon monoxide (CO) at full load with different fuels.

Fuel	HC (g/kWh)	NO_x (g/kWh)	CO (g/kWh)
LFO	0.39	15.2	0.39
Kerosene	0.39	16.3	0.37
MGO	0.40	15.3	0.40
Naphtha-LFO	0.34	15.1	0.39

The oxygen content of the engine exhaust is presented in Figure 8. The oxygen content was almost equal for all fuels.

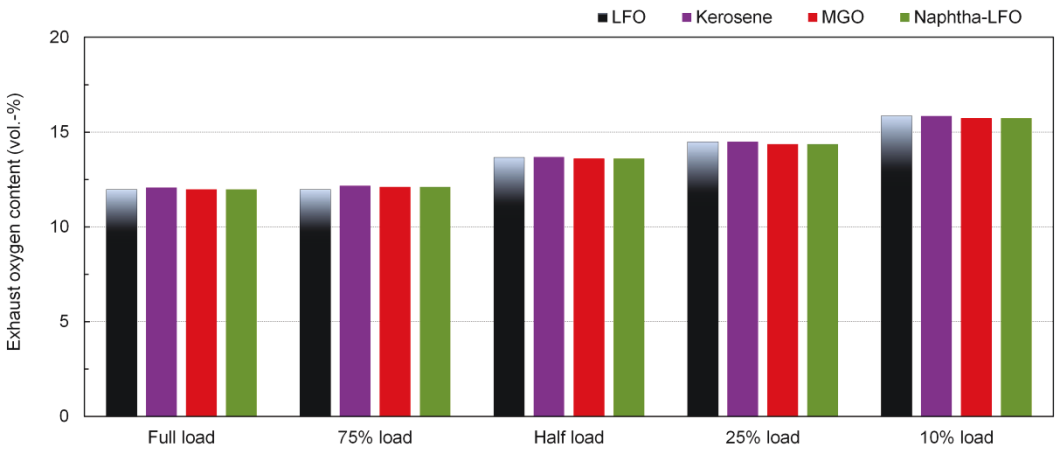

Figure 8. Dry exhaust oxygen content at different engine loads for studied fuels.

4. Discussion

The formation of exhaust particles depends on several issues related to fuel injection and combustion. The physical properties of the liquid fuel tend to control fuel spray characteristics, whereas the fuel composition determines the pathways of chemical reactions during combustion [22]. Besides the fuel sulfur content, fuel characteristics, such as the fuel density [23,24], viscosity [25,26], cetane number [27,28], and fuel contents of aromatic compounds [29], influence particle formation.

All alternative fuels selected for this study had fairly good quality in terms density and viscosity. If the fuel viscosity is extremely low or high, poor fuel injection and increased fuel consumption result. Due to low fuel viscosity, the fuel injection system performance can deteriorate and fuel pump wear and leakage through the nozzle sealing may occur [10,30]. Higher fuel viscosity may lead to incomplete combustion due to less favorable fuel atomization, and the soot emission may increase [13,31]. In this study, kerosene had the lowest kinematic viscosity at 40 °C (0.99 mm^2/s), whereas the blend was the second lowest (1.77 mm^2/s), and MGO the highest (3.74 mm^2/s). At 40 °C, the viscosity of LFO (3.12 mm^2/s) was between the blend and MGO.

High fuel density may deteriorate fuel spray formation during fuel injection. As a result, fuel burns incompletely and high emissions may occur [30]. At 15 °C, the density was the lowest for kerosene (787 kg/m^3), second lowest for naphtha-LFO blend (810 kg/m^3), and the highest for MGO (838 kg/m^3). The density of reference fuel LFO (836 kg/m^3) was almost equal to that of MGO.

Kerosene-based jet fuel typically has lower viscosity and cetane number compared to LFO or MGO used in CI engines in marine and land-use applications. The higher the cetane number, the shorter the ignition delay plus advanced combustion. Cold-starting performance, combustion noise level, and exhaust emissions may change due to the extended delay [10,13,31].

In this study, MGO emitted the lowest PN at several loads despite its highest viscosity and density. The cetane number, viscosity, and density of MGO were, however, within an appropriate range for a CI engine.

The lowest density and viscosity of kerosene may explain the favorable PN result at full load, although the cetane number was the lowest and the sulfur content the highest. The high sulfur content of kerosene may still be the most evident reason for the high PN result at all part loads. All fuel properties, presented in Table 2, including cetane number, density, sulfur content, and kinematic viscosity, were the second lowest for naphtha-LFO. Therefore, naphtha-LFO emitted the lowest TPN at full and half loads and always lower TPN than neat LFO.

In this study, the detected PSDs were bimodal but the peak at a particle size of ca. 10 nm was rather low compared to the maximum within 30–100 nm.

No consistent conclusions could be drawn concerning the particle numbers under the size category of 20 nm for the following reasons. First, mobility particle size spectrometers, as EEPS, have been found to be best for measuring particle numbers within the size range of 20 to 200 nm [32]. Outside this size range, increased uncertainties may exist, as described by Wiedensohler et al. [33]. Second, the complex nature of nucleation mode PN has to be considered. The engine parameters [34], fuel and lubricating oil characteristics [35], and exhaust after-treatment [36] are not the only factors that influence the formation of the nucleation mode PN. The dilution conditions, such as dilution ratio, temperature, and relative humidity of the dilution air [37], also affect the formation. Rönkkö et al. [6] reported that nucleation mode PN formation was insensitive to the fuel sulfur content, dilution air temperature, and relative humidity of ambient air.

Figure 9 illustrates the actual TPN versus the measurement time at full load. Each fuel had a stable TPN level over the extended measurement period of eight minutes. Thus, during data curation, the arithmetic mean was calculated over each measured dataset by means of EEPS, including each fuel at each load, to describe the variation in the PN during the measurements.

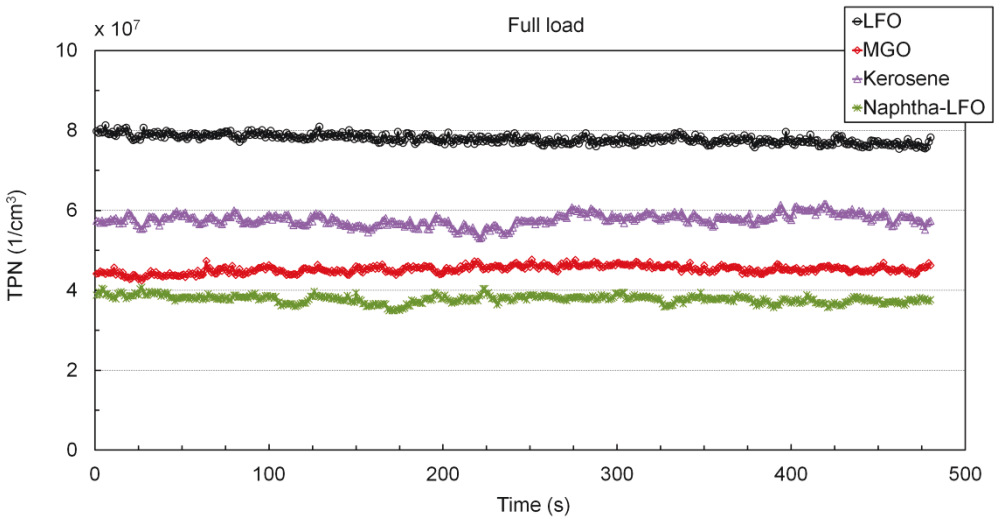

Figure 9. The actual TPN during eight-minute measurement time at full load.

For full load, Figure 10 illustrates the variation in the PN between three consecutive one-minute EEPS scans. The average values, shown in Figure 10, were calculated from the recordings of four EEPS measurement channels. As shown, the average PNs remained almost constant in relation to time.

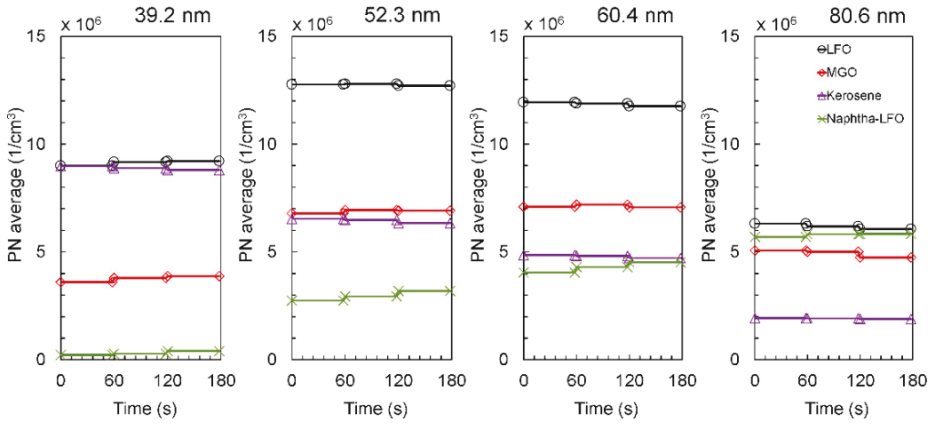

Figure 10. The average particle number between the three consecutive one-minute EEPS scans at the four channels.

In future studies, engine parameters should be optimized because no parameter optimization was applied to any fuels in this study. The fuels were first chosen for comparison without any modifications. Further experiments for different operational conditions should be designed to obtain a wider viewpoint on the NO_x and particulate matter (PM) emissions. Those studies should also include the effects of the humidity of the supplied air [38].

5. Conclusions

The current study determined the effects of three fuel options on PN emissions of a medium-speed diesel engine. The fuels were circulation-economy-derived MGO, a blend of renewable naphtha and low-sulfur LFO, and kerosene. Neat LFO formed the baseline. The engine was run at five alternator output loads at a constant engine speed. The PN was measured by means of an EEPS analyzer.

Based on the results, the following conclusions could be drawn:

(1) Bimodal PSDs were detected for all fuels and loads. However, the peak of the nucleation mode particles was always lower by two orders of magnitude than that of larger particles.

(2) Circulation-economy-based MGO emitted the lowest PN at several loads despite its slightly higher viscosity, density, and sulfur content.
(3) In terms of TPN, MGO and the blend of renewable naphtha and LFO were more beneficial compared to LFO. At full, 75%, and half loads, the blend emitted clearly fewer particles than LFO, but at low loads, the difference in TPN was smaller.
(4) For all fuels within the entire load range, the share of particles larger than 23 nm was high—80–99%. The highest load-averaged share was measured for the naphtha-LFO blend.
(5) Compared with the other fuels, the NO_x emissions were slightly higher with kerosene. The blend generated the lowest HC.

Author Contributions: Conceptualization, T.O., S.N., K.P., T.A., and K.S.; methodology, S.N., T.O., and S.H.; software, T.O.; validation, K.P., T.A., and S.N.; formal analysis, T.O. and K.S.; investigation, T.O., K.S., and S.H.; resources, S.N., K.P., and T.A.; data curation, T.O.; writing—original draft preparation, T.O. and S.N.; writing—review and editing, T.O., S.N., and K.S.; visualization, T.O.; supervision, S.N.; project administration, S.N.; funding acquisition, K.P., T.A., and S.N.

Funding: This project received funding from the European Union's Horizon 2020 research and innovation programme under grant agreement No. 634135 (Hercules-2).

Acknowledgments: This project received funding from the European Union's Horizon 2020 research and innovation programme under grant agreement No. 634135 (Hercules-2). The authors wish to thank Olav Nilsson, Saana Hautala, Kirsi Spoof-Tuomi, Janne Suomela, Antti Niemi, and Antti Kiikeri for their assistance during the measurement campaigns. In addition, the authors express their gratitude to Krister Ekman from Turku University of Applied Sciences for his assistance during the measurements.

Conflicts of Interest: The authors declare no conflict of interest. The funders had no role in the design of the study; in the collection, analyses, or interpretation of data; in the writing of the manuscript, or in the decision to publish the results.

Nomenclature

Symbol	
D_p	mobility diameter of a particle
$dN/d\log D_p$	normalized particle number concentration, $1/cm^3$
N	particle concentration
Abbreviations	
ASTM	American Society for Testing and Materials
CO	Carbon Monoxide
CTO	Crude Tall Oil
EEPS	Engine Exhaust Particle Sizer
DMX	Distillate marine fuel category ISO-F-DMX
EN	European Standard
HC	Hydrocarbon
HFID	Heated Flame Ionization Detection
HFO	Heavy Fuel Oil
ICE	Internal Combustion Engine
ISO	International Organization for Standardization
LFO	Light Fuel Oil
MGO	Marine Gas Oil
NDIR	Non-Dispersive Infra-Red
NO_x	Nitrogen Oxides
NRMM	Non-Road Mobile Machinery
PN	Particle Number
PM	Particulate Matter
PSD	Particle Size Distribution
RDD	Rotating Disc Diluter
TPN	Total Particle Number
UV	University of Vaasa
VEBIC	Vaasa Energy Business Innovation Centre

References

1. EU Regulation 2016/1628. Regulation of the European Parliament and of the Council on Requirements Relating to Gaseous and Particulate Pollutant Emission Limits and Type-Approval for Internal Combustion Engines for Non-Road Mobile Machinery. Available online: http://data.europa.eu/eli/reg/2016/1628/oj (accessed on 16 January 2019).
2. Sarvi, A.; Lyyränen, J.; Jokiniemi, J.; Zevenhoven, R. Particulate emissions from large-scale medium-speed diesel engines: 1. Particle size distribution. *Fuel Process. Technol.* **2011**, *92*, 1855–1861. [CrossRef]
3. Zetterdahl, M.; Moldanová, J.; Pei, X.; Pathak, R.K.; Demirdjian, B. Impact of the 0.1% fuel sulfur content limit in SECA on particle and gaseous emissions from marine vessels. *Atmos. Environ.* **2016**, *145*, 338–345. [CrossRef]
4. Kittelson, D.B. Engines and nanoparticles: A review. *J. Aerosol Sci.* **1998**, *29*, 575–588. [CrossRef]
5. Rönkkö, T.; Virtanen, A.; Vaaraslahti, K.; Keskinen, J.; Pirjola, L.; Lappi, M. Effect of dilution conditions and driving parameters on nucleation mode particles in diesel exhaust: Laboratory and on-road study. *Atmos. Environ.* **2006**, *40*, 2893–2901. [CrossRef]
6. Rönkkö, T.; Virtanen, A.; Kannosto, J.; Keskinen, J.; Lappi, M.; Pirjola, L. Nucleation mode particles with a nonvolatile core in the exhaust of a heavy duty diesel vehicle. *Environ. Sci. Technol.* **2007**, *41*, 6384–6389. [CrossRef] [PubMed]
7. Filippo, A.D.; Maricq, M.M. Diesel nucleation mode particles: Semivolatile or solid? *Environ. Sci. Technol.* **2008**, *42*, 7957–7962. [CrossRef]
8. Lähde, T.; Rönkkö, T.; Virtanen, A.; Solla, A.; Kytö, M.; Söderström, C.; Keskinen, J. Dependence between nonvolatile nucleation mode particle and soot number concentrations in an EGR equipped heavy-duty diesel engine exhaust. *Environ. Sci. Technol.* **2010**, *44*, 3175–3180. [CrossRef] [PubMed]
9. Nousiainen, P.; Niemi, S.; Rönkkö, T.; Karjalainen, P.; Keskinen, J.; Kuuluvainen, H.; Pirjola, L.; Saveljeff, H. Effect of Injection Parameters on Exhaust Gaseous and Nucleation Mode Particle Emissions of a Tier 4i Nonroad Diesel Engine. Available online: https://dx.doi.org/10.4271/2013-01-2575 (accessed on 15 April 2019).
10. Fernandes, G.; Fuschetto, J.; Filipi, Z.; Assanis, D.; McKee, H. Impact of military JP-8 fuel on heavy-duty diesel engine performance and emissions. *Proc. Inst. Mech. Eng. Part D J. Automobile Eng.* **2007**, *221*, 957–970. [CrossRef]
11. Anderson, M.; Salo, K.; Hallquist, Å.M.; Fridell, E. Characterization of particles from a marine engine operating at low loads. *Atmos. Environ.* **2015**, *101*, 65–71. [CrossRef]
12. Ntziachristos, L.; Saukko, E.; Lehtoranta, K.; Rönkkö, T.; Timonen, H.; Simonen, P.; Karjalainen, P.; Keskinen, J. Particle emissions characterization from a medium-speed marine diesel engine with two fuels at different sampling conditions. *Fuel* **2016**, *186*, 456–465. [CrossRef]
13. Nabi, M.N.; Brown, R.J.; Ristovski, Z.; Hustad, J.E. A comparative study of the number and mass of fine particles emitted with diesel fuel and marine gas oil (MGO). *Atmos. Environ.* **2012**, *57*, 22–28. [CrossRef]
14. Ovaska, T.; Niemi, S.; Sirviö, K.; Nilsson, O.; Portin, K.; Asplund, T. Effects of alternative marine diesel fuels on the exhaust particle size distributions of an off-road diesel engine. *Appl. Therm. Eng.* **2019**, *150*, 1168–1176. [CrossRef]
15. Jääskeläinen, S. *Alternative Transport Fuels Infrastructure—Finland's National Plan*; Publications of the Ministry of Transport and Communications: Helsinki, Finland, 2017. Available online: https://julkaisut.valtioneuvosto.fi/bitstream/handle/10024/80230/Report%205-2017.pdf?sequence=1 (accessed on 15 April 2019).
16. Patel, P.D.; Lakdawala, A.; Chourasia, S.; Patel, R.N. Bio fuels for compression ignition engine: A review on engine performance, emission and life cycle analysis. *Renew. Sust. Energ. Rev.* **2016**, *65*, 24–43. [CrossRef]
17. Sirviö, K.; Heikkilä, S.; Hiltunen, E.; Niemi, S. Kinematic viscosity studies for medium-speed CI engine fuel blends. *Agronomy Res.* **2018**, *16*, 1247–1256.
18. Sirviö, K. Issues of various alternative fuel blends for off-road, marine and power plant diesel engines. Ph.D. Thesis, University of Vaasa, Vaasa, Finland, 15 June 2018.
19. ISO 8217:2017(E). *Petroleum Products. Fuels (class F). Specifications of Marine Fuels*; ISO: Geneva, Switzerland, 2017.
20. Wang, X.; Grose, M.A.; Caldow, R.; Osmondson, B.L.; Swanson, J.J.; Chow, J.C.; Watson, J.G.; Kittelson, D.B.; Li, Y.; Xue, J.; et al. Improvement of Engine Exhaust Particle Sizer (EEPS) Size Distribution Measurement – II. Engine Exhaust Aerosols. *J. Aerosol Sci.* **2016**, *92*, 83–94. [CrossRef]

21. EN ISO, 8178-2:2008. *Reciprocating Internal Combustion Engines. Exhaust Emission Measurement*; Part 2: Measurement of Gaseous and Particulate Exhaust Emissions under Feld Conditions; ISO: Geneva, Switzerland, 2008.
22. Eastwood, P. *Particulate Emissions from Vehicles*; John Wiley & Sons Ltd: Chichester, UK, 2008; p. 494.
23. Bach, F.; Tschöke, H.; Simon, H. Influence of Alternative Fuels on Diesel Engine Aftertreatment. In Proceedings of the 7th International Colloquium Fuels of the TAE Technische Akademie, Esslingen, Germany, 10–11 January 2009; p. 685.
24. Szybist, J.P.; Song, J.; Alam, M.; Boehman, A.L. Biodiesel combustion, emissions and emission control. *Fuel Process. Technol.* **2007**, *88*, 679–691. [CrossRef]
25. Mathis, U.; Mohr, M.; Kaegi, R.; Bertola, A.; Boulouchos, K. Influence of diesel engine combustion parameters on primary soot particle diameter. *Environ. Sci. Technol.* **2005**, *39*, 1887–1892. [CrossRef]
26. Tsolakis, A. Effects on particle size distribution from the diesel engine operating on RME-biodiesel with EGR. *Energy Fuels* **2006**, *20*, 1418–1424. [CrossRef]
27. Alrefaai, M.M.; Peña, G.D.G.; Raj, A.; Stephen, S.; Anjana, T.; Dindi, A. Impact of dicyclopentadiene addition to diesel on cetane number, sooting propensity, and soot characteristics. *Fuel* **2018**, *216*, 110–120. [CrossRef]
28. Li, R.; Wang, Z.; Ni, P.; Zhao, Y.; Li, M.; Li, L. Effects of cetane number improvers on the performance of diesel engine fuelled with methanol/biodiesel blend. *Fuel* **2014**, *128*, 180–187. [CrossRef]
29. Violi, A.; Voth, G.A.; Sarofim, A.F. The relative roles of acetylene and aromatic precursors during soot particle inception. *P. Combust. Inst.* **2005**, *30*, 1343–1351. [CrossRef]
30. Hissa, M.; Sirviö, K.; Niemi, S. Combustion property analyses with variable liquid marine fuels in combustion research unit. *Agronomy Res.* **2018**, *16*, 1032–1045.
31. Kegl, B.; Kegl, M.; Pehan, S. Green diesel engine. In *Biodiesel Usage in Diesel Engines*; Springer: London, UK, 2013; p. 263.
32. Wiedensohler, A.; Birmili, W.; Nowak, A.; Sonntag, A.; Weinhold, K.; Merkel, M.; Wehner, B.; Tuch, T.; Pfeifer, S.; Fiebig, M.; et al. Mobility particle size spectrometers: harmonization of technical standards and data structure to facilitate high quality long-term observations of atmospheric particle number size distributions. *Atmos. Meas. Tech.* **2012**, *5*, 657–685. [CrossRef]
33. Wiedensohler, A.; Wiesner, A.; Weinhold, K.; Birmili, W.; Hermann, M.; Merkel, M.; Müller, T.; Pfeifer, S.; Schmidt, A.; Tuch, T.; et al. Mobility particle size spectrometers: Calibration procedures and measurement uncertainties. *Aerosol Sci. Technol.* **2018**, *52*, 146–164. [CrossRef]
34. Lähde, T.; Rönkkö, T.; Happonen, M.; Söderström, C.; Virtanen, A.; Solla, A.; Kytö, M.; Rothe, D.; Keskinen, J. Effect of fuel injection pressure on a heavy-duty diesel engine nonvolatile particle emission. *Environ. Sci. Technol.* **2011**, *45*, 2504–2509. [CrossRef]
35. Vaaraslahti, K.; Keskinen, J.; Giechaskiel, B.; Solla, A.; Murtonen, T.; Vesala, H. Effect of lubricant on the formation of heavy-duty diesel exhaust nanoparticles. *Environ. Sci. Technol.* **2005**, *39*, 8497–8504. [CrossRef]
36. Maricq, M.M.; Chase, R.E.; Xu, N.; Laing, P.M. The effects of the catalytic converter and fuel sulfur level on motor vehicle particulate matter emissions: light duty diesel vehicles. *Environ. Sci. Technol.* **2002**, *36*, 283–289. [CrossRef]
37. Mathis, U.; Ristimaki, J.; Mohr, M.; Keskinen, J.; Ntziachristos, L.; Samaras, Z.; Mikkanen, P. Sampling conditions for the measurement of nucleation mode particles in the exhaust of a diesel vehicle. *Aerosol Sci. Technol.* **2004**, *38*, 1149–1160. [CrossRef]
38. Chybowski, L.; Laskowski, R.; Gawdzińska, K. An overview of systems supplying water into the combustion chamber of diesel engines to decrease the amount of nitrogen oxides in exhaust gas. *J. Mar. Sci. Technol.* **2015**, *20*, 393–405. [CrossRef]